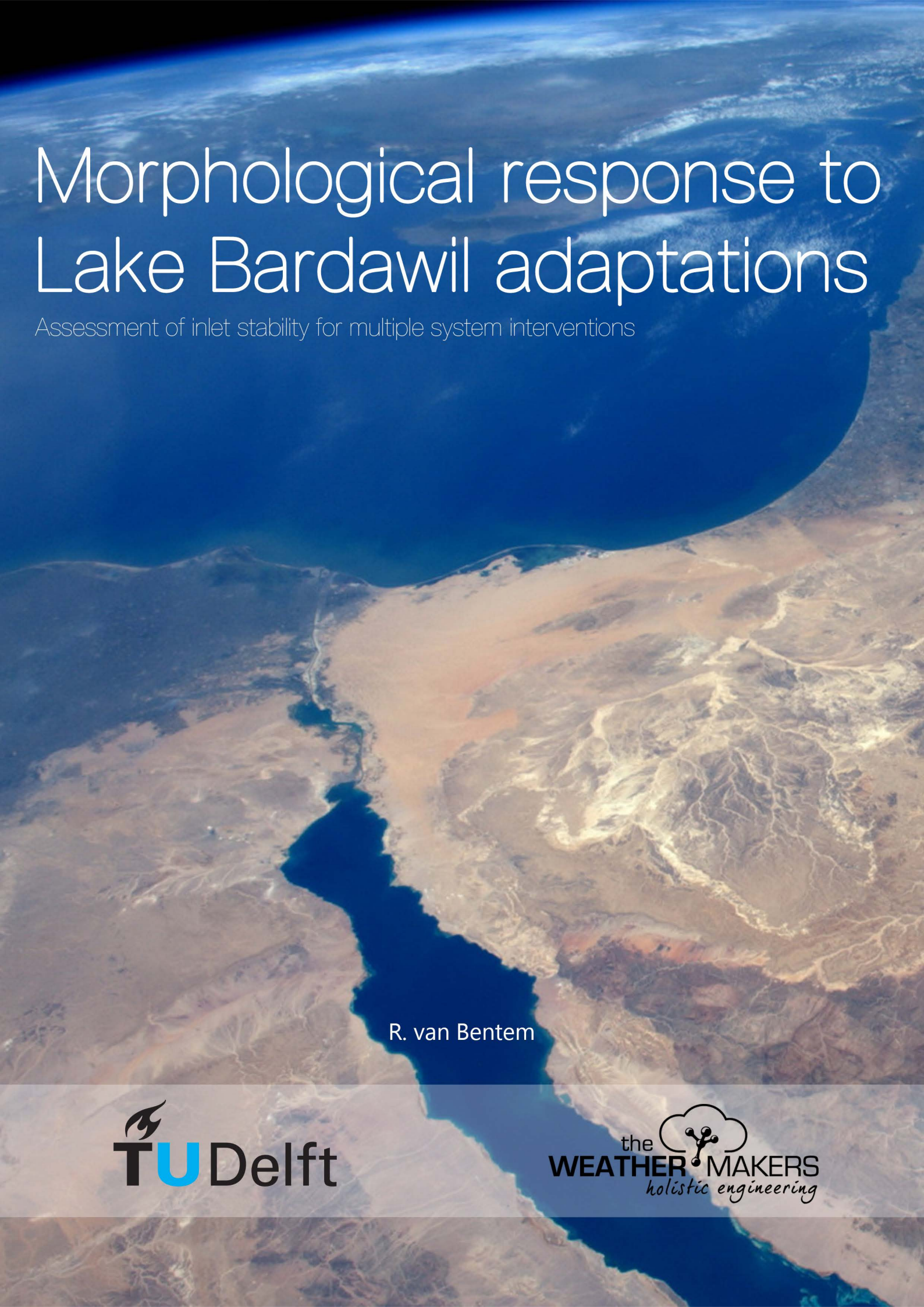

Morphological response to Lake Bardawil adaptations

Assessment of inlet stability for multiple system interventions

R. van Bentem

TU Delft

the WEATHER MAKERS holistic engineering

MORPHOLOGICAL RESPONSE TO LAKE BARDAWIL ADAPTATIONS

A thesis submitted to the Delft University of Technology in partial fulfillment of the requirements for the degree of

Master of Science in Civil Engineering

by

Rick van Bentem
4098773

25 March 2020

Rick van Bentem: *Morphological response to Lake Bardawil adaptations* (2020)

The work in this thesis was made in the:

Department of Coastal Engineering
Faculty of Civil Engineering
Delft University of Technology

Supervisors:	Prof. dr. ir. S.G.J. (Stefan) Aarninkhof	TU Delft
	dr. ir. J. (Judith) Bosboom	TU Delft
	Prof. dr. P.M.J. (Peter) Herman	TU Delft
	ir. J. (Jan) van Overeem	TU Delft
	ir. M.L.E.B. (Ties) van der Hoeven	The Weather Makers
	ir. A.C.S. (Arjan) Mol	DEME

ABSTRACT

Bardawil Lagoon is a tidal lagoon situated at the northern coast of the Sinai Peninsula in Egypt. It's two artificial inlets, Boughaz 1 in the West and Boughaz 2 in the East, provide a connection to the Mediterranean Sea. They enable the water bodies to interact and support fish migration. Currently, regular maintenance dredging works are necessary to keep the two inlets open. The objective of this thesis is to analyse the effect of interventions applied to the two inlets on the lagoon-sea interaction, with the goal of transforming the present, unstable inlet system towards a stable tidal inlet lagoon by adapting one or both of the present inlets.

This study is conducted on three system phases, being Phase 0, Phase 1 and Phase 2. Phase 0 consists of the initial situation without any interventions; Phase 1 contains the effect of adaptations to the Boughaz 1 inlet, and Phase 2 includes adaptations to Boughaz 2 in addition to the changes made in Phase 1. The new design in Phase 1 and Phase 2 consists of a deeper inlet cross-sectional area, the dredging of an approach channel, the addition of a nourishment, and the removal of the present breakwaters. Design elements are processed using a 2D-H Delft3D Flexible Mesh model and analysed under tide-only conditions with and without a prevailing wind climate added. Evaporation effects are included after the model calculations are made. The results are mainly assessed are the interaction with the Mediterranean Sea, the sediment transport character, and the inlet stability according to the Escoffier curve. Moreover, an analysis is made on the flushing of the lagoon and the effect of a prevailing wind pattern on the system.

It is clear from both literature and the initial model results of Phase 0 that Bardawil Lagoon currently does not function as a morphologically stable tidal inlet system, as sedimentation occurs in both inlets. The water exchange between the Mediterranean Sea and Bardawil Lagoon is restricted by the inlets, which is indicated by the difference in tidal elevation on both sides of the inlet. Both inlets are positioned near the unstable equilibrium point on the Escoffier curve, indicating possible closure of the inlets in the future. Hence, interventions are required to establish a morphologically stable lagoon inlet system. By applying the proposed designs in Phase 1 and Phase 2, the limitations on the incoming tide shift from the inlets to the inner basin induces friction, thus removing the inlets as limiting factor. Moreover, taking into account both the prevailing winds and high evaporation effects, the total system is classified as having a sediment exporting character after Phase 2. High evaporation rates have a significant importing effect on the sediment transport character of the inlets. However, after Phase 2, these effects are reduced by a factor 3-5 compared to Phase 0, depending on the wind. The new cross-sectional area design also results in both inlets being positioned near the stable equilibrium point on the Escoffier curve after Phase 2, which is supported by the sensitivity analysis. Hence, it is concluded that the proposed adaptations achieve the goal of developing Bardawil Lagoon into a morphologically stable inlet system.

The study provides good insight into the effect of system interventions on the morphodynamic stability of the inlets as well as the flow dominance regarding those inlets. It is recommended to construct a validated morphological 3D model which can provide insight in the long term response of the system to those adaptations.

ACKNOWLEDGEMENTS

First of all I would like to express my very great appreciation to Judith for our sparring sessions on the topic and the time you made available to guide me through this thesis. My plans didn't always work out as planned, but your encouragement helped me to stay focused. Stefan, thank you for your guidance, chairing the committee, and for being the mediator during the final months. Jan, thank you for taking the place of Judith during these final months and providing constructive feedback. Peter, your thorough assessment helped lifting the quality of my work. I hope my thesis will not evaporate as fast as Bardawil does. Thank you, Arjan, for all your modelling advice and feedback. Ties, a special thanks to you for the unlimited stream of ideas, enthusiasm, and support which form the basis of this thesis; I really enjoyed our collaboration.

Furthermore I would like to thank everybody else at The Weather Makers for making me feel welcome and appreciated. I highly enjoyed my time there and I hope we can re-green the Sinai together! Especially Maarten, thank you all the support you provided while I was working on this thesis and thank you for being a good friend.

I hope my family still knows me, they never stopped encouraging me, thank you, I will visit again soon if Corona allows it! A special thanks to my friends in Delft for all the coffee breaks and moral support while being patient with my mood, I owe you all! Thank you Niek, Wouter en Brecht for not only checking my work, but also providing the necessary distraction. Hanna, you made it all possible, thank you for carrying this team!

CONTENTS

1 INTRODUCTION

The Bardawil Lagoon is situated at the Northern coast of the Sinai Peninsula of Egypt. This tidal lagoon consists of a basin enclosed by a coastal barrier island and forms, like for example beach and dune systems, a transition between the land and the sea. Two artificial inlets, Boughaz 1 in the West and Boughaz 2 in the East, connect the lagoon with the Mediterranean Sea, as can be seen in Figure 1.1. The lagoon has an extent of almost 80 km and a maximum width of 20 km and it covers an area of about 550 km^2 (Khalil and Shaltout, 2006).

Figure 1.1: Bardawil Lagoon and the two artificial inlets connecting the lagoon to the Mediterranean Sea

The prosperity of thousands of families around Lake Bardawil largely depends on fishing yield, which subsequently depends on an ecological robust tidal lagoon system. Due to the absence of inland fresh water inflow, the lagoon depends on the inflow of less saline Mediterranean Sea water to maintain a viable habitat. However, a near full closure of the inlets in 1970 resulted in extreme salinity observations (up to 70-100‰). Reopening the inlets in the 1980's caused a significant reduction in salinity, but with an average salinity around 50‰the lagoon is still classified as hypersaline.

This research is set up with the goal to determine whether it is possible to adapt Boughaz 1 and Boughaz 2 to two morphologically stable inlets which enhance natural sediment export out of system. A naturally deepening lagoon with morphologically stable inlets prevents the inlets from closure and hence the drying up of the lagoon and the subsequent loss of biological and economic value (El-Aiatt et al., 2019).

1.1 PROBLEM DESCRIPTION

The current hypersaline environment has led to an unsustainable situation at Bardawil Lagoon. Abnormally high salinities prevent both adult and young fish from settling in the lagoon (Ben-Tuvia, 1979), hence the fish migration into the lagoon is degrading, causing the fisherman to concentrate their fishing activities in and around the inlets (Khalil and Shaltout, 2006; Lanters, 2016). The current demand for fish is exceeding the supply of the lagoon, causing a negative feedback loop in fish catch rates (Khalil and Shaltout, 2006). While the fish catchment rates show an increase between 2014 and 2015, the fishing yield consists mainly (67.3%) of juvenile fish, which is non-sustainable (El-Aiatt et al., 2019). Moreover, sedimentation inside both inlets is reducing the interaction between the two water bodies, leading to even higher salinity values, which in their turn are a threat to the fish migration and thus the living conditions of the fishermen in Bardawil Lagoon (Abd Ellah and Hussein, 2009; Abohadima et al., 2013; Lanters, 2016; El-Aiatt et al., 2019). Due to sedimentation regular maintenance dredging works are needed to keep both inlets , Boughaz 1 and Boughaz 2, open to provide sufficient interaction with the Mediterranean Sea (Linnersund and Mårtensson, 2008; Lanters, 2016; Nassar et al., 2018).

1.2 RESEARCH SCOPE

This research is part of a larger study currently conducted by The Weather Makers (TWM) and will build further on previous research done by Lanters (2016) and Georgiou (2019), who both conducted their thesis under the same supervisor currently working at TWM. The overarching goal of the Sinai project conducted by The Weather Makers is to contribute to a sustainable future for those communities living in the northern part of the Sinai Peninsula. This will be done through restoration of the marine, coastal and terrestrial ecosystems, on the functioning of which these communities depend. The objective of the project is to restore the aquatic and terrestrial ecosystem of the Northern Sinai desert through well-designed restoration activities. The main activities to achieve the objective are (i) dredging to improve the water quality of the lagoon and so increase the fish population, and with it the fishing yield; (ii) intelligent re-ruse of the materials dredged from the lagoon for reinforcement of the coastline, construction of dams for flash-flood management, and as soil enhancer for land-based activities; (iii) restoration and development of wetlands and salt marshlands around the lagoon; and (iv) improving the hydrological cycle through the construction of wetlands and reducing salinity of the lagoon surface water by increasing tidal influence, flash flood management, and vegetation and canopy cover. This thesis study will focus on the lagoon related interventions of the Sinai project (i): resource-based dredging to improve the water quality of the lagoon and thus increase the fish migration into the lagoon. As described this study will continue on the work previously done by Lanters (2016) and Georgiou (2019), an extensive analysis of their work can be found in Chapter 2. Results from previous studies are used for further analysis of this thesis. The study of Lanters (2016) gave good insight in the hydrological processes governing the lagoon which forms a solid base for this study. Georgiou (2019) proposed an innovative inlet design by mimicking nature for the Boughaz 1

inlet. The cross-sectional area and approach channel design from that study will be applied on both inlets in this research.

The scope of this research is to analyse the hydraulic processes taking place after adapting the double inlet system of the Bardawil Lagoon and the stability concerning those inlets. The study will concentrate on the hydraulic and morphodynamic response of the inlets and their adjacent areas. The inner lagoon areas will be discussed, but no extensive quantitative analysis is performed on these parts. Furthermore, baroclinic processes due to salinity and density differences are not considered in the results of this part of the study, which does not mean they can be neglected for the overarching project, as is described in the discussion. The methodology of the study can be described as a circle flow chart, as will be done in Section 1.4.

A morphologically stable inlet system provides a constant interaction with the Mediterranean Sea and reduces regular maintenance dredging works. The objective of this research is therefore to analyse the effect of inlet adaptations on the lagoon-sea interaction, with the goal of transforming the present, sediment importing, system towards a morphologically stable inlet system by adapting one or both of the present inlets.

1.3 RESEARCH QUESTIONS

The key concept of the objective as described in this section can be summarized as follows:

> **How can the Bardawil Lagoon multiple inlet system be transformed from a morphologically unstable towards a morphologically stable inlet system by adapting one or both inlets?**

To support the main research question the following sub-questions have been defined:

- How can the current hydrodynamic and morphological character and inlet stability of Bardawil Lagoon be classified?
- What effect do the inlet adaptations have on the sediment transport character of the inlets?
- What effect do the inlet adaptations have on the stability of the inlets?
- To what extent does the wind climate contribute to sediment transport and inlet stability of the system?
- What effect do the adaptations and wind climate have on the renewal time and flushing of the lagoon?

1.4 METHODOLOGY

A methodology is developed to determine the effect of interventions to the functioning of Bardawil Lagoon. Such interventions can be assessed according to the flow chart in Figure 1.2 below. For the start of each cycle it is important to properly define the functioning of the system and locate the current limitations that prevent the system from the desired functioning. The next step is to propose and implement system interventions to counter

such limitations and enhance the system functioning. In the third step the proposed adaptations are processed in a numerical model to determine the effect, followed by a careful elaboration of the results in the fourth step. The final step is to discuss the results of the numerical model and elaborate the previously proposed system interventions, followed by a discussion on other relevant processes which could further influence the results, but are not included in the model.

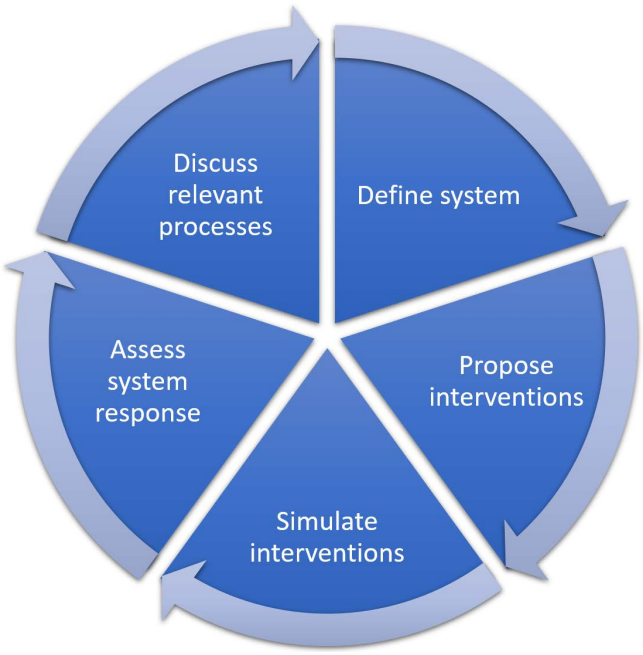

Figure 1.2: The research methodology followed for this thesis

As described in the scope this particular study focuses on the hydraulic and morphological response of the system to the application of a new design to the inlets and the directly adjacent areas. Effects of for example baroclinic processes on the system or a detailed response of the inner lagoon area can be assessed according to this methodology, but these steps will not be performed for this thesis.

The system will be assessed according to several hydraulic parameters, including an analysis on the shape of the tidal harmonic in predefined locations in the lagoon. Changes in the tidal elevation curve can indicate the limiting factor in lagoon-sea interaction, this will be further elaborated in Chapter 3.

The proposed system interventions are studied in three phases in order to determine their individual response to the system and are listed as follows:

- Phase 0: Assessment of the present functioning of Bardawil Lagoon
- Phase 1: New design to Boughaz 1 and determine the response
- Phase 2: New design to Boughaz 2 in addition to Phase 1 and determine the response

The present functioning of the lagoon is further elaborated in Chapter 2, while the design of Phase 1 and 2 can be found in Chapter 3.

The study can be divided into two parts. The first part contains a hydrodynamic and stability analysis of the research phases under the influence

of the tide, whereas the second part investigates what effect adding a daily wind pattern has on to the hydrodynamics, stability and lagoon-sea interaction through the system. Figure 1.3 depicts the research timeline.

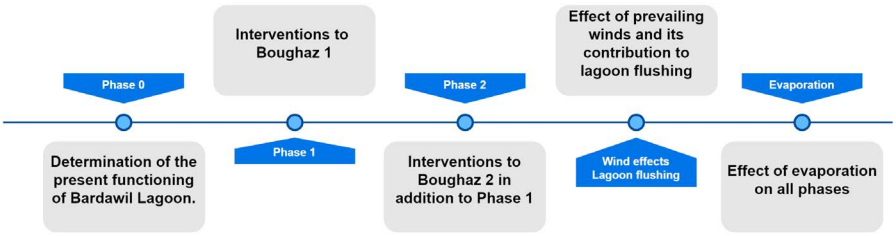

Figure 1.3: Visualization of the research steps conducted in this study

The inlet adaptations considered in this study consist of the inlet cross-sectional area, the inlet approach channel, and the design of the inlet surroundings including the removal of the breakwaters and adding a nourishment. An extensive description of the methodology and the Delft3D FM model used in this study can be found in Chapter 3

1.4.1 Reading guide

The report is built up as follows: Chapter 2 provides insight in the history of the lagoon and the processes determining its functioning. Furthermore, it gives insight into relevant studies which are previously carried out. The methodology is described in Chapter 3, including the elaboration of the modelling software used. Chapter 4 provides results for all research steps, which are then discussed in Chapter 5. The thesis is concluded in Chapter 6, which contains conclusions and recommendations.

2 BACKGROUND INFORMATION

2.1 INTRODUCTION TO BARDAWIL LAGOON

2.1.1 Lagoon history

Bardawil Lagoon, also referred to as Lake Bardawil, is located at the Northern of the Sinai Peninsula in Egypt and is one of the major features of the coastline, located at latitude 31°03'-31°15'N and longitude 32°40'-33°32'E, see Figure 2.1. The lagoon is bordered from the north by the Mediterranean Sea, from the east by the Arish-Rafah sector, from the west by the eastern margin of the Nile Delta plain, and from the south by sabkhas (a flat coastal plain with a salt crust), extensive playas, sand sheets and sand dune fields reaching up to 40 meters above sea level (Khalil and Shaltout, 2006). The eastern part of the lagoon consists of the Zaranik protected area, a nature reserve currently exploited for salt production.

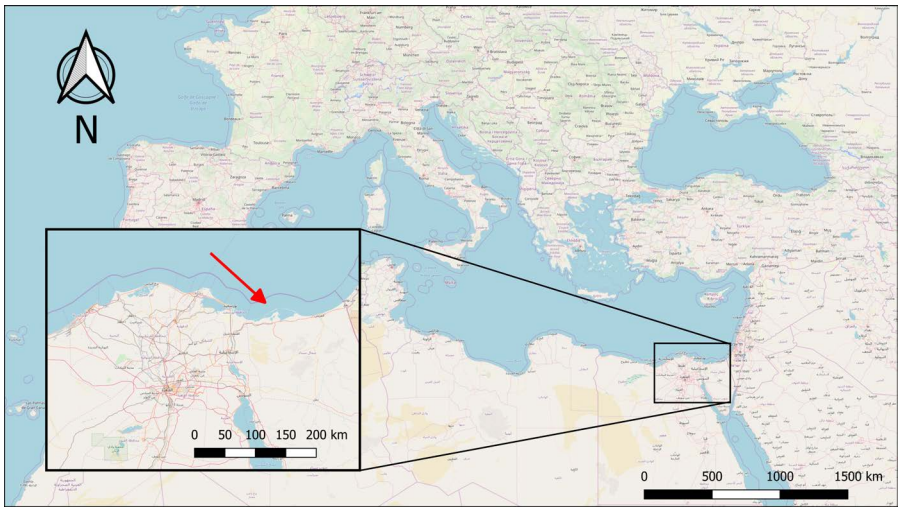

Figure 2.1: The location of Bardawil Lagoon, indicated with the red arrow

While other Mediterranean Egyptian lagoons are of deltaic origin (the Nile River Delta), Bardawil Lagoon is of tectonic origin (El-Bana et al., 2002). During the Roman period, in which the lagoon was called "Sirbonis lake" (Hamdan and Hassan, 2020), interaction with the sea was high enough to allow permanent water flow from the Mediterranean Sea into the basin. During later periods Bardawil Lagoon was a sabkha and was called "Bardawil Sabkha" as its surface was not permanently covered by water (Embabi and Moawad, 2014). Bardawil Lagoon was artificially opened in the beginning of the 20th century so it could be used for fishing purposes. An opening and closing cycle of approximately three years was established, of which 6 months were required for digging the inlets connecting the lagoon with the sea, followed by 24 months of fishing before the inlets were closed due to

the littoral drift. The final 6 months the lagoon dried up again due to evaporation (Linnersund and Mårtensson, 2008). Attempts have been made since 1927 to maintain permanent artificial inlets in the lagoon barrier, which did not succeed until 25 years later (Klein, 1986; Linnersund and Mårtensson, 2008). The present inlets, Boughaz 1 in the west and Boughaz 2 in the east (Figure 2.2), were constructed between 1953-1955 with concrete jetties on both sides and were maintained open by continuous dredging operations (Khalil and Shaltout, 2006; Linnersund and Mårtensson, 2008). However, the efforts were insufficient and around 1970 Boughaz 1 nearly closed and Boughaz 2 experienced a full closure (Inman, 1970; Klein, 1986; Khalil and Shaltout, 2006). Dredging operations were continued in 1972 and the inlets have been kept open since, but with a constant changing shape (Klein, 1986). Klein (1986) conducted research on the morphological changes of the inlets after the construction of the High Aswan Dam in 1970, which altered the sediment budget in the littoral zone. He concluded that the inlets act as a groin, trapping longshore sediment at the inlet entrance, which is then moved into the inlet by waves entering the lagoon. Deposition of sediment in the inlets results in severe downstream erosion. Furthermore, he concluded that sedimentation occurs mainly in summer and Boughaz 2 traps the most sediment. While no clear numbers were defined, Klein (1986) estimates the sedimentation in the inlets after the construction of the High Aswan Dam about 50% of the values predicted by the studies of Inman (1970) and Vinja (1970). The construction of the High Aswan Dam resulted in near absence of Nile River flow and complete loss of the Nile River as an active sediment source for the delta and the coastline of the Nile littoral cell (Inman and Jenkins, 1984).

To maintain and protect the inlets from the accumulation of coastal sediments breakwaters have been constructed to the east and west of both inlets around 1990. The breakwaters helped to maintain the inlets open, but their presence has led to an undesirable evolution of the shoreline by causing coastal erosion on the downdrift eastern side and accumulation of sediment on the western side of the inlet. Meanwhile, until today, there is still a significant accumulation of sediment in front of the inlets, leading to gradually shallowing waters which affect the water exchange between Bardawil Lagoon and the Mediterranean Sea (Nassar et al., 2018). In its current state the lagoon is still dependent on continuous dredging works to keep the inlets open and ensure the water exchange with the sea, overcome salinity increasing, and conserve the lagoon ecosystem (Khalil and Shaltout, 2006; Linnersund and Mårtensson, 2008; Embabi and Moawad, 2014).

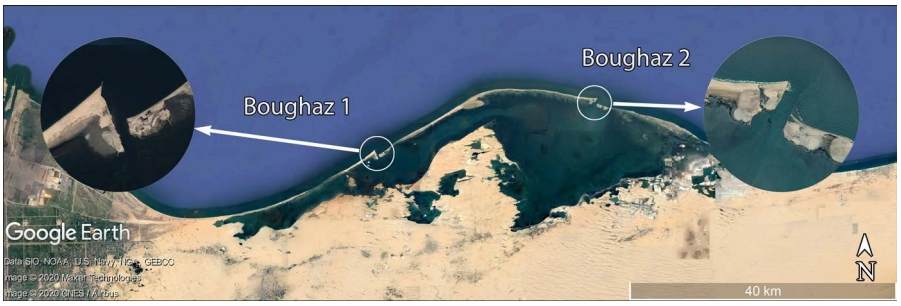

Figure 2.2: Bardawil Lagoon and the two artificial inlets Boughaz 1 (west) and Boughaz 2 (east) (From Google Earth)

2.1.2 Lagoon dimensions

The lagoon is separated from the Mediterranean Sea by a long convex shaped sand bar, between 300 and 1000 meters wide (Khalil and Shaltout, 2006). Although various sources write about the area of the lagoon, their estimates differentiate per study, or even in the study itself. Inman (1970) reports an area of 600 km^2 while Khalil and Shaltout (2006) mentions different sizes in the range between 600 and 680 km^2. Abd Ellah and Hussein (2009) reports a change in area from 600 km^2 in 1991 to 518 km^2 in 2004, describing the lost areas to be the result of natural processes, man made dried, or cut off by embankment or extensive salina and super tidal salt flats, or all of these reasons (Abd Ellah and Hussein, 2009). A Google Earth study provided an area of approximately 550 km^2, a value which will further be used in this study.

Abd Ellah and Hussein (2009) classified the lagoon water depth into four categories, which can be found in Table 2.1. The lagoon is very shallow with an average depth around 1.2 m (Khalil and Shaltout, 2006; Abd Ellah and Hussein, 2009; Embabi and Moawad, 2014). Except for the areas close to the inlets the lagoon water depth never exceeds 3 m. Different values for the depth around the inlets are presented, with estimated values between 5.75 and 8.50 m (Abd Ellah and Hussein, 2009; Embabi and Moawad, 2014). For this study the depth profile provided by Egypt and The Weather Makers is used, which can be found in Figure 2.3. The average depth of 1.2 m and the approximated area of 550 km^2 provide a lagoon volume of 660 million cubic meters. Depth values of the inlets we found to have a maximum depth of 6 meter, thus not reaching the 8.5 meters described in literature. The dimensions of the inlets can be found in Table 2.2. An overview of the key numbers required for establishing a clear view of the lagoon can be found in Table 2.3, the values are elaborated more extensively later on in this chapter.

Depth [m]	Percentage	Area [m^2]
$<$ 1.0	21.0%	115
1.0 - 1.5	62.0%	341
1.5 - 2.5	16.5%	91
$>$ 2.5	0.5%	3

Table 2.1: Percentage of depths observed inside Bardawil Lagoon (Abd Ellah and Hussein, 2009)

Inlet	Width [m]	Depth [m]	Cross-sectional area [m^2]
Boughaz 1	270	3-5	954
Boughaz 2	350	3-6	1386

Table 2.2: The inlet characteristics of Boughaz 1 and Boughaz 2

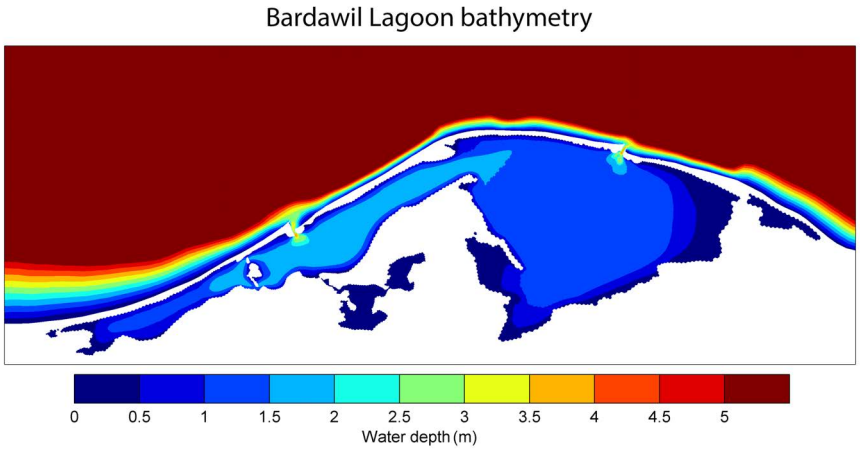

Figure 2.3: The bathymetry of Bardawil Lagoon used in this study, values relative to MSL

Key numbers	Value
Lagoon area	550 km^2
Mean lagoon depth	1.2 m
Mean lagoon volume	660.000.000 m^3
Mean air temperature	20.8 °Celsius
Mean water temperature	21.5 °Celsius
Median spring tide	0.37 m
Median neap tide	0.14 m
Precipitation	80-100 mm/year
Evaporation	1505 mm/year
Average lagoon salinity	50‰

Table 2.3: Key numbers of processes affecting Bardawil Lagoon

2.2 DATA REVIEW

2.2.1 Tide

The Mediterranean Sea tide governs the water exchange between the Mediterranean Sea and Bardawil Lagoon. It is characterized by a micro tidal regime (Abd Ellah and Hussein, 2009), indicating a tidal range less than 2 m (Embabi and Moawad, 2014). Furthermore the tidal environment can be characterized as semi-diurnal and with mixed energy. While no periodic data measurements are available for this thesis, multiple studies (both measurements and computational) have been conducted with various results. Inman and Jenkins (1985) estimated an average tidal range of 0.30 m along the coast of the Mediterranean Sea, Frihy et al. (2002) found similar results with measurements at El Arish, east of Bardawil Lagoon, with a tidal range of 31 cm. Linnersund and Mårtensson (2008) computed tidal motion for Port Said data with WxTide, resulting in an average of 0.30 m outside the lagoon, varying 0.05 m with neap and spring tide. The amplitudes inside the lagoon and in Boughaz 1 inlet are estimated to be less than 0.16 m (Linnersund and Mårtensson, 2008). The dataset from Nassar et al. (2018) varies from previous studies and estimates the spring tidal range to be 0.55 m.

Georgiou (2019) computed an offshore tidal range of 0.40 m, reducing to 0.075 m inside the lagoon.

Data on tide induced flow velocities are more scarce, the only study is from Embabi and Moawad (2014) which estimates approximately equal inflow and outflow velocities through the inlets with a magnitude equal to 0.70 m/s.

Like the study by Georgiou, this study will work with the predictions made by Lanters (2016) who used a Mediterranean Sea model to determine the water level conditions at the system boundaries. The tidal range observed offshore of Bardawil Lagoon is shown in Figure 2.4, which shows a median spring tidal range of 0.37 m and a median neap tidal range over 0.14 m.

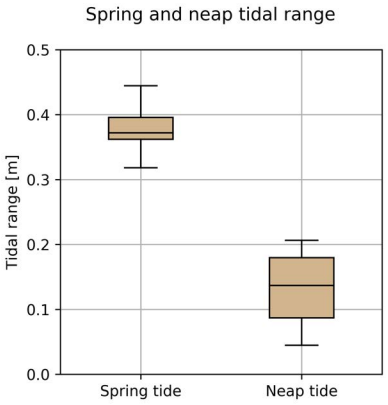

Figure 2.4: Spring and neap tidal range offshore of Bardawil Lagoon

2.2.2 Wave climate

The wave climate can be divided into three seasons; Winter (November to March), spring (April to May), and summer (June to September) (Frihy et al., 2002). Low-swell waves prevail during spring and summer, with wave heights rarely exceeding 1-1.5 m for waves originating from the WNW and NE. Winter waves are fluctuating between stormy and calm intervals and coming from the N, NNW, and NW sectors and are the predominant cause of morphological changes (Frihy et al., 2002).

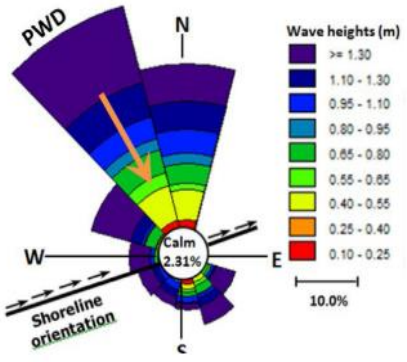

Figure 2.5: Wave rose indicating wave height and direction from in situ measurements, measured over the year 2010 (Nassar et al., 2018) The dominant wave direction is indicated with PWD (Prevailing wave direction)

Average wave height and period were found to be 0.5 m and 6.3 s. Linnersund and Mårtensson (2008) studied measurements from a wave gauge located at Port Said, recordings ranging from August 1999 to July 2000 with 3 hours interval. Important note is that the measurements were taken in shallow water. Results confirm earlier studies with a dominant wave direction from NNW. Maximum recorded wave height is 2.10 meter with an average height of 0.53 m and a period of 3.35 s.

Measurements done in 2010 using a current and wave gauge at a depth of 14m near the western inlet gives the wave rose shown in Figure 2.5 (Nassar et al., 2018). The measurements indicate a predominant wave direction from the NW (51%), while 32% of the waves originate from the N and 5% originate from the SE. These prevailing wave directions generate an eastward-flowing alongshore current. The maximum wave height during the strongest storms is almost 4.0 m. The wave period is between 2 and 6 s for 80% of the time (Nassar et al., 2018).

To summarize: an average wave height of 0.5 m with a period of 6 seconds and with a prevailing North-West to North origin can be found for the wave climate outside of Bardawil Lagoon (Frihy et al., 2002; Linnersund and Mårtensson, 2008; Georgiou, 2019).

Previous research on Bardawil Lagoon showed that the system is predominantly influenced by the tide, with little influence of waves (Linnersund and Mårtensson, 2008; Georgiou, 2019). Therefore waves will not be added separately to the model. However, an analysis of the wave climate is made to estimate the littoral drift along the North Sinai coastline. The BMT ARGOSS model from Waveclimate is used for acquiring a representative wave climate dataset along the North Sinai coastline.

2.2.3 Wind climate

Wind induced stresses generate waves and surface currents in a body of water more or less in the same direction as the wind direction (Bosboom and Stive, 2015). These currents are important for maintaining a good circulation of water within Bardawil Lagoon as well as exchange with the Mediterranean Sea (Miller et al., 1990; Linnersund and Mårtensson, 2008; Lanters, 2016). Wind induced waves generate longshore currents transporting sediment along the North Sinai coast (Linnersund and Mårtensson, 2008). Frihy et al. (2002) determined the dominant wind direction to be WNW. Linnersund and Mårtensson (2008) processed measurement data from Port Said, 60 km west of Lake Bardawil. They found the most frequent wind direction to be between NW and N, with 44% of the winds approaching from these directions, but a seasonal variation can be observed, see Figure 2.6. The winter months are characterised by strong winds approaching from SW to W, while spring can be recognised by strong winds from the SSW and WSW and moderate ones from ENE. Little variation of wind direction is observed during the summer months. The dominant northwestern winds are responsible for generating waves and longshore currents in an easterly direction. During spring, the wind direction is reversed coming from N, NNE and NE, contributing to a longshore current towards the west (Embabi and Moawad, 2014).

Average wind speed was found to be between 3.69 - 4.92 m/s, with peak velocities around 14 m/s. There is a daily pattern with the strongest winds occurring in the afternoon (12:00 - 17:00) and the weakest at night, in which the strongest winds come from SW and W and do not contribute to the wave climate relevant for Bardawil Lagoon (Linnersund and Mårtensson, 2008). Due to the prevailing wind a spatial distribution of salinity values is observed inside the lagoon. The North-Western winds displace the water masses in the eastern direction. Dry winds during the warm period lead to an increase in evaporation rate, subsequently the salinity increases, espe-

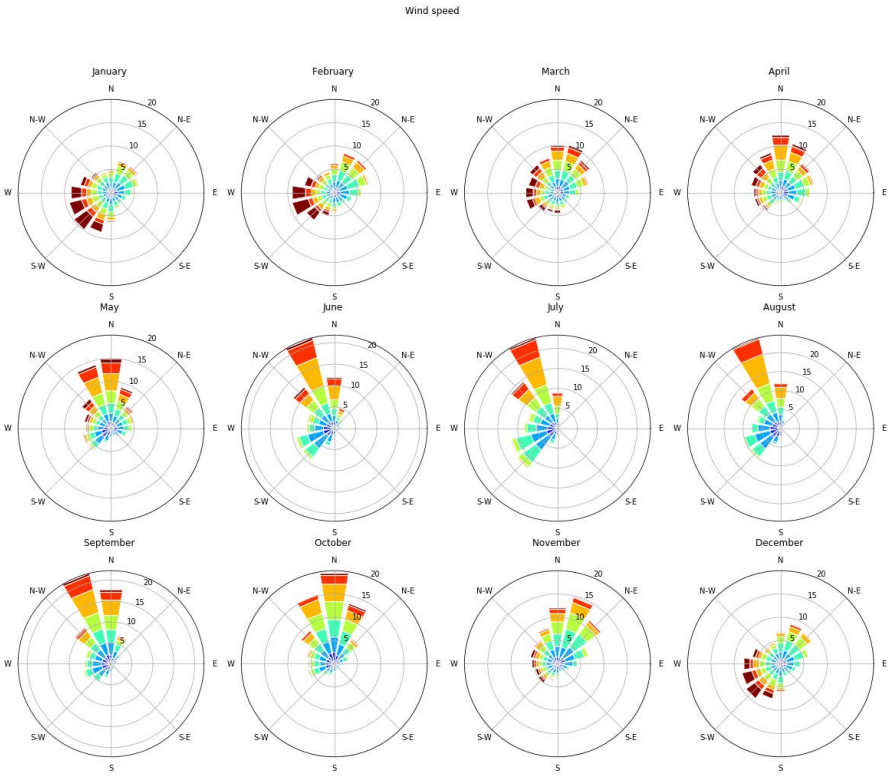

Figure 2.6: The wind magnitude and direction distribution for each month for a 26 year period (1992-2018)

cially in isolated areas (Abd Ellah and Hussein, 2009).

For the implementation of the wind in this research two datasets are assessed, one from the Waveclimate BMT ARGOSS model based on the NOAA GTECCA dataset and one from the Meteoblue data based on the NEMS model. The models differ on location, accuracy and timestep. The BMT ARGOSS model only takes into account offshore locations and provides a grid size of 50 km and a timestep of 3 hours while the Meteoblue model provides a grid size of 30 km and time step of 1 hour and is also available for land based locations. The higher accuracy and smaller timestep are in favor of the Meteoblue model, this data is therefore used as model input.

The climate used in this study is obtained by finding a representative month with a daily occurring wind pattern, which is provided by August 2018, see Figure 2.7. The model input is determined by taking the velocity and direction for each timestep averaged over the whole month. A wind rose of the daily averaged wind pattern of August 2018 can be found in Figure 2.8 (a), in addition to that the averaged morning winds (Figure 2.8 (b)) and afternoon winds (Figure 2.8 (c)).

2.2.4 Climate, salinity and evaporation

An overview of the monthly climate in Bardawil Lagoon can be found in Table 2.4. The salinity of Bardawil Lagoon is much higher than in the open sea as a result of low rainfall (80 – 100 mm/year) and high evaporation rate (1505 mm/year) with a yearly average around 50‰ and can be considered hypersaline (>35‰) (Khalil and Shaltout, 2006). High fluctuations in

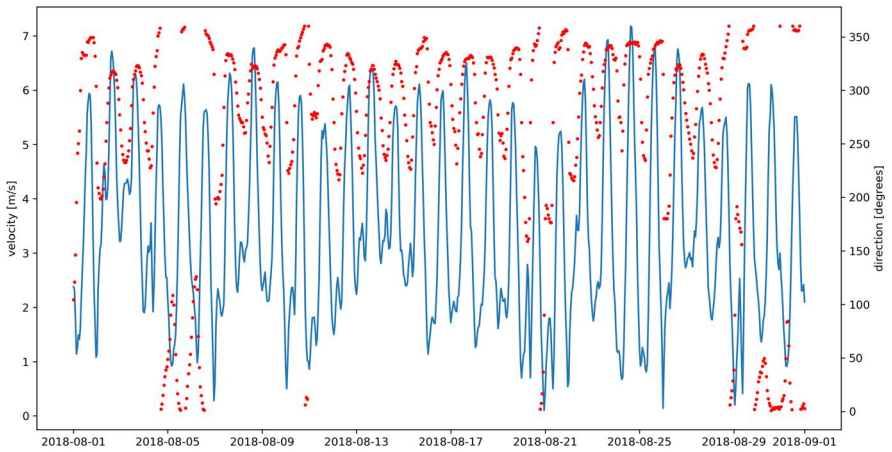

Figure 2.7: The wind climate for the period 2018-08-01 to 2018-09-01 from the Meteoblue dataset

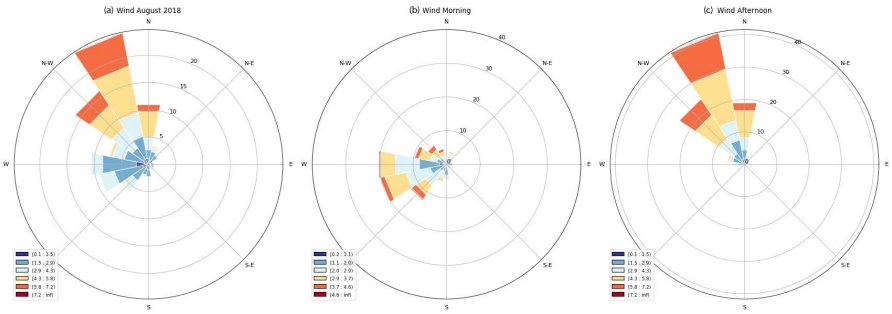

Figure 2.8: The daily occurring wind climate for the period 2018-08-01 to 2018-09-01 from the Meteoblue dataset. With (a) the daily average wind velocity and direction, (b) the morning climate, and (c) the afternoon climate

salinity range can be found, the lowest value being 38.3‰ and the highest 71.1‰ (Abd Ellah and Hussein, 2009).

	j	f	m	a	m	j	j	a	s	o	n	d
Mean temperature (°C)	14	15	16	19	22	24	26	27	25	24	21	15
Precipitation (mm)	13	10	9	7	5	0	0	0	0	0	18	20
Evaporation rate (mm)	56	84	96	132	167	189	192	177	153	146	63	50
Net water loss (mm/day)	1.4	2.6	2.8	4.2	5.2	6.3	6.2	5.7	5.1	4.7	1.5	1.0
Net water loss ($\cdot 10^6 m^3$)	0.77	1.43	1.54	2.31	2.86	3.47	3.41	3.14	2.81	2.59	0.83	0.55

Table 2.4: The climatic data and net water loss in Bardawil Lagoon (Euroconsult, 1995)

Euroconsult (1995) determined the highest net water loss up to 3.5 million m^3 of water per day during the summer months and the lowest net water loss about 0.5 million m^3. These losses of water have to be compensated by water inflow through the inlets from the Mediterranean Sea, resulting in a residual flow into the lagoon.

This water exchange therefore plays a crucial role in water salinity variations (Ferrarin and Umgiesser, 2005). A relative variation in salinity between the inlets and the inside of the lagoon can be observed with increased distance from the inlets (Khalil and Shaltout, 2006). These spatial distributions of water salinity are affected by prevailing wind, the predominant Northern

and Western winds cause water masses to displace towards the east. The dry winds in warm periods also lead to an increase in the evaporation rate from the Lagoon's surface (Abd Ellah and Hussein, 2009). Due to higher precipitation in winter and high evaporation in summer, the lowest salinity values are observed during the winter months and the highest in summer. A spatial distribution inside the lagoon per quarter can be found in Figure 2.9 below, notable is the constant high value of at least 65‰ in the Western part of the lagoon. During the warm periods the dry winds enhance evaporation, consequently increasing salinity, especially in isolated areas (Khalil and Shaltout, 2006). The increase in salinity is compensated during winter season by rainfall and sea water entrance through the inlets (Abd Ellah and Hussein, 2009).

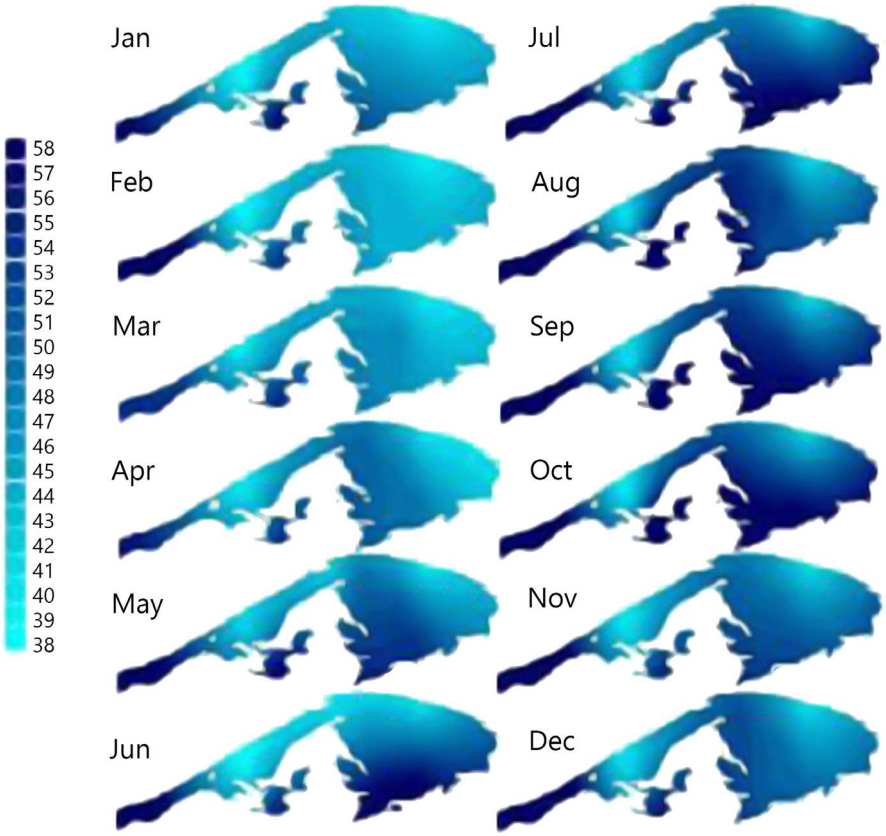

Figure 2.9: Salinity distribution throughout Bardawil Lagoon for each month, adapted from Abd Ellah and Hussein (2009)

2.2.5 Sediment characteristics

Bardawil lagoon consists mainly of clayey sand, with sand near the inlets of the lagoon area and with silty clay in the deepest parts (Khalil and Shaltout, 2006). Farahat (2006) performed a series of sediment grain size studies during 2004 at 12 stations across Bardawil Lagoon. The findings show both a spatial and time variation of sediment composition during the year. Inside the lagoon the sediment composition consists of mainly sand (72%), mud (19%), and very little amount of gravel (9%). The inlets have a significantly higher sand fraction (98%) complemented with gravel (2%), mud is absent.

At the center of the lagoon area at Boughaz 2 the lowest sandy fractions are found (61.2%) which coincide with the highest mud fractions (27.5%) (Khalil and Shaltout, 2006). The finer sediments form a great part of the bottom sediments of the lagoon, along with biological products like shells (Euroconsult, 1995).

The distribution of sediment particle sizes depends on two different processes; the availability of different particle sizes in the parent material and the processes operating where the particles were deposited (Folk and Sanders, 1978). Studies on the outside of the lagoon showed that in the accreted area West of Boughaz 1 the sediment is coarser compared to the sediment at the east side (Emanuelsson and Mirchi, 2007).

2.2.6 Littoral drift

Littoral drift (or longshore sediment transport) can be defined as the transport of non-cohesive sediments due to the action of breaking waves and longshore currents parallel to the shoreline in the littoral zone (DHI, 2019). Transport rates are dependent on the nearshore wave exposure and wave incidence angle and the littoral drift gradients can contribute to an eroding of accreding shoreline (Bosboom and Stive, 2015). In the littoral system of Bardawil Lagoon longshore transport is the most dominant coastal process for transport of non-cohesive sediments (Frihy et al., 2002). The longshore sediment transport is almost unidirectional eastward all year long, with only short periods of westward transport (Frihy et al., 2002). The eastward longshore transport assumption is supported by several indicators, for example: sand accumulation versus beach erosion on opposite sides of breakwaters, changes in shoreline position resulting from erosion and accretion trend, longshore growth of spits, and patterns of beach sand variation in grain sizes (Frihy and Lotfy, 1997). A schematic view of sediment transport along the North Sinai coast can be found in Figure 2.10. Sediment fluxes derived from longshore drift generate sediment infilling in the inlets which are regularly addressed by dredging (Bek and Cowles, 2018).

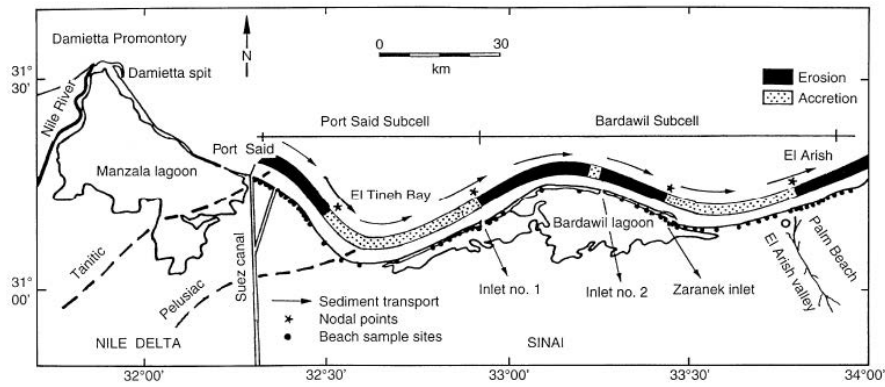

Figure 2.10: Erosion and accretion patterns along the North Sinai coast. Net sediment transport directions are indicated with arrows (Modified by Linnersund and Mårtensson (2008) after Frihy and Lotfy (1997))

Over the past decades several studies have been conducted on determining the littoral drift along the North Sinai coast, of which the results can be found in Table 2.5. This table shows the gross transport found by vari-

ous studies, which are required for the stability calculations by Bruun and Gerritsen (1960). A more extensive table can be found in Appendix A.1 containing net values as well. The first studies of littoral drift in the area were performed by Inman (1970) and Vinja (1970), who both estimated the sediment entrapment in the two inlets before the construction of the breakwaters and High Aswan Dam in the Nile in 1970 (Klein, 1986). Because of unknown transport rates in the area Inman (1970) used figures of entrapment in the inlets, emphasizing that these accumulation rates are lower limits of actual transport. Vinja (1970) determined the transport rates with the CERC formula, based on the wave height and shoreline orientation. The different shoreline orientations of the coastal stretch in which each inlet is located explains the difference between Boughaz 1 and Boughaz 2 inlet, with a more oblique approach at Boughaz 2. This is supported by Klein (1986), who performed research on the sedimentation character of the inlets during the 1970s and observed a closure of Boughaz 2 while Boughaz 1 remained open. Later studies by Suez Canal Authority (1983) and Emanuelsson and Mirchi (2007) were both carried out by using the CERC formula, thus covering a stretch of coastline. Notable is the higher transport for Boughaz 1 according to the Suez Canal Authority, this in contrast with the other studies.

Study	**Boughaz 1** (m^3/y)	**Boughaz 2** (m^3/y)	**Direction**	**Location**
Inman (1970)	300 000	500 000	Gross	Inlet
Vinja (1970)	480 000	700 000	Gross	Coastline
Suez Canal Authority (1983) (from Linnersund and Mårtensson (2008))	725 500	415 000	Gross	Coastline
Euroconsult (1995)	500 000	800 000	Gross	Coastline
Emanuelsson and Mirchi (2007)	40 000	258 000	Net East	Coastline

Table 2.5: Littoral drift studies along the North Sinai coastline, results obtained with aerial observations (Inman, 1970) and CERC formula (1984), (Vinja, 1970; Euroconsult, 1995; Emanuelsson and Mirchi, 2007) (Suez Canal Authority, 1983)

A separate study is performed for this thesis with the calculation sheets provided by van Rijn. The results of this study can be found in Table 2.6 and the full table can be found in Section A.1. The table shows the gross littoral drift values for four methods; Kamphuis (1991), Modified Kamphuis (Mil-Homens et al., 2013), CERC Shore Protection Manual (1984), and van Rijn (2013). Notable is the high difference between the methods, this can be due to the fact that CERC disregards the sediment properties and beach slope. van Rijn (2013) concluded that the CERC formula yields results which are too large (factor 2) for storm conditions and significantly too large (factor 5) for low wave conditions. Furthermore, he concluded that the Kamphuis (1991) formula yields results which are slightly too small (factor 1.5) for storm conditions, but too large (factor 3) for low wave conditions. The modified Kamphuis formula (Mil-Homens et al., 2013) also underpredicts for high waves and overpredicts for low waves, but not as much compared to the original formula (van Rijn, 2013).

In relation to the literature the CERC result of Boughaz 2 is in line with earlier findings. Boughaz 1 seems on the higher end, however the value

Method	Boughaz 1 (m^3/y)	Boughaz 2 (m^3/y)	Direction	Location
Kamphuis (1991)	147 100	152 300	Gross	Coastline
CERC (Shore Protection Manual, 1984)	596 800	700 400	Gross	Coastline
Mil-Homens et al. (2013)	101 700	91 300	Gross	Coastline
van Rijn (2013)	220 300	245 000	Gross	Coastline

Table 2.6: Gross transport along the coastline stretches of Boughaz 1 and Boughaz 2 determined using the methods of Kamphuis (1991), Modified Kamphuis (Mil-Homens et al., 2013), CERC (Shore Protection Manual, 1984), and van Rijn (2013)

is smaller compared to the value determined by the Suez Canal Authority (1983). The studies by Kamphuis and van Rijn all predict significantly lower values compared to CERC, which can be explained by the reasons discussed earlier. Smaller littoral drift values favourable for the stability method of Bruun and Gerritsen (1960), discussed in the next section.

It can be concluded that a high variability can be found in the results from both literature and the study conducted for this thesis. Taking into account the general overprediction of the CERC formula, but also the underprediction of the Kamphuis formulas, it is chosen to use the values determined by Inman (1970) for further analysis, since these values form an average between all studies.

2.3 STABILITY OF TIDAL INLETS

Two stability relations have been proposed to describe the stability of a tidal inlet and will be elaborated in this section. The first method by Bruun and Gerritsen (1960) relates the stability to the ratio between the littoral drift and the tidal prism. With this method it is possible to determine the bypassing type of an inlet. The second study by Escoffier (1940) determines the stability of an inlet with the depth averaged equilibrium velocity in relation to the cross-sectional area and the observed depth averaged inlet velocity.

2.3.1 Tidal prism

The tidal prism is defined as the volume of water (excluding any fresh water inflow) that has to flow in and out through an inlet during one tidal cycle (Bosboom and Stive, 2015). The tidal prism can be described as:

$$P = \int_0^{T/2} Q \quad dt$$

In which P is the tidal prism (m^3), T the tidal period (s) and Q the discharge through an inlet (m^3/s). In the case of Bardawil Lagoon two inlets are present in the system, each with a discharge contributing to the tidal prism.

2.3.2 Bruun & Gerritsen

Sediment bypassing is defined as the way sediment is transported from updrift to the downdrift coast of a tidal inlet. Through this process sand is returned to the littoral zone after an interruption on the ebb tidal delta and in the inlet (Van de Kreeke and Brouwer, 2017). The first proposition of bypassing mechanisms was done by Bruun and Gerritsen (1959), who reasoned that the type of bypassing is the combined result of waves and tidal currents. Bruun and Gerritsen (1960) and Bruun (1978) proposed the ratio parameter r to indicate the type of bypassing, which is given by:

$$r = P/M_{tot}$$

In which P is the tidal prism under spring tide conditions (m^3) and M_{tot} the yearly gross littoral drift (m^3). The parameter r expresses the relative influence of the waves/tide at the inlet. Large values of r indicate tide-dominated bypassing (tidal flow bypassing), whilst low r-values indicate wave dominated bypassing mechanisms (bar bypassing) (Bosboom and Stive, 2015). Increasing the value of r results in a greater seaward displacement of inlet bars (Oertel, 1988). In total there are eight bypassing mechanisms categorized of which not all fit the mode of bar bypassing or tidal flow bypassing (FitzGerald et al., 2000). Spit formation will be, besides bar bypassing and tidal flow bypassing, also considered for this research.

$r = P/M_{tot}$	**Stability**	**Bypassing type**	**Dominant process**
$r < 20$	Poor	Bar bypassing	Wave
$20 < r < 50$	Poor	Bar bypassing	Wave/Tide
$50 < r < 150$	Fair to good	Bar and flow bypassing	Tide/Wave
$r > 150$	Good	Flow bypassing	Tide

Table 2.7: Stability parameter conditions with the associated bypassing type and dominant bypassing process (de Vriend et al., 2002)

With **bar bypassing** (r $<$ 50) sediment is directly transferred from the updrift coast to the downdrift coast via the terminal lobe and the swash platform on the ebb delta. The terminal lobe and swash platform act as a bridge over which the sand is transported to the downdrift side, a schematic representation can be found in figure 2.11 (Van de Kreeke and Brouwer, 2017).

During **tidal flow bypassing** (r $>$ 150) sand is transported into the inlet and main ebb channel, partly across the channel margin linear bars, as can be seen in figure 2.11. The ebb tidal currents transport the sediment out of the main ebb channel and deposit it at the far seaward end of the channel, resulting in the formation of swash bars. Swash bars move onshore over the swash platform and can form bar complexes on their way to the beach (Van de Kreeke and Brouwer, 2017).

Spit formation (r $<$ 20) implies that littoral drift is deposited as a sand-spit in front of the inlet, rather than being transferred to the ebb delta (Van de Kreeke and Brouwer, 2017). With an increasing spit both the ebb delta and the inlet move in a downdrift direction, until the spit is breached again at the original location. It is suggested that spit breaching is a result of a washover forced by a storm (Friedrichs et al., 1993).

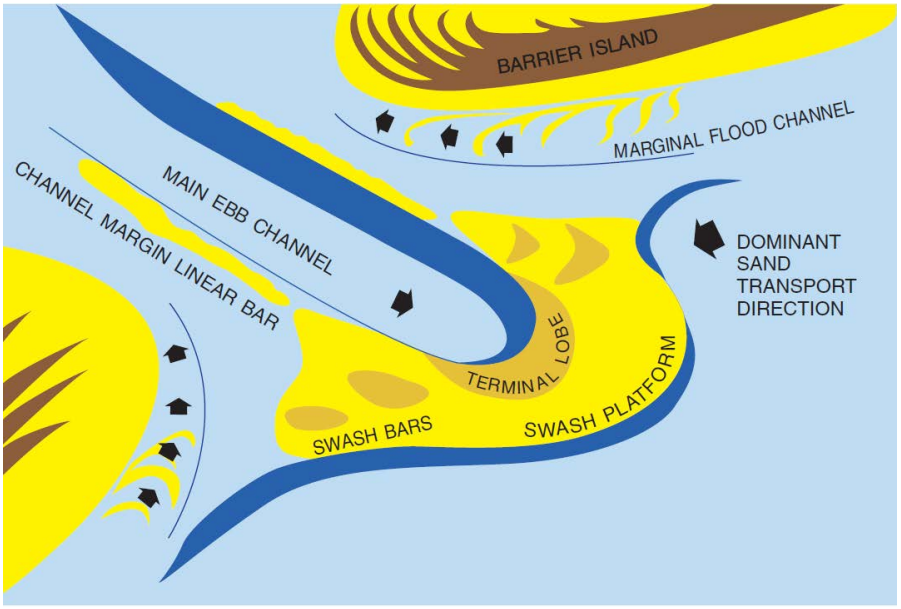

Figure 2.11: Idealized ebb delta, adapted by Van de Kreeke and Brouwer (2017) from Davis & FitzGerald (2004)

2.3.3 Escoffier

Escoffier (1940) model incorporates feedback between hydrodynamics and morphology and can therefore be seen as a morphodynamic model for the entrance of a tidal basin (Bosboom and Stive, 2015). The Escoffier model is described as the balance between the volume of sediment entering and leaving the inlet, assuming average weather conditions (storm events are not included) (Brouwer et al., 2012). The volume entering the inlet is taken as a constant fraction of the littoral drift and the volume leaving the inlet is taken proportional to a power of the ebb tidal velocity amplitude (Van de Kreeke and Robaczewska, 1993). The model describes the latter as the expression for the maximum cross-sectional averaged entrance velocity (u_e [m/s]) for a given estuary or inlet over a tidal cycle, also known as the closure curve. The velocity is related to the tidal prism (P [m^3]), tidal period (T [s]), and inlet cross-sectional area (A [m^2]). The relation can be expressed as:

$$u_e = \frac{\pi P}{AT}$$

The closure curve is depicted as the blue line in Figure 2.12. In the range from point A to C on the curve, the entrance channel is so small that it chokes off the tidal flow so that the tidal difference within the basin will be less than at sea. Increasing the size of the inlet in this situation will thus also result in an increase in velocity. On section C-E of the curve the tidal flow is not choked off any longer, such that the maximum current velocity decreases as the channel becomes larger (Bosboom and Stive, 2015).

The sediment erosion capacity is included as the equilibrium maximum velocity u_{eq}, below which the velocity in the channel is too low to erode sediment and keep the entrance channel open (Bosboom and Stive, 2015). According to Escoffier (1940), this critical velocity is more or less indepen-

dent of the channel geometry and in the study the value is determined to be 0.9 m/s. Later, Bruun (1978) suggested a value of 1.0 m/s, this value will be used in this thesis. Hence, the inlet is in equilibrium if the amplitude of the inlet velocity u_e equals the equilibrium velocity u_{eq}.

The behaviour of a tidal inlet can be predicted by examining the closure curve (blue line) in relation to the equilibrium maximum velocity u_{eq} (red dashed line). If the maximum channel velocity is surpassed by the equilibrium velocity sediments will deposit in the inlet entrance and the channel cross-sectional area will decrease in size. However, if the channel velocity is higher than the equilibrium velocity the sediments inside the inlet will erode and the inlet cross-sectional area will increase in magnitude. Hence, if the inlet is located between A and B, the inlet is too small and the velocity magnitude insufficient to maintain the inlet, thus the inlet will be closed by natural processes. If the inlet cross-sectional area is placed between point D and E, the velocity is also too small and deposition of sediments will take place. However, in this case it results in an increase in velocity; sedimentation will continue until point D is reached. If the inlet is placed between B-D the velocity is exceeding the equilibrium maximum velocity and the inlet will erode until it reaches point D. Hence point D represents a stable equilibrium situation. Point A and B can also be identified as equilibrium points, but are less desired for engineering purposes. Point A represents a full closure of the inlet, making it a stable equilibrium point. Point B is an unstable equilibrium point; inlets with an area close to B will always increase or decrease in size depending on the maximum inlet velocities. For this study it is desired to know the location of the present inlets on the Escoffier curve, as well as the cross-sectional area necessary to migrate the inlet close to point D.

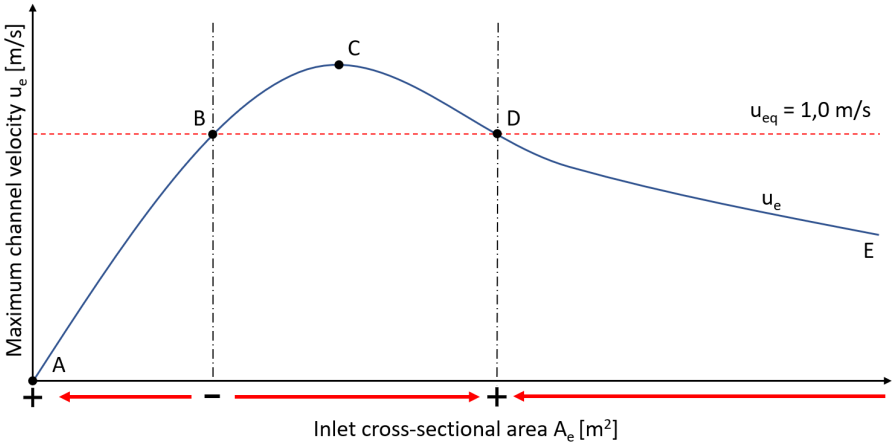

Figure 2.12: Escoffier stability curve indicating equilibrium states of an inlet

Multiple inlets

Back-barrier lagoon systems with multiple inlets capture a smaller or larger part of the tidal prism, depending on the hydraulic efficiency. The cross-sectional stability of the inlet is determined by the fraction of the tidal prism entering the individual inlet. A too small tidal prism fraction results in a closing inlet. This is important to take into account when opening a new inlet, for the new inlet could reduce the tidal prisms of the existing inlets, caus-

ing a probability of unstable inlets which result in closing (Van de Kreeke and Brouwer, 2017).

2.4 RELATED PREVIOUS STUDIES

2.4.1 Lanters

Lanters (2016) related hydrodynamics with fish population in Lake Bardawil. Non-juvenile fishing yield in the lagoon have been reduced dramatically due to a combination of declining fish populations and water quality combined with overfishing. As a response to the declining conditions the fishing effort shifted to juvenile fish, a non-sustainable solution. The report states that according to the research at the Institute for Marine Resources and Ecosystem Studies (IMARES), an increase in fish population in Lake Bardawil can be expected after increasing the tidal prism and decreasing the lagoon salinity.

The research describes four different design phases and their influence on the hydrodynamic conditions. The first phase consists of the revision and extension of the current inlets and the dredging of a new inlet in the far western end of the lake. The second phase consists of the dredging of a channel through the lake between all three inlets. The third phase contains the yearly dredging of channels and the fourth and final phase adds extensive nourishments at the erosion side (Eastern side) of the inlets. Wind was initially excluded for a better understanding of the influence of tidal currents, waves, and sediment properties, and later added to investigate wind driven circulations. A Delft3D Flexible Mesh model was developed to investigate the impact of these adaptations.

The tidal prism and flow velocity changes at several lagoon locations were examined for all phases. A difference in velocities was found in the initial phase between the inlets; Boughaz 1 showing a velocity around 0.7 m/s (both ebb and flood) and Boughaz 2 a value between 0.9 m/s (ebb) and 1.0 m/s (flood). From the differences between ebb and flood velocity it was concluded that the system is sediment importing. After phase 4 the tidal prism results show a possible increase of tidal prism of 400%. Furthermore, differences in sediment size between the Mediterranean Sea and lagoon can stimulate sediment export of the system, but no clear elaboration on this topic is made. From a comparison between the different phases it is concluded that the basin geometry plays a crucial role for changes of water level movement and flow conditions within the basin. Increasing the inlet depth without changing the inner basin geometry shows an increase in tidal prism, but a reduction in flow conditions is still present. However, after dredging channels in the last phase, a significant increase of water levels and flow velocities is observed.

The hydrodynamic response of the aforementioned phases was also examined under the influence of four different wind conditions. The influence of wind in the initial state of the system affects the circulation within the lake, which subsequently affects the ecosystem and the hydrodynamics. With the presence of wind forces, a net water export from the east inlet is observed during the simulation period. Furthermore, it was determined that the tidal prism increases with the influence of the South-West (SW), West (W) and North-North-East (NNE) winds to about 4.5% while a reduction of 3.3%

was found with the west northwest winds (WNW). Lanters (2016) first mentioned the presence of a tidal divide between the two inlets, but no further research is done on the topic.

2.4.2 Georgiou

Georgiou (2019) continued on the work from Lanters (2016). The research aimed to improve the functionality of the Boughaz 1 inlet by mimicking nature in such a way it allows the system to function naturally, without the presence of any hard structures. The dimensions of the Boughaz 2 inlet are kept constant in all simulations.

Three design elements are considered in the research; approach channel, nourishment and the shape of the inlet cross-sectional area. The purpose of the approach channel is to concentrate the tidal energy and wave energy to enhance interaction of water between the two water bodies. The inlet nourishment is intended to increase the water setup through the inlet and also reinforce the coast directly East of the inlet. Lastly, the shape of the cross-sectional area of the inlet can stimulate flow and local deepening of the inlet channel if constructed in the right way. For the classification of all design parameters is referred to the report of Georgiou (2019). The results of the research of Georgiou are obtained using a Delft3D model instead of the Delft3D FM model used by Lanters, this is due to the fact that FM was at the time of the study not yet capable of modelling morphological changes.

For the results of the initial (current state) situation at Bardawil Lagoon, Georgiou found, in contrast to the results of Lanters, higher inlet velocities in Boughaz 1. The results for Boughaz 2 were found to be similar with 0.9 m/s (flood) and 1.0 m/s (ebb). This could be due to the difference in modelling software, or a minor change in bathymetry. A tidal divide was again identified between the two inlets, see Figure 2.13. Here the tidal flow was found to be approximately zero whilst the water level variations of the points inside the lake were found to have the same response, this allows settling of fine materials which are still in suspension.

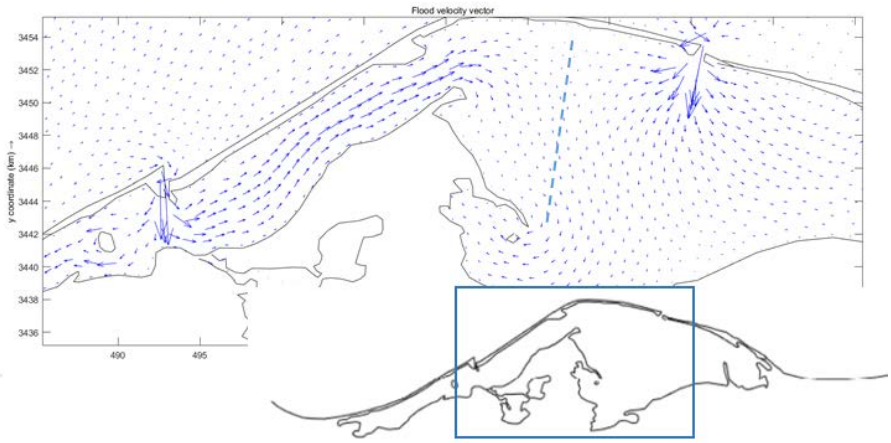

Figure 2.13: Flow velocity magnitude (indicated by arrow size) inside Lake Bardawil, tidal divide indicated with a blue dashed line (Georgiou, 2019)

In the research the three design elements are assessed individually after which the best results of each element were combined in a final design. The chosen design for the inlet cross-sectional area showed a 43% increase in

tidal prism with an area of 2250 m^2. Using the same area for the approach channel in combination with a length of 2400 m and deepening the lagoon itself the tidal prism is increased with an extra 36% on top of the cross-sectional area only design. However, without deepening the lagoon itself only an extra 10% is added to this value. The inlet nourishment did not affect the hydrodynamics of the system significantly and shows only a 2% increase of tidal prism.

The final combined design choice results for a tide only situation in a tidal range increase of 61% compared to the initial situation of the Boughaz 1 inlet. Flow velocities remained in the same order of magnitude (0.81 m/s) but the tidal range increased with 25%. The design is thought not to be affected much by the current wave climate and different sediment properties, showing a maximum tidal prism decrease of only 2.5% during various combinations. This entails that the design methodology that is adapted to a tide dominant system is appropriate.

The ebb-flood delta system created with the model shows a mimic of nature in Boughaz 1. East of the ebb channel a swash bar is formed, which indicates high interaction between waves and tidal currents. Within the inlet and around the inlet nourishment erosion is observed, while limited accretion is observed in the approach channel. It is found that the tidal currents dominate the morphological changes within the inlet system and thus the system can be characterized as tide dominated.

To understand the feasibility of the design methodology, the stability ratio according to Bruun and Gerritsen (1960) is determined during neap, mean and spring tide for two different littoral drift situations. With the initial state only during optimal scenario (low littoral drift, high tide) fair stability ($P/M > 50$) can be reached, otherwise the stability is indicated as poor. The final design classifies mostly as a fairly stable system with bar and tidal bypassing system, which indicates that the entrance bars are still pronounced (de Vriend et al., 2002).

2.5 LIMITATIONS PREVIOUS RELATED STUDIES

The limitations from these two studies should be a guideline for determining a solid approach for this research and should be carefully elaborated for their implications.

First when taking a look at the computational modelling software used in the studies. Both modelling grids used by Lanters (2016) and Georgiou (2019) are relatively coarse compared to the smaller scale processes happening around the inlets. For example, the situation of the present breakwaters is not included in these grids. A finer grid allows for the implementation of such structures and might give a more realistic overview of the bathymetry due to the increased amount of nodes in the grid. Furthermore, looking at the input data the previous studies relied on generic estimates for the sediment size from literature. With new data available a more accurate representation of the sediment distribution and transport can be made. The study of Lanters (2016) investigated the effect of 4 different wind directions and magnitudes, but as described earlier in this chapter a daily wind velocity and magnitude pattern can be observed, which could have significant influence on the functioning of the lagoon.

An error is discovered in the representation of the tidal prism data provided by both Lanters (2016) and Georgiou (2019). In both studies the tidal prism is calculated as the total amount of water entering and leaving the lagoon through an inlet, instead of the amount of water stored in the lagoon during one tidal cycle. In the previous studies the tidal prism value is linked to several conclusions and it is therefore important to reevaluate those findings. Lanters performed calculations on the refresh rate of the lagoon. However, the very limited interaction between several lagoon areas is not further discussed and might be important for the interpretation of the results.

Concerning the stability the method of Bruun and Gerritsen (1960) is used for determining the stability of the inlets. However, an error was found in the calculation of the tidal prism values, which should be half of the values shown in the report of Georgiou (2019). The principle of Escoffier (1940) is discussed in both studies, but the results are not re-evaluated according to this method. The design of an inlet is highly dependent on the position of the inlet on the curve and should therefore be evaluated accordingly. Moreover, the recognised tidal divide is mentioned, but not coupled to further conclusions. The true implication on the stability is still uncertain.

The study done by Lanters provides insight as a rough estimate on the functioning of Bardawil Lagoon and opened the door for further research to be conducted on this topic. The study of Georgiou gave a clear insight in the functioning of Boughaz 1 in the total picture. However, no insight is given in the effect on the total system and the effect of adapting Boughaz 2 as well. A study providing more detailed insight in the functioning of the lagoon including adaptations to both inlets should give a solid overview of the potential of Bardawil Lagoon.

3 METHODOLOGY

The desired result of this study is to show the possibility to transform the present (sediment importing) system towards a stable (sediment exporting) system by adapting one or more of the inlets. This chapter describes the process on how the study is conducted and the results are obtained.

3.1 INTRODUCTION TO THE STUDY

The research is a desk study on the effect of adaptations to the current Bardawil Lagoon system and can roughly be divided into two parts. The first part consists of a hydrodynamic and stability analysis of the three research phases under the influence of the tide, which are elaborated in the next paragraph. The second part will investigate what effect adding a daily wind pattern has on the hydrodynamics, stability, and the interaction with the Mediterranean Sea.
The three research phases are performed as follows:

Phase 0 investigates the present functioning of Bardawil Lagoon, also referred to as the initial situation. The focus lays on quantifying the interaction between the lagoon and the Mediterranean Sea and the functionality of the inlets. This phase forms the base case of the study, all future adaptations will be compared to the results of the analysis of Phase 0.

Phase 1 consists of adaptations to Boughaz 1, the Western inlet of Bardawil Lagoon. The inlet cross-sectional area and approach channel is adapted according to the design parameters provided by Georgiou (2019) and the nourishment according to a design provided by The Weather Makers. A visualization of the adaptations can be found in Figure 3.1. A nourishment will be made on the green area, in addition to the sand supplementation above water a submerged nourishment is attached to this area. The red area indicates the present breakwater and surrounding area, these will be removed in Phase 1. Lastly the design of the inlet and approach channel cross-sectional area is shown, these will be further elaborated later in this chapter.

Phase 2 consists of adaptations to Boughaz 2, the Eastern inlet of Bardawil Lagoon. As is the case with Phase 1, the adaptations to the inlet and approach channel are made according to design parameters provided by Georgiou (2019) and the nourishment from design parameters from The Weather Makers (2016). The adaptations made in Phase 2 are an addition to Phase 1. Thus, in this phase both inlets are adapted according to the new design. A visualization can be found in Figure 3.2, where the nourishments are indicated with green. The to be removed breakwater is indicated with red. The inlet and approach channel cross-sectional area design can be

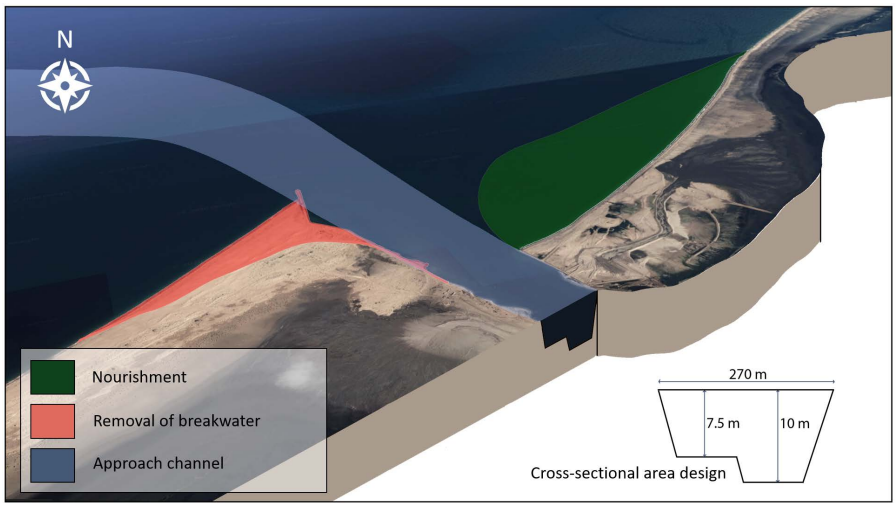

Figure 3.1: The new design of Boughaz 1 applied to the system in Phase 1

found in the bottom right corner of the figure. Details on the design parameters can be found in Section 3.3

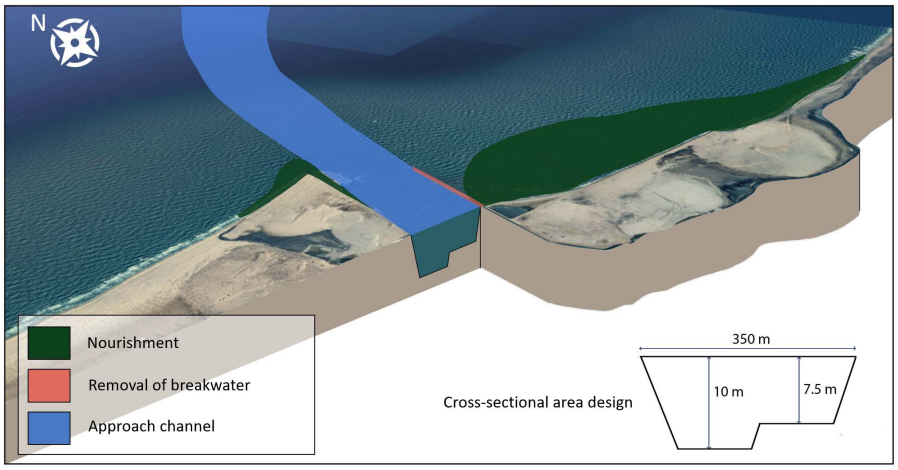

Figure 3.2: The new design of Boughaz 2 applied to the system in Phase 2

After an assessment of the hydrodynamics and stability under tide-only conditions the significance of the present wind climate is investigated. It is known from previous studies that the wind contributes to the circulation patterns inside the lagoon, as well as the interaction with the Mediterranean Sea (Linnersund and Mårtensson, 2008; Lanters, 2016). However, the significance of a daily occurring pattern is yet to be determined. Furthermore, a study is conducted on the flushing of the lagoon. The addition of wind to the system is applied to all three research phases to determine the effect of these phenomena on the hydrodynamics and stability of the inlets. Finally the effect of evaporation inside the lagoon on the hydrodynamic behaviour of the lagoon is determined. The complete research timeline can be found in Figure 3.3

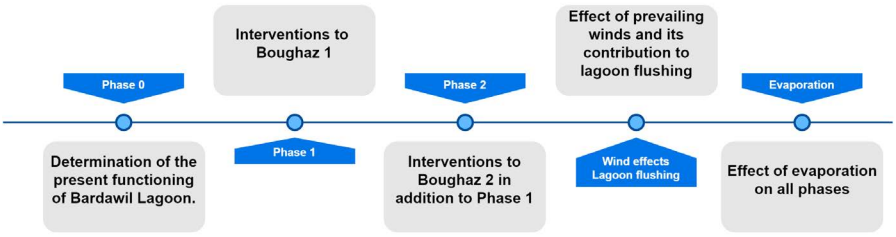

Figure 3.3: Visualization of the research steps conducted in this study

3.2 SYSTEM UNDERSTANDING

The goal of the study is to answer the research questions provided in Chapter 1. Moreover, it is important to determine when the adaptations can be described as successful. Thus, all research steps have to be assessed according to the method described below:

First of all it is determined whether or not the system can be classified as sediment importing or sediment exporting. Sediment transport is induced by waves and currents acting on the sediments at the bottom of Bardawil Lagoon. A tidal basin can be either sediment importing or exporting, depending on the dominant character of the inlet. The maximum flow velocities are determined to give insight in this dominance and in addition to that the sediment transport capacity function is used to give better insight in these processes.

The second goal of the study is to develop a double inlet system in which both inlets are considered dynamically stable. Due to varying tidal conditions and the effect of storms, tidal inlets cannot have one set of stable parameters. To determine the stability it is important to know the position of the inlets on the Escoffier Curve. Due to unknown parameters for determining the shape of the curve it cannot easily be determined where on the curve the present inlets are located. However, by assessing the hydrodynamic parameters the current stability parameter is derived. The maximum inlet velocities provide insight on the position of the vertical axis in the Escoffier plot, which is further elaborated in Section 2.3. In addition to that the rate of interaction between the Mediterranean Sea and Bardawil Lagoon is assessed by determining the difference in tidal amplitude on both sides of the inlet. Finally, the sediment dominance of the inlet is determined to indicate whether or not an inlet is sediment importing or sediment exporting.

Another method used to assess stability is the method described in Bruun and Gerritsen (1960). For the successful application of this method the tidal prism under spring tide conditions is determined for both Boughaz 1 and Boughaz 2. Along with the littoral drift a ratio classifying the stability of the inlet, including the bypassing type, is determined.
Finally, it is important to determine if the interaction between the inlets is significant. Tidal basin systems with multiple inlets can influence each other, possibly causing one of the two inlets to eventually close. Differences in net tidal discharge rates through the inlets are determined to give insight into this interaction, as well as visualising the flow velocities inside the lagoon. It should be noted again that the analysis is restricted to tidal flow through the

inlet and does not include other natural phenomena such as baroclinic circulations, which can also play an important role in determining inlet velocities. Evaporation effects are mentions in the results and further elaborated in the discussion in Chapter 5. A visualization of the important processes governing Bardawil Lagoon can be found in Figure 3.4

From the assessment above the important parameters can be summarized as described below.
The parameters desired for the determination of the sediment transport character of the inlets:

- Maximum and minimum flow velocities in Boughaz 1 and Boughaz 2 for both ebb and flood currents.
- The sediment transport capacity

The parameters desired for the determination of inlet stability:

- The maximum observed flow velocities in both inlets
- The distribution of water level throughout both water bodies
- Both the average and spring tidal prism for both inlets, including ebb and flood prisms
- A representative value for the littoral drift
- The sediment transport dominance of both inlets

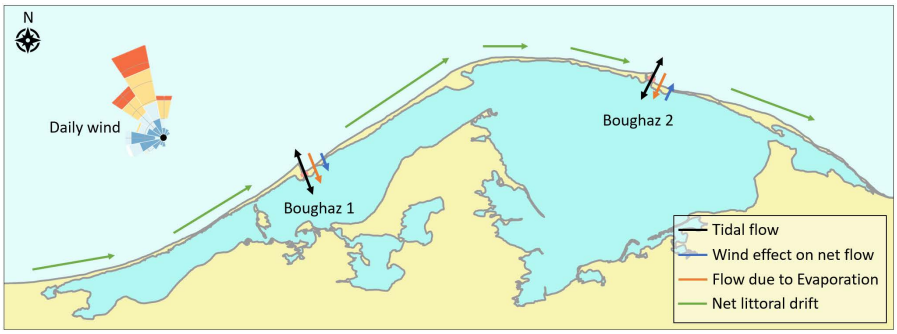

Figure 3.4: Overview of the processes influencing the water exchange at Bardawil Lagoon

3.3 SYSTEM ADAPTATIONS

As described in Chapter 2 a tidal inlet system can be divided into three segments: the ebb tidal delta, the flood tidal delta and the inlet itself. This research focuses on adaptations to the ebb tidal delta and the inlet. The flood tidal delta is not included, because of the goal to investigate natural deepening of the lagoon. This does however not imply it's not useful to propose adaptations to the flood delta, for earlier research shows that deepening of the lagoon does increase the sea-lagoon interactions and enhances the functioning of the approach channel (Georgiou, 2019). Adaptations to the inlet are applied on the inlet cross-sectional area, the ebb tidal delta segment is adapted with the addition of an approach channel. Furthermore, changes are made to the adjacent coastline of the inlet, with the removal of the present breakwaters and the addition of a nourishment on the downdrift eastern side of the inlet. The design elements will be further elaborated below.

3.3.1 Inlet cross-sectional area

The inlet cross-sectional area is directly related to the tidal prism and plays a crucial role in the magnitude of the tidal prism, flow velocities and, subsequently, the functionality of the tidal inlet system (Georgiou, 2019). The cross-sectional area is in equilibrium with the hydrodynamic environment when the volume of sand entering through the inlet equals the volume of sand leaving through the inlet (Van de Kreeke and Brouwer, 2017). This equilibrium is dynamic; the inlet cross-sectional area oscillates around a mean value. For a natural deepening system the inlet is initially (morphologically) out of equilibrium, as the amount of sediment leaving the inlet is desired to surpass the amount entering. However, in time the inlet should be moving to a morphologically dynamically stable inlet.

The inlet cross-sectional areas of both Boughaz 1 and Boughaz 2 are adapted according to the design proposed by Georgiou (2019). Georgiou investigated the hydrodynamic and morphological response of three cross-sectional area shapes, which are depicted in Figure 3.5. From the results of that research it can be concluded that the triangular design (blue dotted line) was the least efficient adaptation to the system. Both the trapezoidal (orange dotted line) and the two depth steps trapezoidal (green dotted line) gave equal promising results with a depth of 10 meters. But by choosing the two depth steps trapezoidal design one can significantly reduce the amount of sediments to be dredged, therefore this design is considered to be the most efficient one. The design is applied on the system on Boughaz 1 (Phase 1) and Boughaz 2 (Phase 2). The inlet cross-sectional parameters for both the initial situation and the inlet adaptations can be found in Table 3.1

3.3.2 Approach channel

The intention of the approach channel design is to concentrate the tidal and wave energy in the channel with the purpose of enhancing the tidal prism and flow velocities through the inlet. From the research of Georgiou (2019) it is determined that an approach channel 90 degrees in the direction of the coastline provides the most promising results, which is therefore implemented in this study. The layout of the approach channel of the research of

Initial	Width [m]	Depth [m]	Area [m^2]
Boughaz 1	270	3-5	954
Boughaz 2	350	3-6	1386
Adapted	**Width [m]**	**Depth [m]**	**Area [m^2]**
Boughaz 1	270	7.5/10	2323
Boughaz 2	350	10/7.5	3221

Table 3.1: The inlet dimensions of the initial situation and the dimensions of the new design applied in Phase 1 and Phase 2

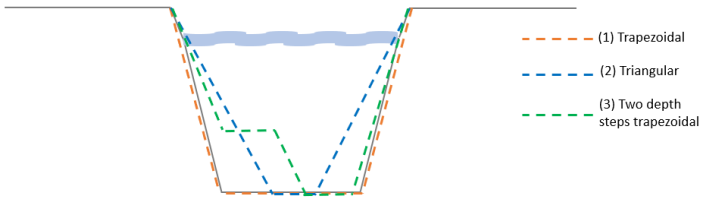

Figure 3.5: The examined cross-sectional area designs by Georgiou (2019)

Georgiou (2019) can be found in Figure 3.6 and the design parameters can be found in Table 3.2.

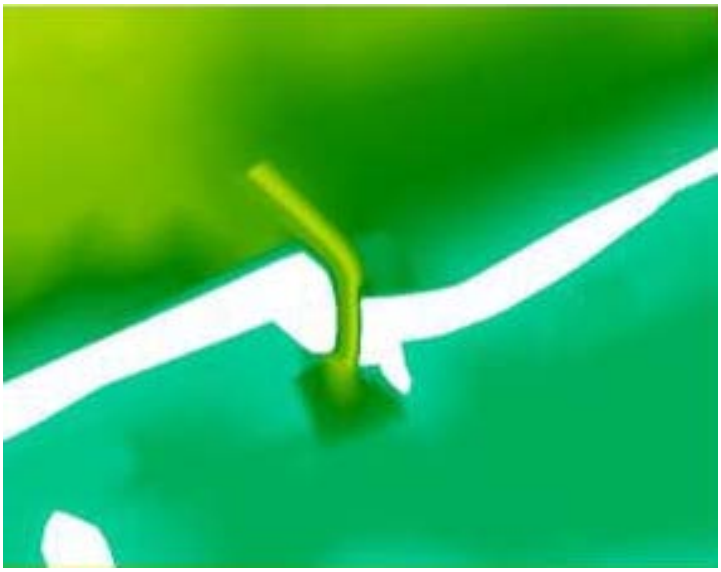

Figure 3.6: The proposed approach channel from the study of Georgiou (2019)

Approach channel	Width [m]	Length [m]	Depth [m]	Orientation to shoreline
Boughaz 1	270	2400	7.5/10	90 degrees
Boughaz 2	350	2400	10/7.5	90 degrees

Table 3.2: The approach channel design parameters applied to the system in Phase 1 and Phase 2

3.3.3 Nourishment and removal of the breakwaters

The addition of a large-scale nourishment with a submerged shoal on the East side of the inlet entrance is thought to have the capability to increase the water set-up near the inlet by catching the incoming tide (The Weather Makers) and thus increase the tidal flow velocities, and reinforce the eroding coastline East of the inlet. These coasts have had a significant lack of sediment input due to the presence of breakwaters, which disturbed the natural sediment transport patterns (Nassar et al., 2018). The nourishment applied in this study is according to design requirements defined by The Weather Makers and can be seen in Figure 3.1 and Figure 3.2. A submerged nourishment is constructed adjacent to the nourishment as seen in the figures. The design of the submerged nourishment can be found in Figure 3.7.

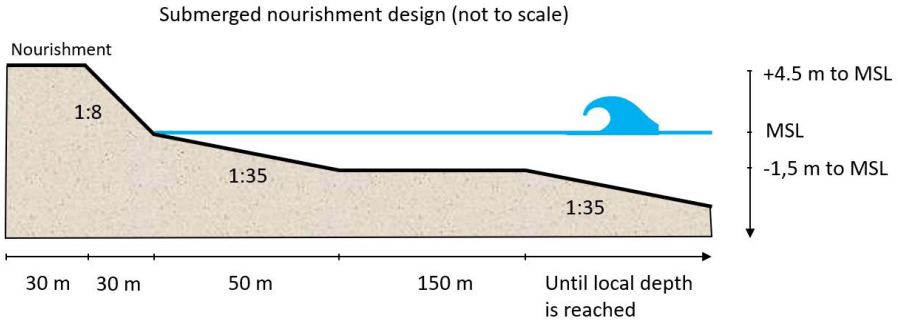

Figure 3.7: Cross-section of the submerged nourishment design applied in the study

The current breakwaters are obstructing the natural ebb and flood currents, causing sedimentation directly behind the inlets, worsening the sediment infilling of the inlets (TWM, 2018). The Weather Makers (2018) proposed a new design for the inlet surroundings at Boughaz 1 and Boughaz 2, which is implemented in this study. The following adaptations to the present situation are made:

- Removal of the current breakwaters
- Dredging the shore at the Western side of the Boughaz 1 in order to enable a smooth incoming tidal current.
- Dredged material will be used for construction of nourishment at East side of inlet

3.4 MODELLING

Design elements are processed using the Delft3D Flexible Mesh (Delft3D FM) numerical model. Delft3D Flexible Mesh Suite is composed of several models, of which D-Flow FM is used for this thesis. D-Flow FM is a multi-dimensional hydrodynamic and transport simulation program which calculates non-steady flow and transport phenomena that result from tidal and meteorological forcing on structured and unstructured boundary fitted grids (Deltares, 2019).

The flexible mesh suite is chosen above the longer available Delft3D-FLOW module for several reasons. First of all the flexible mesh allows for

the use of unstructured grids: large regions with quadrangles can be coupled with much greater freedom compared to the Delft3D-FLOW model. The Bardawil Lagoon system represent a large area for which only certain points desire high accuracy, other lagoon areas can be represented by larger grid cells. Therefore, by applying the finer grids only locally, much shorter calculation times are achieved for the same accuracy of certain points of interest. Another advantage is the use of dynamic time-step limitation which is automatically set based on the Courant criterion, the model adapts to larger time-steps when possible, further reducing calculation time.

3.4.1 Model setup

The D-Flow model is used for determining the hydrodynamic response of the system after implementing the proposed adaptations. All simulations will be performed on a 48 day timescale, allowing sufficient time for the model spin-up time. The results obtained will be averaged over a full tide cycle.

Grid

The main grid used for this research can be found in Figure 3.8. The outer North and West boundaries of the grid are adopted from the grid of Lanters (2016), while the more detailed grid area close to the lagoon is constructed newly for this study. While many adaptations are made compared to the grids used by Lanters (2016) and Georgiou (2019), two main differences stand out. First of all, the shape of the inlets was inaccurately implemented in previous studies, disregarding the breakwaters and the distinct shape of the inlets. Moreover, a higher accuracy is achieved in the latest grid, accurately acquiring the hydrodynamic data for both Boughaz 1 and Boughaz 2, see Figure 3.9 and Figure 3.10. The size of the grid cells varies from 4500 m offshore and 25 m in the inlets.

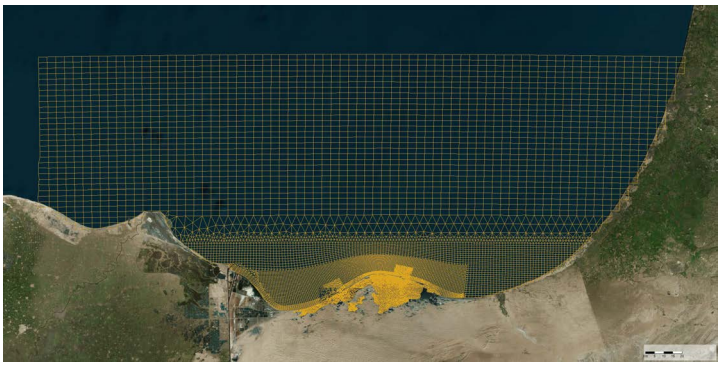

Figure 3.8: The Delft3D FM grid used for the model simulations in Phase 0

The implementation of the nourishment is clearly visible in Figure 3.9 and Figure 3.10.

Bathymetry

In line with the previous studies no recent bathymetric data is available covering the whole of Bardawil Lagoon. The most up-to-date bathymetric data on the nearshore of the lagoon is acquired from a 2011 map, based on data originating from 1856 (Section A.2). The inner lagoon bathymetry is

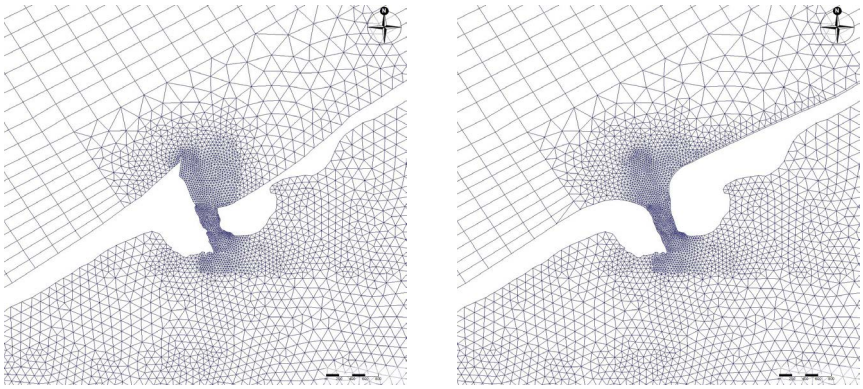

Figure 3.9: The local grid constructed for Boughaz 1 in Phase 0 (left) and after the adaptations in Phase 1 (right)

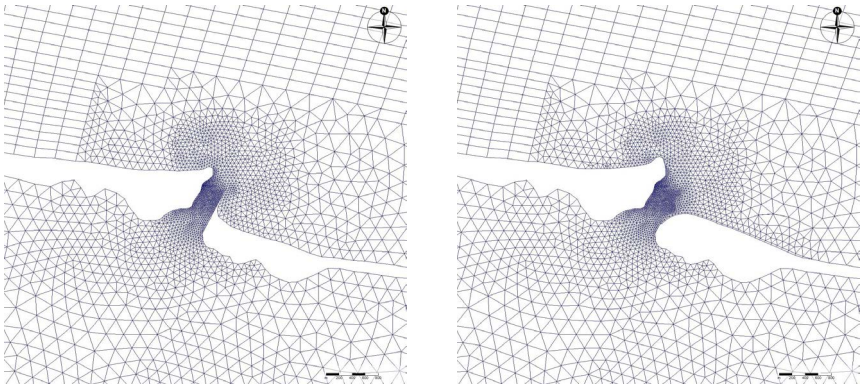

Figure 3.10: The local grid constructed for Boughaz 2 in Phase 0 (left) and after the adaptations in Phase 2 (right)

derived from a previous study conducted by Linnersund and Mårtensson (2008) which can be found in Section A.2. The bathymetry implemented in the model can be found in Figure 3.11

In addition to the bathymetric data used by the previous studies, a recent study from 2017 provides a detailed bathymetric map of Boughaz 2 (Appendix A.2). This allows for a more accurate representation of the lagoon and a more reliable hydrodynamic study.

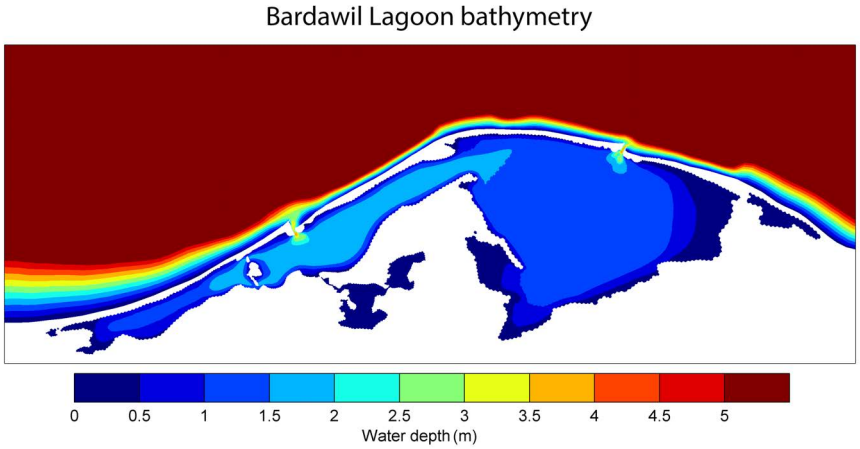

Figure 3.11: The bathymetry of Bardawil Lagoon, relative to MSL, used in this study

4 RESULTS

This chapter will describe the processes affecting the Bardawil Lagoon hydrodynamics and morphodynamics based on the D-Flow results for the initial lagoon situation, Phase 0, and the situations in which a new design is implemented on the inlets in Phase 1 (Boughaz 1 adapted) and Phase 2 (Boughaz 1 and 2 adapted).

4.1 PHASE 0 – THE INITIAL SITUATION

Before any adaptations to the Bardawil Lagoon system can be analysed it is important to properly evaluate the current system.

4.1.1 Processes

Hydrodynamics

Hydrodynamics play an important role in tidal basin morphology. Therefore, proper qualification of the hydrodynamic observations forms the basis for further conclusions. Figure 4.1 shows the maximum (a) and minimum (b) observed tidal elevation during the simulation period of 2 months. What stands out immediately is the significant elevation difference between the Mediterranean Sea and Bardawil Lagoon. The offshore tidal range exceeds 0.4 meter, while in the inner basin the tidal range is less than half of that. A minor difference in elevation between the Boughaz 1 area and Boughaz 2 area is observed.

If we take a closer look at the tidal elevation at specific points, an interesting trend is visible. Figure 4.1 (c) shows the water level elevation for seven observation points located between Boughaz 1 (Blue) and Boughaz 2 (Red), as well as the offshore elevation. The specific location of the observations points can be found in Figure 4.1 (d). The color gradient indicates the respective position of the observation point to Boughaz 1. Two observations can be made from this figure: the observation points inside the lagoon show no significant difference in maximum and minimum elevation, and the tidal range becomes more out of phase for observation points further away from the inlets inside the lagoon with respect to the offshore tidal range.

Furthermore, insight is gained in tidal elevation inside the two inlets compared to an offshore and inner basin elevation, see Figure 4.3 and Figure 4.2, the latter shows the location of the observation points. As is the case with the maximum elevation map, a clear difference between the inside and outside of the basin can be observed in the plot. The offshore elevation curve coincides with the negative elevation of Boughaz 1, but the positive elevation of Boughaz 1 is only half the offshore value. Boughaz 2 is significantly lower, both the negative and positive elevation, and almost completely lacks a positive elevation. A closer look shows a higher harmonic on the positive

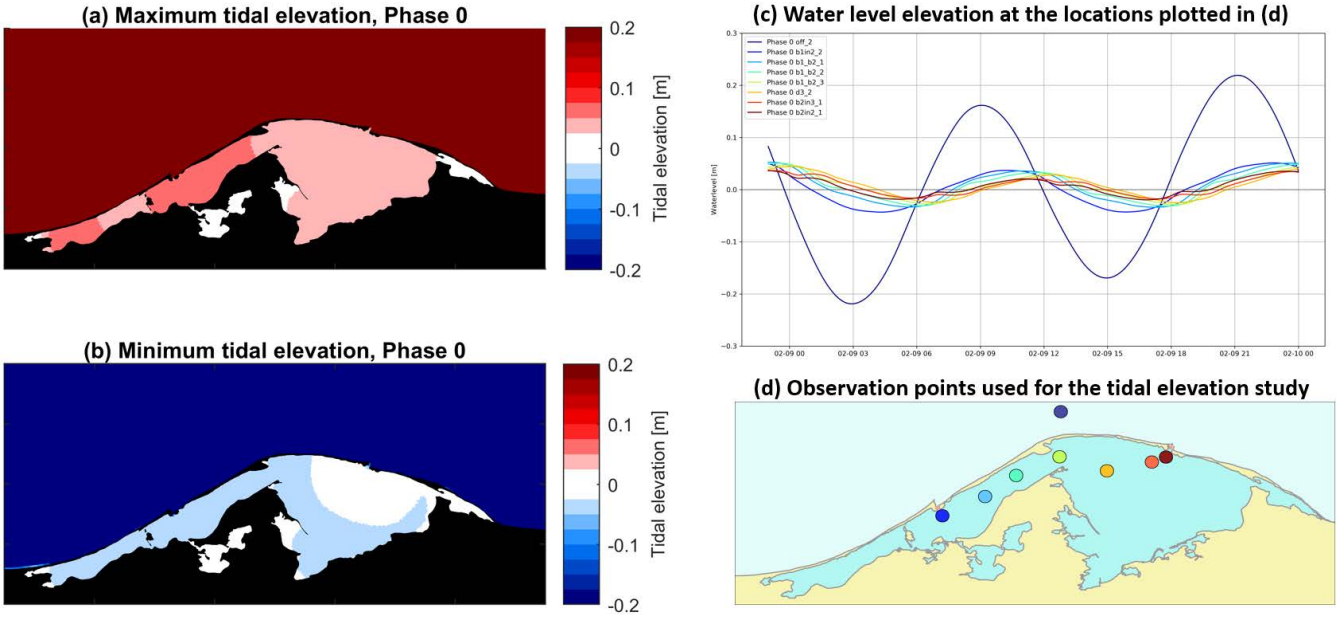

Figure 4.1: Tidal elevation of Phase 0 with: (a) Maximum and (b) minimum tidal elevation over the modelling period during spring tide conditions for the initial situation, (c) the water level elevation through the lake plotted for the observation points in (d)

elevation of Boughaz 2. A phase difference can be observed for all observation points in the lagoon, especially the inner basin point, which is more than 90 degrees out of phase.

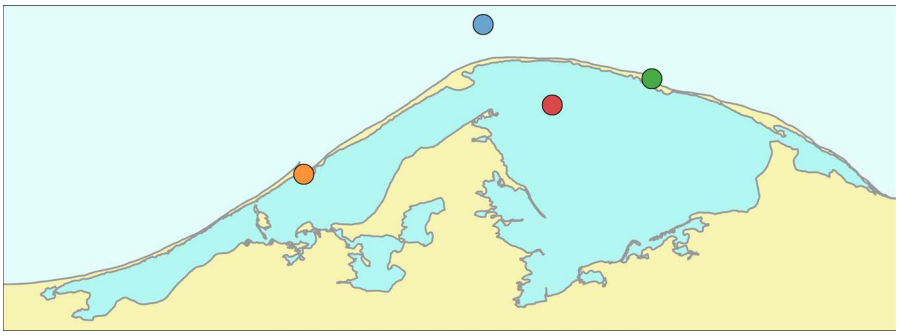

Figure 4.2: Observation points offshore, inside the inlets and inside the lagoon used in Figure 4.3 below, the color coincides with the respective line in this figure

Variations in inlet water elevation are expected to be visible in the shape of the inlet velocity over time as well. If we look at Figure 4.4, no clear disturbance is observed in the velocity signal where the water level signal is distorted. Furthermore, like with the water elevation, a difference in velocity magnitude can be observed between the ebb velocity and flood velocity for Boughaz 1 and Boughaz 2, as well as a difference in velocity magnitude between the two. If we look at the velocity distribution in the total Bardawil system, a divide between the two inlets is visible, see Figure 4.5. The figure shows the observed absolute maximum flow velocities over the simulation period. From Figure 4.4 we know the inlet velocities exceed 0.5 m/s, but for a better insight into the velocities inside the lagoon the boundary is set at

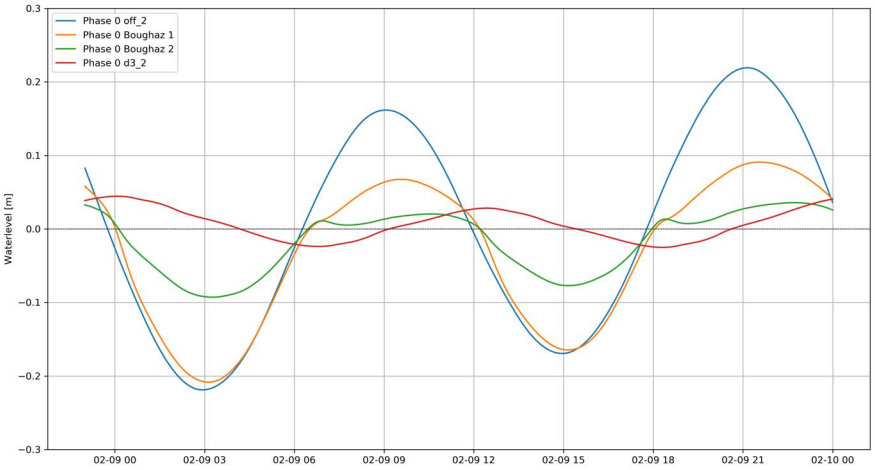

Figure 4.3: Water level elevation at four observation points (offshore, blue; Boughaz 1, orange; Boughaz 2, green; between the inlets, red)

0.5 m/s. The reach of the horizontal tide is visible in the lagoon and an area without much action can be observed further away from the inlets.

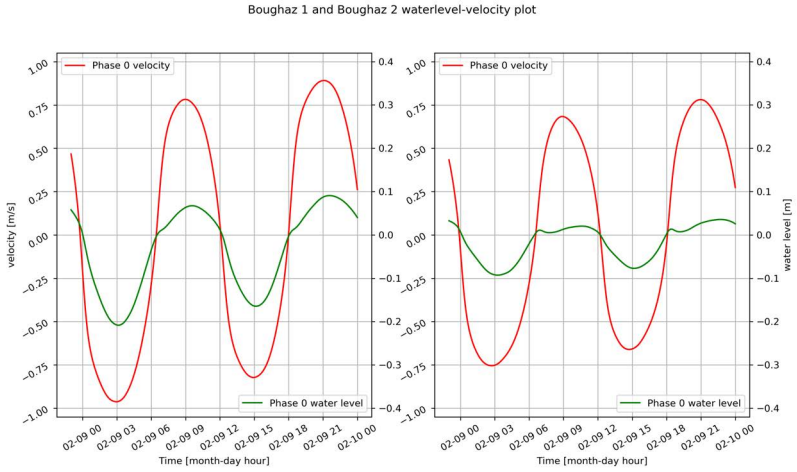

Figure 4.4: Water level and depth averaged velocity plots for Boughaz 1 (left) and Boughaz 2 (right)

Observations of the maximum current velocity data provided by Table 4.1 show a maximum ebb velocity of 0.96 m/s and a flood velocity of 0.91 m/s for Boughaz 1, indicating a 0.05 m/s difference in favor of the ebb current. Boughaz 2 however, shows a 0.04 m/s difference in favor of the flood current.

The flow velocities show ebb dominance for Boughaz 1 and flood dominance for Boughaz 2. However, due to the fact that sediments do not react linearly to the flow velocity, but with the power n, the tidally averaged transport is determined by calculating the (flood and ebb) tide averaged sediment transport capacity of the flow velocities observed in the inlets, see Table 4.2. Along with the maximum current velocities in the previous table the transport capacity shows for Boughaz 1 a net transport in ebb direction and for Boughaz 2 a net transport in flood direction.

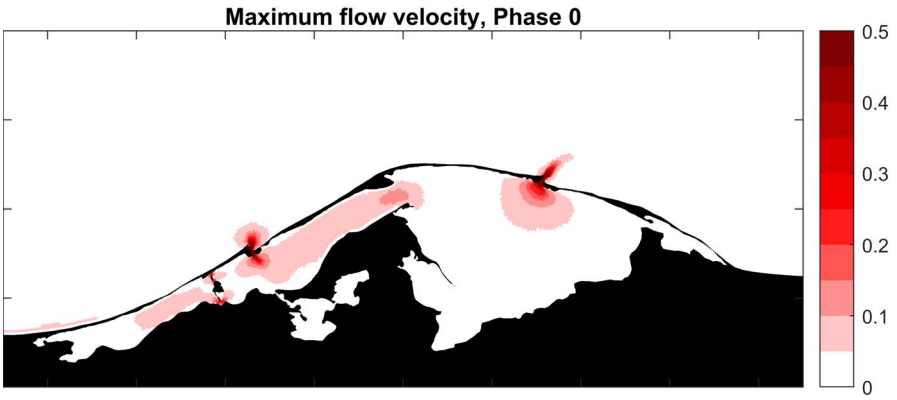

Figure 4.5: The maximum flow velocities during the simulation period for spring tide conditions in m/s. Legend limited to 0.5 m/s, inlet velocities exceed this value, as can be found in Table 4.1

	Max u ebb [m/s]	Max u flood [m/s]
Boughaz 1 (Phase 0)	0.96	0.91
Boughaz 2 (Phase 0)	0.75	0.79

Table 4.1: The maximum velocities during ebb and flood flow for Boughaz 1 and Boughaz 2

Tidal Prism

The tidal prism is determined cross-sectional discharge of both inlets and results in the data presented in Table 4.3. Boughaz 2 has a tidal prism of about 13 million cubic meters per cycle which accounts for 55% of the total volume entering and leaving the lagoon during one tidal cycle, 45% flows through Boughaz 1. The average flood and ebb prism for both inlets are very close, with only a 1.5% net difference for Boughaz 1 and 1% net difference for Boughaz 2.

The hydraulic processes dominating Bardawil Lagoon in Phase 0 are visualized in Figure 4.6. Inhere the black arrow represents the tide averaged tidal prism, the orange arrow the net evaporation effect during daytime and the blue arrow the net transport between the inlets. The direction of the arrow indicates the net direction of the flow. From this map it is clear that for the initial situation without wind, a flow of water can be observed from Boughaz 2 to Boughaz 1. However, this flow only consists of just over 1% of the volume entering the lagoon in a tidal cycle from the model results. It should be noted that the effects of net flow due to evaporation is not included in these interactions, an elaboration of evaporation effects can be found in Section 5.1.

Interpretation of the results

The significant difference between inner and outer basin water amplitude suggests that the inflow and outflow of the basin is limited by the inlets. Compared to the offshore amplitude, the amplitudes observed inside the lagoon are significantly damped, while no distinct difference is observed between the inner lagoon points. The elevation difference between the Boughaz 1 area and Boughaz 2 area is thought to be the result of the limited capacity of the inlets, with Boughaz 2 being more limited in its water ex-

Phase	Boughaz 1 Net transport 10^{-3} $[m^3/s]$	Boughaz 2 Net transport 10^{-3} $[m^3/s]$	System Net transport 10^{-3} $[m^3/s]$	System Dominant transport
0	-6.19	1.28	-4.91	Ebb

Table 4.2: The sediment transport capacity per inlet for Phase 0 with their dominant transport direction

	Phase	Tide averaged prism $[m^3]$	Spring tidal prism $[m^3]$	Net flow $[m^3/\text{cycle}]$	% of total
Boughaz 1	Phase 0	10 425 000	15 370 000	-160 000	45%
Boughaz 2	Phase 0	12 874 000	18 833 000	151 000	55%
Total	Phase 0	23 299 000	34 202 000	-9000	-

Table 4.3: The tidal prism for Phase 0 for both inlets and the total system. Net flow is defined as the flood flow minus the ebb flow.

change. The tidal range observed in the inlets also shows a high distortion in relation to the offshore amplitude. A closer look at the inlet water elevation shows a higher harmonic on the positive elevation curve of Boughaz 2, possibly a result of basin geometry. A phase difference can be observed for all observation points in the lagoon, especially the inner basin points, which are more than 90 degrees out of phase. This indicates a significant restriction on tidal propagation into the deeper lagoon areas due to friction and/or reflection and the lower wave celerity resulting from the shallowness of the lagoon. The high flow velocity values are all concentrated around the inlets and no significant velocity values are observed inside the lagoon. Hence, it is assumed that there is no connection between the two inlets velocity wise, and thus that the inlets act as two separate basins.
A system can be classified as either importing or exporting, depending on the dominance of the inlets. Ebb dominance results in a sediment exporting system while flood dominance results in a sediment importing system. Based on the maximum current velocity data provided by Table 4.1 it is indicated that for the initial system Boughaz 1 is sediment exporting and Boughaz 2 is sediment importing for coarse sediments, although the magnitude of the velocities is quite similar. The transport capacity can give more insight in the transport patterns, indicating ebb dominance for Boughaz 1. The differences in ebb and flood transport capacity for Boughaz 2 are more equal, but indicating sediment import.

4.1.2 Stability

Connecting the processes discussed in this section so far allows for some conclusions to be drawn about the stability of the present inlets. As described before, the Escoffier closure curve consists of two equilibrium points: a stable and unstable point, see Figure 2.12. Both points are indicated on the location where the equilibrium velocity curve and closure curve intersect. A constant approximated value of 1.0 m/s proposed by Bruun (1978) is used for the analytical approach for determining the current stability of the system.

The large difference between the inner and outer tidal elevation suggests the inlets are nowhere near the stable equilibrium point. A significant difference between the water elevation on both sides of the inlets suggests a

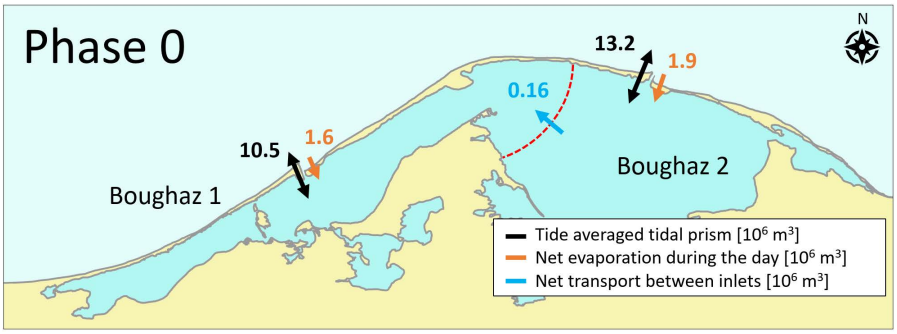

Figure 4.6: Overview of the hydraulic processes present in the Bardawil Lagoon inlet system in Phase 0

value on the left side of the peak of the Escoffier curve. The maximum depth averaged flow velocities in both inlets Table 4.1 can be an indication of the position of the inlets in respect to the equilibrium velocity curve along with the cross-sectional area of the inlet (Table 4.4). The inlet velocities of Boughaz 1 are between 0.9 and 1.0 m/s, in the same order of magnitude as the equilibrium velocity. The fact that Boughaz 1 is considered sediment exporting suggests the inlet is going towards a stable equilibrium, however the effect of evaporation is not yet included in this result. Taking into account the high distortion of tidal elevation, Boughaz 1 is assumed to be near the unstable equilibrium point, which is supported by the sensitivity analysis, see Figure 4.7 and Section B.1. Boughaz 2, on the contrary, is sediment importing and has inlet velocities in the range of 0.7 m/s. These are well below the equilibrium velocity, which supports, in combination with the limited water exchange, the assumption that the Boughaz 2 inlet is on the left of the unstable equilibrium point, thus eventually resulting in a closure of the inlet. This is again supported by the sensitivity analysis in Section B.1. Without interventions the inlet will keep accumulating sediments and reduce its size until it eventually closes.

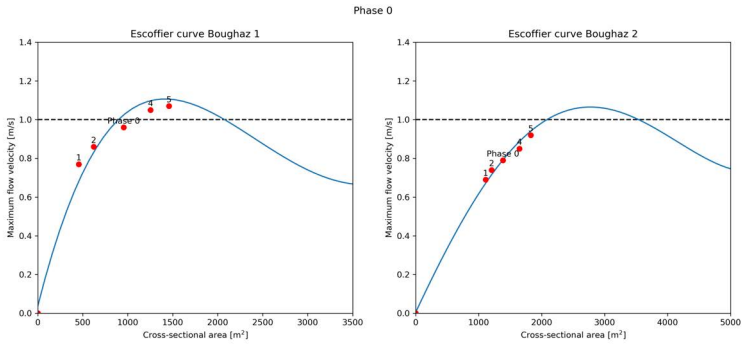

Figure 4.7: The Escoffier curve for Boughaz 1 (left) and Boughaz 2 (right). The closure curve is indicated by the blue line and the equilibrium velocity by the horizontal dashed line. Phase 0 indicates the location of the inlet on the curve, point 1, 2 ,4, 5 are the results of the sensitivity analysis, which can be found in Section B.1

Referring to the theory explained in Section 2.3 the inlets can also be assessed according to the method of Bruun and Gerritsen (1960). Following this method, the stability of the current system varies per inlet, see Table 4.5.

	Maximum velocity $[m/s]$	Cross-sectional area $[m^2]$
Boughaz 1	0.96	954
Boughaz 2	0.79	1386

Table 4.4: The maximum inlet velocity and inlet cross-sectional area used for determining the Escoffier curve

Boughaz 1 has a fair stability, but is only just exceeding the requirement of not being poor, indicating a bar bypassing system both dominated by waves and tide. Boughaz 2, however, has a poor stability and is mainly dominated by waves for its bypassing mechanism. Both inlets are still far away from a stability value exceeding 150.

	Spring Prism $[m^3]$	Littoral Drift $[m^3]$	r [-]	Bypassing type	Stability
Boughaz 1	15 370 000	300 000	51	Bar bypassing	Fair
Boughaz 2	18 833 000	500 000	37	Bar bypassing	Poor

Table 4.5: Inlet stability parameter and bypassing type according to Bruun and Gerritsen (1960)

4.2 PHASE 1 – BOUGHAZ 1 ADAPTED

As described in Chapter 3 phase 1 describes the situation in which Boughaz 1 is adapted according to the design requirements stated in this chapter. The results can be found below.

4.2.1 Processes

Increasing the inlet cross-sectional area and the implementation of the approach channel and nourishment at the Boughaz 1 inlet now shows a similar minimum and maximum tidal elevation at the Mediterranean Sea and the lagoon, see figure Figure 4.8 (a) and (b). The area directly behind Boughaz 1 shows a maximum elevation which coincides with the offshore elevation, a significant difference in relation to the initial situation in Phase 0. A similar trend is visible for the minimum elevation, although the minimum elevation 'intrusion' is smaller in this case. For the whole lagoon area an increase in both positive and negative tidal elevation is visible, but the increase of minimum and maximum elevation at the western side of the islands in the west is limited compared to the change visible east of these islands.

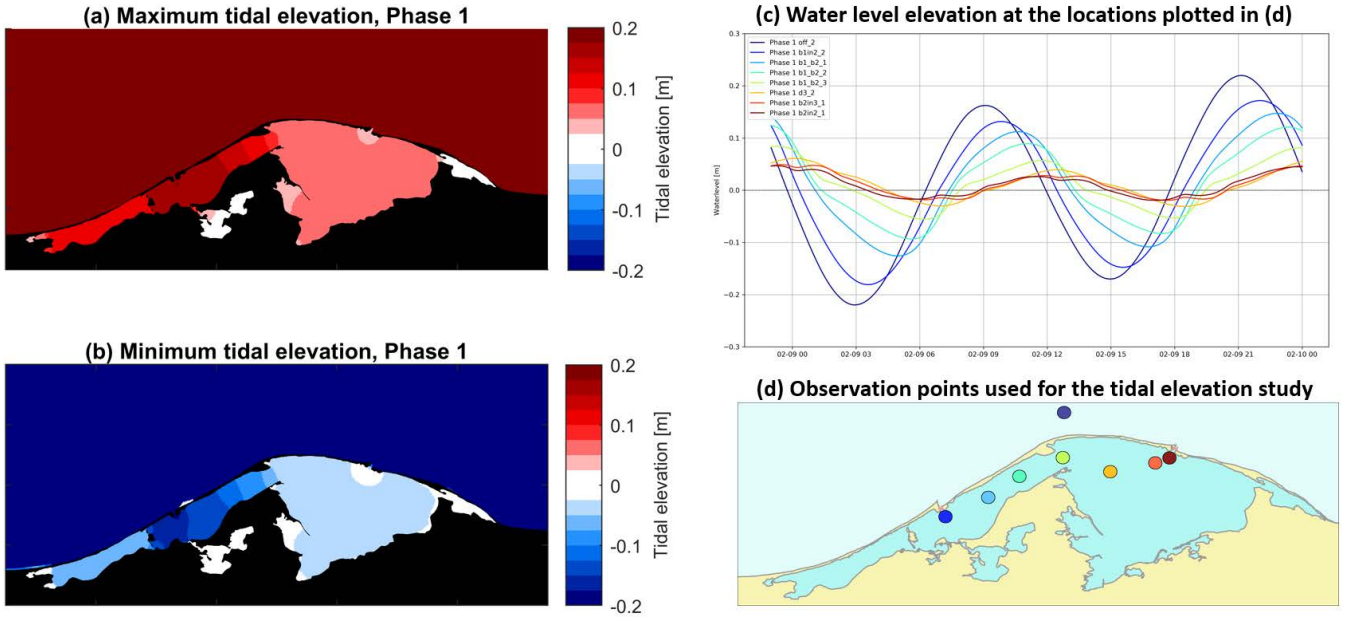

Figure 4.8: Tidal elevation of Phase 1 with: (a) Maximum and (b) minimum tidal elevation over the modelling period during spring tide conditions for the initial situation, (c) the water level elevation through the lake plotted for the observation points in (d)

The change to the system is visible throughout the observation points in the lagoon. The initial situation showed no difference in amplitude for the observation points in the lagoon, but if we take a look at Figure 4.8 (c) a different trend is visible. The observation points close to Boughaz 1 show a curve similar to the offshore amplitude, with a small phase difference visible. Moving further away from this point towards Boughaz 2 each point decreases in amplitude, with the smallest amplitudes observed near the Boughaz 2 inlet. The two red lines representing the tidal elevation near

Boughaz 2 show a disturbed curve, presumably the effect of the tidal wave progressing from Boughaz 1.

If we compare the tidal amplitudes in the inlets to the offshore amplitude and the amplitude inside the lagoon a similar trend is visible. Where for the initial situation only the negative elevation matched the offshore amplitude, for the adapted situation the positive elevation coincides with the offshore amplitude as well. No significant change is visible for Boughaz 2, which is still highly damped. An increase for the inner lagoon observation point is present, presumably the result of more water flowing in from Boughaz 1.

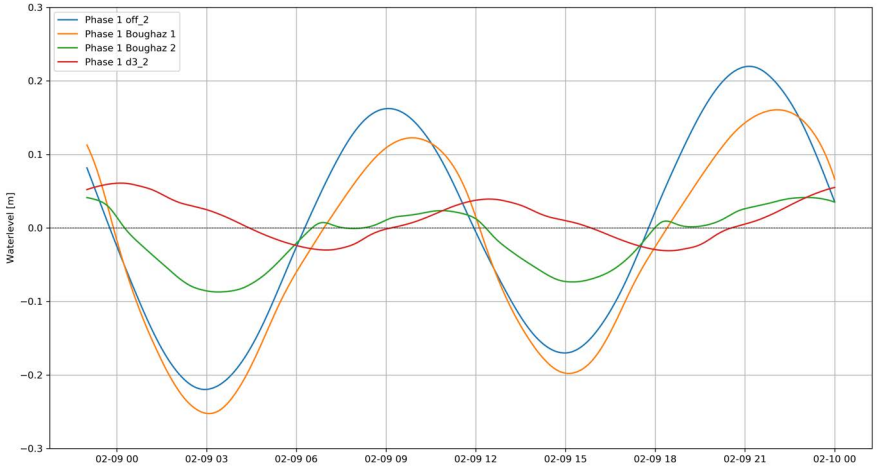

Figure 4.9: Water level elevation at four observation points (offshore, blue; Boughaz 1, orange; Boughaz 2, green; between the inlets, red)

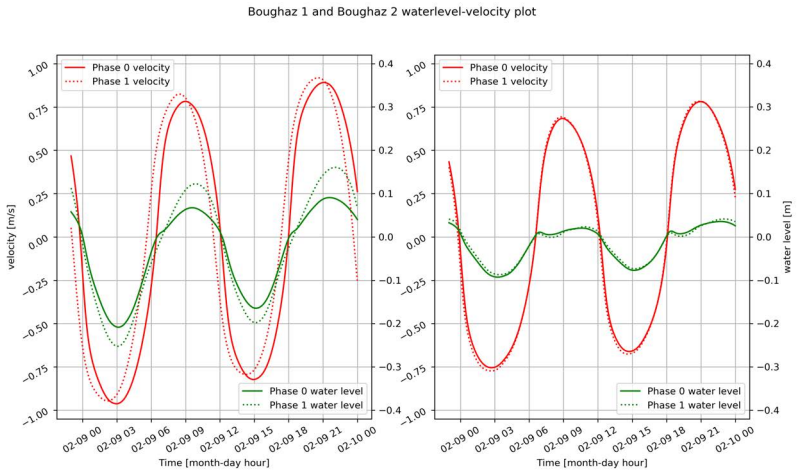

Figure 4.10: Water level and depth averaged velocity plots for Boughaz 1 (left) and Boughaz 2 (right) for Phase 1

Figure 4.10 displays the velocity and water level for Phase 0 (solid line) and phase 1 (dotted line). Increasing the cross-sectional area of Boughaz 1 to 2323 m^2 does not result in significant velocity changes. A minimal increase in flood velocity is present, but the ebb velocity is reduced by the same amount. However, a shift in phase can be observed for the velocity peak, reaching its peak earlier. As expected from the previous figures, the

magnitude of the flood water levels almost doubled and the ebb magnitude increases as well. No significant changes are observed for Boughaz 2.

While the inlet velocities show similar values compared to Phase 0, the velocities inside the lagoon show a significant growth (Figure 4.11. Especially the narrower part of the lagoon (the bottleneck) shows velocities nearing the sediment transport threshold. The flow velocities of the Boughaz 1 and 2 area do connect for Phase 1.

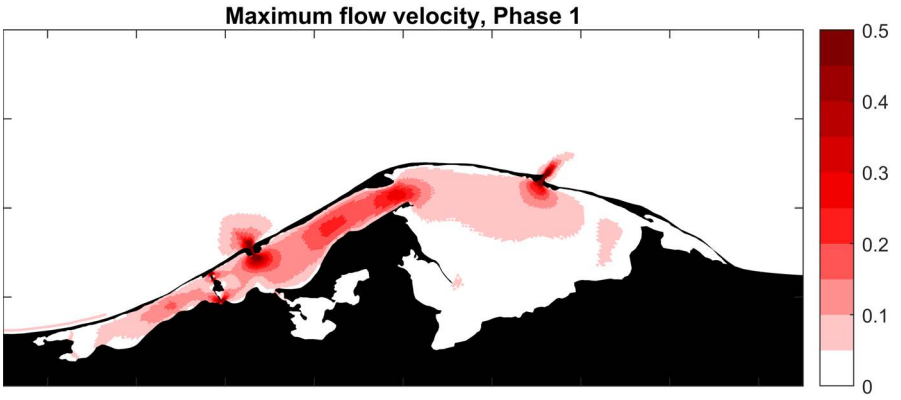

Figure 4.11: The maximum flow velocities during the simulation period for spring tide conditions in m/s. Legend limited to 0.5 m/s, inlet velocities exceed this value, as can be found in Table 4.6

The observed inlet velocities are presented in Table 4.6. The max ebb and flood velocity for both inlets differs only 0.02 m/s, a reduced value compared to Phase 0.

	Max u ebb [m/s]	Max u flood [m/s]
Boughaz 1 (Phase 0)	0.96	0.91
Boughaz 1 (Phase 1)	0.95	0.93
Boughaz 2 (Phase 0)	0.75	0.79
Boughaz 2 (Phase 1)	0.77	0.79

Table 4.6: The maximum velocities during ebb and flood flow for Boughaz 1 and Boughaz 2 for Phase 0 and Phase 1

The smaller difference observed between the maximum flow velocities is also visible in the sediment transport capacity calculations, see Table 4.7. The ebb transport at Boughaz 1 is still exceeding the flood capacity, but by a smaller margin. In contrast to the observed maximum velocities, Boughaz 2 shows a different pattern regarding the dominant transport direction, which is now in favor of the ebb current. But, like Boughaz 1, only by a small margin. The effect of evaporation is not shown in these results, for more insight in evaporation effects on the sediment transport capacity is referred to Section 5.1.

Increasing the size of Boughaz 1 leads to an increase of tidal prism of 224% for this inlet (Table 4.8). Adapting Boughaz 1 does not lead to significant change at the other inlet, which grows by just 2%. However, it does result in a switch of net transport for both inlets, of about 450.000 m^3 per tidal cycle. The net transport for Boughaz 1 accounts for 1.3% of the specific prism and Boughaz 2 has a net flow of 3%. While these values are still very

Phase	Boughaz 1 Net transport 10^{-3} $[m^3/s]$	Boughaz 2 Net transport 10^{-3} $[m^3/s]$	System Net transport 10^{-3} $[m^3/s]$	System Dominant transport
0	-6.19	1.28	-4.91	Ebb
1	-1.29	-0.72	-2.02	Ebb

Table 4.7: The transport capacity per inlet for Phase 0 and Phase 1 with their dominant transport direction

small compared to the total prism, they show a small increase in interaction between the inlets.

	Phase	Tide averaged prism $[m^3]$	Spring tidal prism $[m^3]$	Net flow $[m^3/\text{cycle}]$	% of total
Boughaz 1	Phase 0	10 425 000	15 370 000	-160 000	45%
	Phase 1	23 529 000	36 263 000	301 000	64%
Boughaz 2	Phase 0	12 874 000	18 833 000	151 000	55%
	Phase 1	13 174 000	19 277 000	-311 000	36%
Total	Phase 0	23 299 000	34 202 000	-9000	-
	Phase 1	36 552 000	55 540 000	-10000	-

Table 4.8: The tidal prism for Phase 0 and Phase 1 for both inlets and the total system. Net flow is defined as the flood flow minus the ebb flow, a positive value thus indicates import

A visualization of the hydraulic processes governing the system can be found in Figure 4.12. The figure shows the change in net transport direction, which is now from Boughaz 1 to Boughaz 2. The gray arrow shows the value and magnitude of the tidal prism in Phase 0.

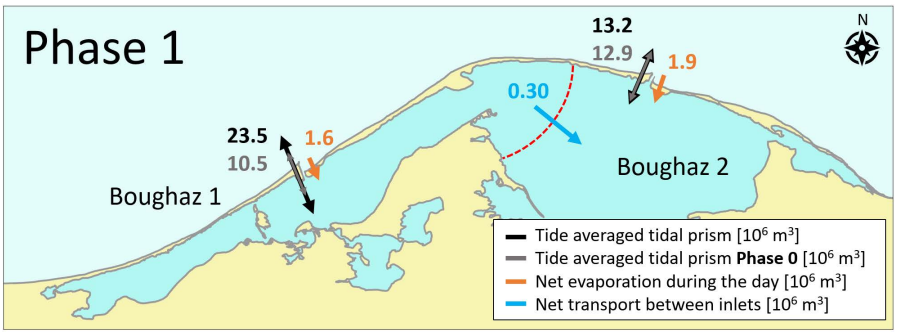

Figure 4.12: Overview of the hydraulic processes present in the Bardawil Lagoon inlet system in Phase 1

Interpretation of the results

Adapting the Boughaz 1 inlet significantly increases the water exchange between the inlet and the Mediterranean Sea. The maximum elevation inside the Boughaz 1 area follows for a large part the offshore amplitude, but the islands in the west are limiting the water exchange to the most western part of the lagoon (Figure 4.8). Although a phase difference between the offshore amplitude and the amplitude of the inner basin observation points is still observed, the variation is less compared to the initial situation. This indicates that friction has a reduced influence on the tidal progression. Combining the results it can be concluded that the inlet is no longer the limiting factor at the Boughaz 1 area. Taking a look at the flow velocity map in Figure 4.11

a connection between Boughaz 1 and 2 is visible but this value is considered too small (<0.1 m/s) for significant exchange of water.

Unlike the initial situation, no ebb or flood dominance can be determined for Phase 1 according to the maximum flow velocities. The difference of 0.02 m/s for both inlets between ebb and flood velocity is considered too small to draw clear conclusions. Also the transport capacity cannot give a solid answer, but Boughaz 1 tends to be more ebb dominant.

4.2.2 Stability

Starting with Boughaz 1, the high minimum and maximum tidal elevation near the inlet inside the lagoon suggest that the inlet is no longer the limiting factor for water trying to enter the system. The inlet velocities for both ebb and flood are approaching 1, the theoretical value of the equilibrium velocity curve proposed by Bruun (1978). To summarize these findings on the closure curve it is suggested that after the adaptations the inlet is close to the stable equilibrium point (Figure 4.13 and Table 4.9), this is supported by the sensitivity analysis in Section B.1. Boughaz 2 however, is still significantly limited by the inlet and experiences little of the changes made to Boughaz 1. A small increase in ebb velocity is observed, but nothing to transfer the inlet from closing on its own to a stable equilibrium.

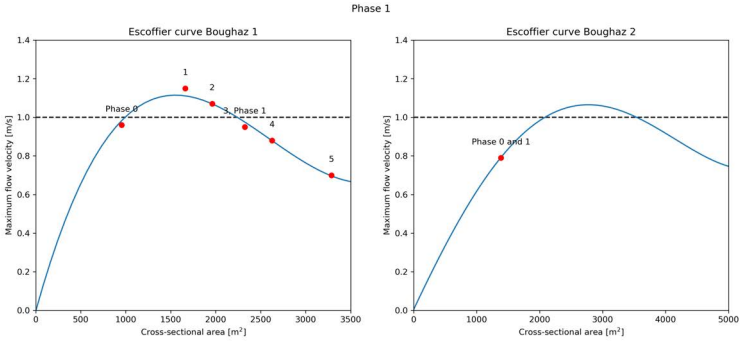

Figure 4.13: The Escoffier curve for Boughaz 1 (left) and Boughaz 2 (right). The closure curve is indicated by the blue line and the equilibrium velocity by the red dashed line. Phase 1 indicates the location of the inlet on the curve, point 1, 2 ,4, 5 are the results of the sensitivity analysis, which can be found in Section B.1

	Maximum velocity $[m/s]$	Cross-sectional area $[m^2]$
Boughaz 1	0.95	2323
Boughaz 2	0.79	1386

Table 4.9: The maximum inlet velocity and inlet cross-sectional area used for determining the Escoffier curve for Phase 1

Looking at the stability values resulting from the Bruun and Gerritsen method in Table 4.10, we can conclude that the stability of Boughaz 1 is significantly improved in Phase 1. It can be classified as fair and the bypassing type is transferring to flow bypassing, more dominated by the tidal currents. No changes are observed for Boughaz 2.

	Spring Prism [m^3]	Littoral Drift [m^3]	r [-]	Bypassing type	Stability
Boughaz 1	38 534 000	300 000	128	Bar bypassing	Fair
Boughaz 2	19 361 000	500 000	39	Bar bypassing	Poor

Table 4.10: Inlet stability parameter and bypassing type according to Bruun and Gerritsen (1960) for Phase 1

4.3 PHASE 2 – BOUGHAZ 1 AND 2 ADAPTED

Phase 2 describes the situation in which both Boughaz 1 and 2 are adapted according to the design requirements stated in this section. The results can be found below.

4.3.1 Processes

As expected, after adapting the second inlet (Boughaz 2) the maximum tidal elevation in the Boughaz 2 area significantly increases, see Figure 4.14 (a), (b), and (c). Except for the hard to reach places, the whole basin has at least a maximum elevation of half the offshore tide. However, low values for the minimum tidal elevation are still concentrated around the inlets, especially for Boughaz 2. The adaptations do not result in significant changes around the Boughaz 1 area compared to Phase 1.

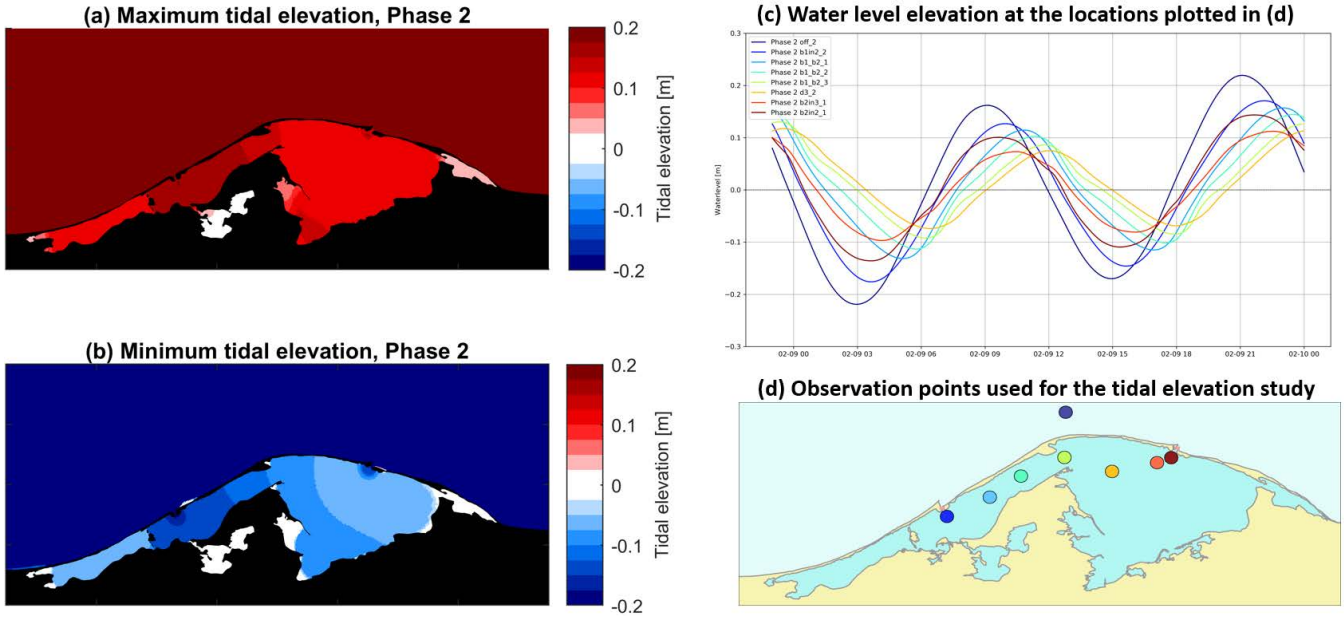

Figure 4.14: Tidal elevation of Phase 2 with: (a) Maximum and (b) minimum tidal elevation over the modelling period during spring tide conditions for the initial situation, (c) the water level elevation through the lake plotted for the observation points in (d)

Interesting to see is the change in water elevation through the lake after adapting Boughaz 2, see Figure 4.14 (c). While for point b1_b2_2, b1_b2_3 a small increase in elevation is visible, point d3_2, b2in3_1 and b2in2_1 show a significant increase in elevation and a complete change in phase, but for some point the elevation is still just half of the potential. A similar trend is visible if we take a closer look at the inlets, of which a full comparison of

the elevation in both inlets can be found Figure 4.15. The higher harmonics in Boughaz 2 disappear after the adaptations and both the positive and negative elevation more than double.

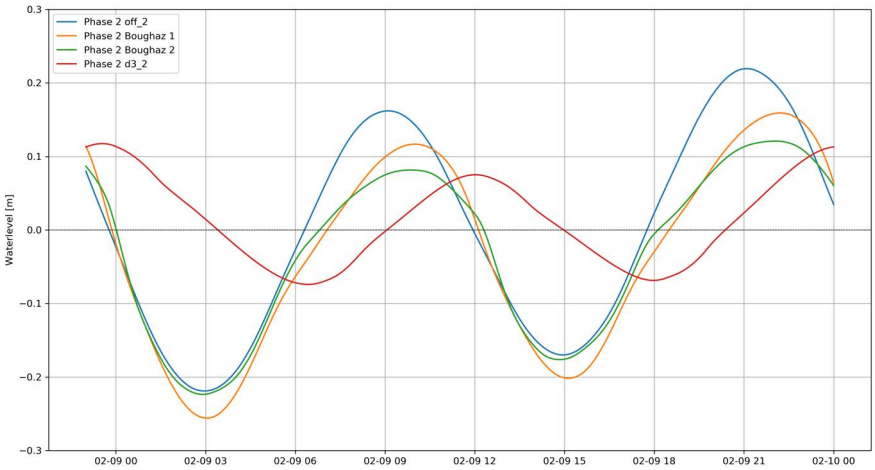

Figure 4.15: Water level elevation at four observation points (offshore, blue; Boughaz 1, orange; Boughaz 2, green; between the inlets, red) during Phase 2

The inlet velocity and water level are again compared in Figure 4.16. The adaptations result in a small increase in inlet velocity for Boughaz 1, but no significant changes are observed. Boughaz 2 experiences a major increase in both velocity and water level, with the velocity now 1 m/s for both ebb and flood. A slight phase difference is notable for Boughaz 2, but not as large as the changes affecting Boughaz 1 in Phase 1.

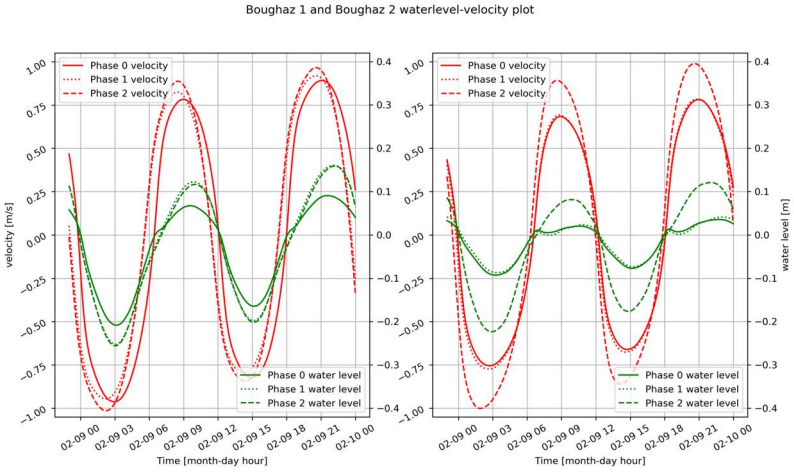

Figure 4.16: Water level and depth averaged velocity plots for Boughaz 1 (left) and Boughaz 2 (right) for Phase 2

If we take a closer look at the velocity distribution through the lagoon a significant increase near Boughaz 2 is visible (Figure 4.17. Although the velocity in the whole Boughaz 2 area increases, the velocity magnitude between the inlets is still minimal.

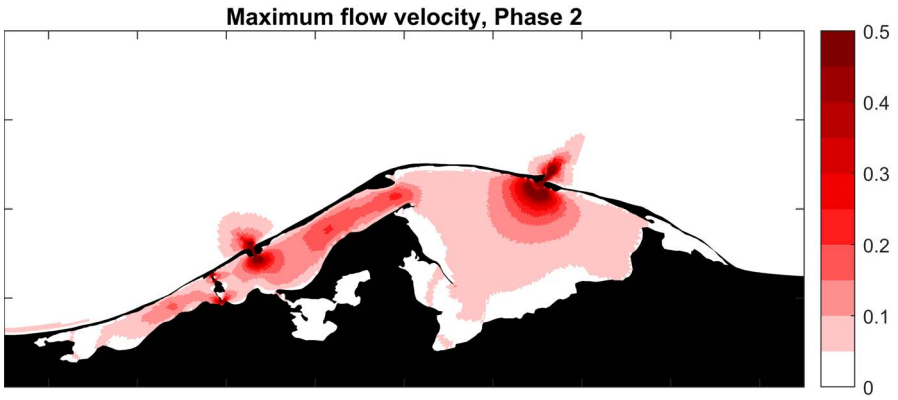

Figure 4.17: The maximum flow velocities during the simulation period for spring tide conditions in m/s. Legend limited to 0.5 m/s, inlet velocities exceed this value, as can be found in Table 4.11

According to the observations shown in Table 4.11, the velocities in Boughaz 2 are 25% higher compared to phase 0 and 1, but there is no difference in the maximum ebb and flood velocity.

	Max u ebb [m/s]	Max u flood [m/s]
Boughaz 1 (Phase 0)	0.96	0.91
Boughaz 1 (Phase 1)	0.95	0.93
Boughaz 1 (Phase 2)	1.01	0.98
Boughaz 2 (Phase 0)	0.75	0.79
Boughaz 2 (Phase 1)	0.77	0.79
Boughaz 2 (Phase 2)	1.00	1.00

Table 4.11: The maximum velocities during ebb and flood flow for Boughaz 1 and Boughaz 2 during all 3 phases.

The significant change in observed velocity at Boughaz 2 is also visible in the transport capacity, see Table 4.12. The net transport capacity of Boughaz 2 more than doubles in Phase 2 and is still characterised as ebb dominant. The net transport of Boughaz 1 also shows a positive effect in de ebb direction, increasing the outward transport with a factor 2. However, the evaporation effects are still not included and will be further discussed in Section 5.1.

Phase	Boughaz 1 Net transport 10^{-3} $[m^3/s]$	Boughaz 2 Net transport 10^{-3} $[m^3/s]$	System Net transport 10^{-3} $[m^3/s]$	System Dominant transport
0	-6.19	1.28	-4.91	Ebb
1	-1.29	-0.72	-2.02	Ebb
2	-2.96	-1.70	-4.66	Ebb

Table 4.12: The transport capacity per inlet for Phase 0, Phase 1, and Phase 2 with their dominant transport direction

The new design of Boughaz 2 results in a significant increase in tidal prism for the inlet, increasing from 13 million to 37 million m^3 per cycle. It seems the extra water flowing in through the inlet counters the flow incoming from Boughaz 1. Where for phase 1 a net flow of around 300000 m^3 per cycle was observed, after phase 2 only about 20% of this exchange remains.

With this situation the net flow through Boughaz 2 is reduced to 0.2%. A visualization of the hydraulic processes governing the system can be found in Figure 4.18

	Phase	Tide averaged prism [m^3]	Spring tidal prism [m^3]	Net flow [m^3/cycle]	% of total
Boughaz 1	Phase 0	10 425 000	15 370 000	-160 000	45%
	Phase 1	23 529 000	36 263 000	301 000	64%
	Phase 2	25 199 000	38 623 000	51 000	40%
Boughaz 2	Phase 0	12 874 000	18 833 000	151 000	55%
	Phase 1	13 174 000	19 277 000	-311 000	36%
	Phase 2	37 363 000	55 137 000	-76 000	60%
Total	Phase 0	23 299 000	34 202 000	-9000	-
	Phase 1	36 552 000	55 540 000	-10000	-
	Phase 2	62 562 000	93 760 000	-25 000	-

Table 4.13: The tidal prism for the first three phases for both inlets and the total system. Net flow is defined as the flood flow minus the ebb flow.

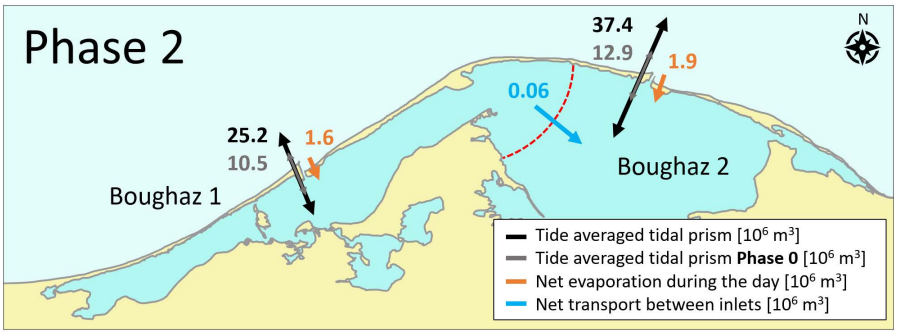

Figure 4.18: Overview of the hydraulic processes present in the Bardawil Lagoon inlet system in Phase 2

Interpretation of the results

The deepening of Boughaz 2 in addition to the deepening of Boughaz 1 leads to an increase in flow velocities through the inlet into the lagoon. The lagoon area at the inlets shows an increase in both minimum and maximum elevation, although the minimum tidal elevation values are still very much concentrated around the inlet. This can either be the effect of bottom topography, or the inlet is still limiting the exchange with the Mediterranean Sea. The observation points inside the lagoon all show a significant difference compared to Phase 0, but a difference in both amplitude and phase is still visible compared to the offshore observation point. This indicates that by opening the inlets the tidal wave celerity increases and the effect of friction on the tidal propagation through the lagoon is significantly reduced. Where Phase 1 showed a more distinct interaction between the inlets, no such thing is present in Phase 2. The net flow from Boughaz 1 to Boughaz 2 accounts for only 0.2% of the total prism, hence the inlets in Phase 2 can be considered as separate basins for these simulations. While the net flow difference between inflow and outflow increases to almost half of the Boughaz 1 inflow, it only accounts for 0.04% of the total average basin prism.

The maximum depth averaged ebb and flood velocities show interesting values. For Boughaz 1 an increase in both values is observed with 0.95 to

1.01 for ebb velocity and 0.93 to 0.98 for flood velocity, these values still tend towards ebb dominance. Boughaz 2 shows for both the ebb and flood velocity a value of 1.00 m/s, indicating an equilibrium position regarding the dominance of the inlet. The transport capacity values give a more distinct difference compared to these maximum flow velocities, especially for Boughaz 2, which is considered ebb dominant looking at the transport capacity and neutral velocity wise. Thus, after Phase 2 both Boughaz 1 and Boughaz 2 can be classified as ebb dominant inlets.

4.3.2 Stability

Increasing the inlet cross-section area of Boughaz 2 positively influences the stability of the inlet. Where the first two phases the hydrodynamics were indicating an unstable equilibrium situation on the closure curve, phase 2 results in maximum ebb and flood velocities indicating a situation close to an equilibrium point (Figure 4.19 and Table 4.14. This is supported by the sensitivity analysis in Section B.1. However, the absence of difference between the inlet velocities does not allow for characterizing a dominance for ebb or flood. The tidal elevation just inside of the basin is not yet approaching the offshore elevation, this is assumed to be the result of the quickly reducing basin depth influencing the incoming tide. Boughaz 1 experiences an increase in inlet velocities, bringing them close to the theoretical 1 m/s of the intersection between the equilibrium velocity and closure curve.

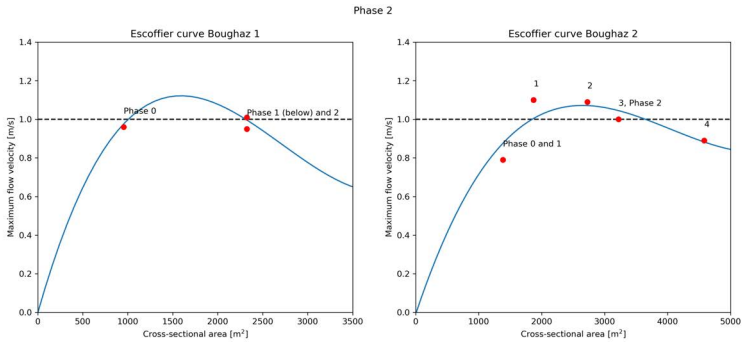

Figure 4.19: The Escoffier curve for Boughaz 1 (left) and Boughaz 2 (right). The closure curve is indicated by the blue line and the equilibrium velocity by the red dashed line. Phase 2 indicates the location of the inlet on the curve, point 1, 2 ,4, 5 are the results of the sensitivity analysis, which can be found in Section B.1

	Maximum velocity $[m/s]$	Cross-sectional area $[m^2]$
Boughaz 1	1.01	2323
Boughaz 2	1.00	3221

Table 4.14: The maximum inlet velocity and inlet cross-sectional area used for determining the Escoffier curve for Phase 2

The stability value of Bruun and Gerritsen shows a positive change for Boughaz 2 (Table 4.15), where the inlet is now considered to have a fair stability while experiencing bar and flow bypassing. The whole system is now moving towards a tide dominated system. The adaptations have no significant influence on the stability of Boughaz 1.

	Spring Prism [m^3]	Littoral Drift [m^3]	r [-]	Bypassing type	Stability
Boughaz 1	38 623 000	300 000	128	Bar bypassing	Fair
Boughaz 2	55 137 000	500 000	110	Bar bypassing	Fair

Table 4.15: Inlet stability parameter and bypassing type according to Bruun and Gerritsen (1960) for Phase 1

4.4 WIND EFFECTS

The daily wind pattern discussed in Chapter 2 might have significant influence on the behaviour of the lagoon. As described in this section the wind blows from the West in the morning, shifting to a North-West to North wind in the afternoon. This section elaborates the contribution of the wind on the system compared to the tide only cases discussed in the previous section.

4.4.1 Processes

Some changes can be observed when looking at the wind effect on the tidal elevations throughout Bardawil Lagoon. Almost all of the lagoon shows a maximum elevation in the same range, with a smaller elevation near Boughaz 2 and a higher elevation at the South-Eastern parts due to wind set-up, as can be seen in Figure 4.20. The effect of the wind set-up is also visible in the minimum tidal elevation, where the values are reduced due to this phenomenon.

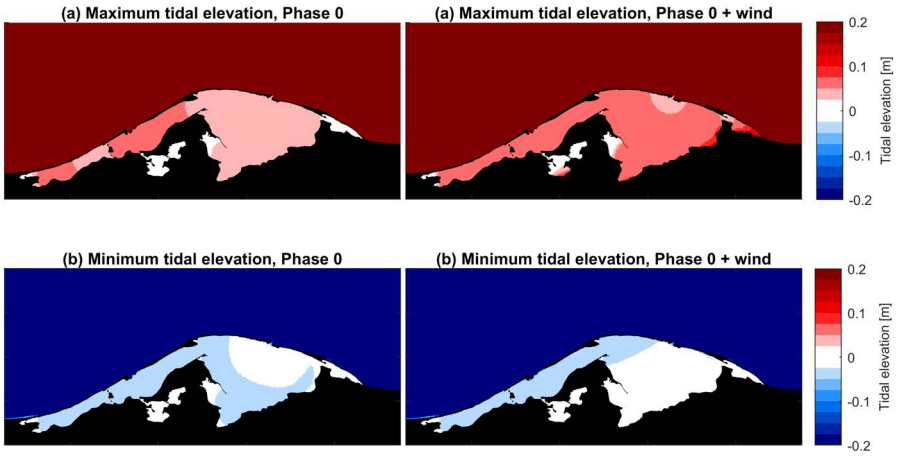

Figure 4.20: Maximum and minimum elevation plots for the situation without (left) and with (right) a daily wind pattern added to the model for Phase 0

A similar pattern can be observed for Phase 1 and Phase 2 for their respective situation without and with wind. The dominant West to North-Western winds cause a set-up at the South-Eastern borders of the lagoon, showing a rise in elevation for both the maximum and minimum tidal elevation plots. Phase 1 and Phase 2 are both characterised by a rise in elevation directly behind Boughaz 1 and east of the bottleneck due to wind set-up. A reduced elevation in most other lagoon areas is observed, as can be seen in Figure 4.21 and Figure 4.22.

Figure 4.23 depicts the effect of wind on the maximum observed flow velocities in (and around) the lagoon. Notable is the significant effect outside the lagoon, where in the initial situation no velocity above the 0.05

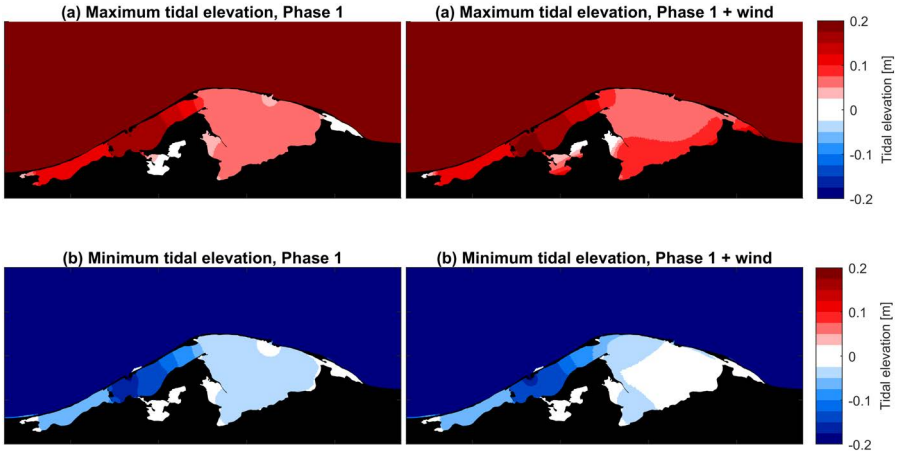

Figure 4.21: Maximum and minimum elevation plots for the situation without (left) and with (right) a daily wind pattern added to the model for Phase 1

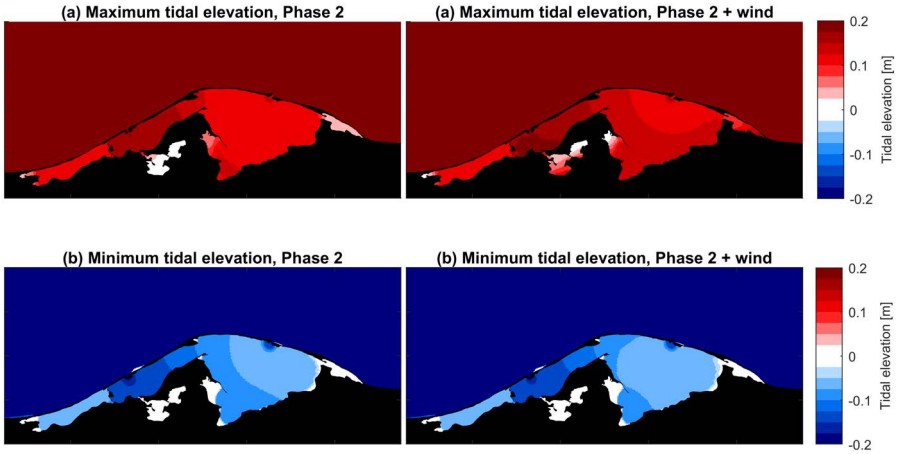

Figure 4.22: Maximum and minimum elevation plots for the situation without (left) and with (right) a daily wind pattern added to the model for Phase 2

m/s threshold is observed. Inside the lagoon an increase of velocity can be observed around the barrier island near Boughaz 2, at the bottleneck, and between Boughaz 1 and the small islands in the west. The maximum velocity plot for the initial situation shows no connection between the Boughaz 1 and Boughaz 2 area.

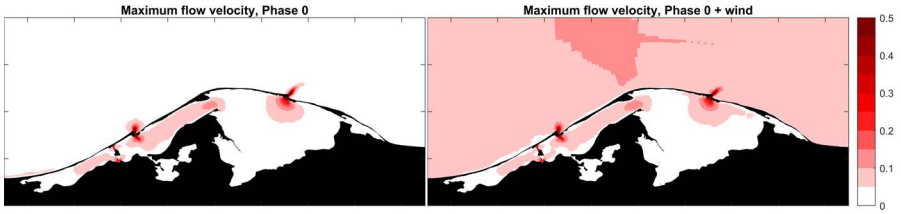

Figure 4.23: The maximum flow velocities during the simulation period of Phase 0 for spring tide conditions in m/s. The left image depicts the situation without wind, the right image with wind added to the model. Legend limited to 0.5 m/s, inlet velocities exceed this value.

Phase 1 (Figure 4.24) and 2 (Figure 4.25) show a similar increase of velocity outside of the lagoon. Inside the lagoon higher velocities are observed at the

most eastern part compared to the associated situation without wind, but furthermore no significant changes are observed the later phases.

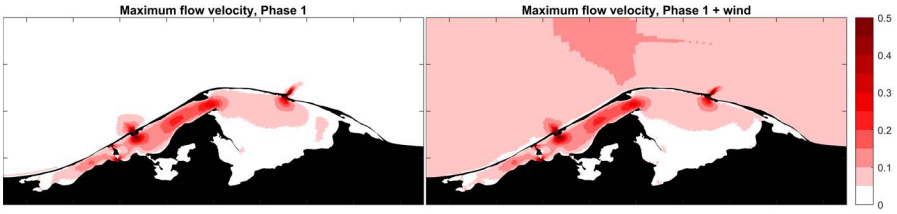

Figure 4.24: The maximum flow velocities during the simulation period of Phase 1 for spring tide conditions in m/s. The left image depicts the situation without wind, the right image with wind added to the model. Legend limited to 0.5 m/s, inlet velocities exceed this value.

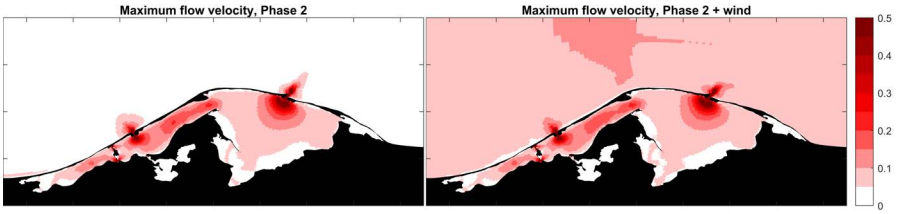

Figure 4.25: The maximum flow velocities during the simulation period of Phase 2 for spring tide conditions in m/s. The left image depicts the situation without wind, the right image with wind added to the model. Legend limited to 0.5 m/s, inlet velocities exceed this value.

In Table 4.16 a comparison between the max ebb and max flood velocities is found for both inlets and for all phases, showing values with and without the added daily wind pattern. Under the prevailing wind conditions the maximum observed velocities for Boughaz 2 show an expected result, with an increase in maximum ebb velocities of about 2-3% and a decrease in maximum flood velocity of 1-3%. However, taking a closer look at the Boughaz 1 velocities, an unexpected increase in ebb velocities is observed, where one would expect a velocity reduction with winds blowing towards the inlet.

Inlet	Phase	Max ebb velocity [m/s]	Max ebb velocity wind [m/s]	Velocity growth	Max flood velocity [m/s]	Max flood velocity wind [m/s]	Velocity growth
Boughaz 1	Phase 0	0.96	0.97	1.0%	0.91	0.91	0.0%
	Phase 1	0.95	0.96	1.1%	0.93	0.94	1.1%
	Phase 2	1.01	1.03	2.0%	0.98	0.98	0.0%
Boughaz 2	Phase 0	0.75	0.77	2.7%	0.79	0.78	-1.3%
	Phase 1	0.77	0.79	2.6%	0.79	0.78	-1.3%
	Phase 2	1.00	1.02	2.0%	1.00	0.98	-2.0%

Table 4.16: Comparison of the max ebb and flood currents for both existing inlets in the Bardawil Lagoon system for each phase with and without wind added to the model

The increase of maximum ebb velocity can be explained by the daily directional variation in winds. The wind velocity and direction pattern gives a difference over time for the velocities observed in both inlets. Looking at Figure 4.26 which shows the velocity differences for Boughaz 1 at spring

tide conditions. The main differences can be found in the ebb velocities, represented by the negative velocity magnitude in the figure. During the afternoon when the velocity magnitude reaches its peak, the North-Western winds are reducing the maximum observed ebb velocities, while during the night the weaker Western winds coincides with a slight increase in maximum ebb velocity. The flood velocities show a slight shift in phase but no significant velocity magnitude change is observed. This explains why the maximum ebb velocity increases where one would expect a decrease in maximum ebb velocities due to the prevailing winds. It should be noted that these results are a snapshot in time to explain the change in maximum observed velocity for this case. Due to the difference in period (24 hour day, 12 hour 25.2 minute tidal cycle) the effect changes per day and the peak wind velocities do not always coincide with the peak tidal velocities, but they do for the particular time frame of this simulation.

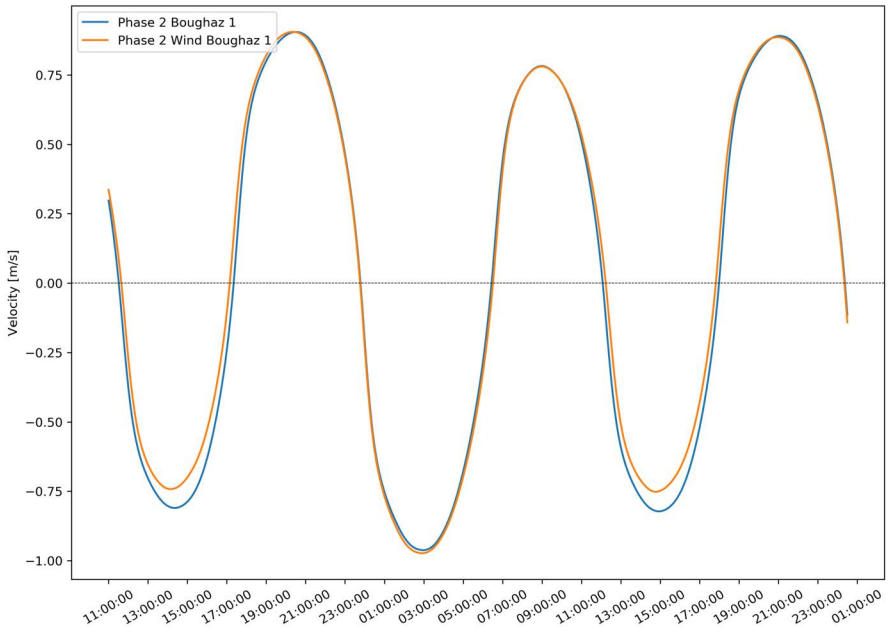

Figure 4.26: Tidal inlet velocity plot for Boughaz 1 during Phase 0 describing the case with only flow (blue line) and the situation with flow and wind (orange line)

Boughaz 2, see Figure 4.27, also shows a reduction in ebb velocity during the stronger North-Western winds in the afternoon, but the difference is smaller compared to the difference observed at Boughaz 1. An increase in ebb velocity during the weaker Western winds is seen, which is larger compared to the Boughaz 1 difference. In contrast to Boughaz 1 the observed velocity difference at Boughaz 2 does show a reduction of flood velocity magnitude during all cases, especially later in the day.

Due to the differences in maximum and minimum inlet velocities per tidal cycle a better method for describing the (ebb or flood) dominance of the inlet is by determining the transport capacity over time. In Table 4.17 the transport per inlet per phase can be found, where the transport is determined as the ebb and flood transport calculated per time-step and averaged per tidal cycle for bedload transport. Without wind Boughaz 1 shows a large difference in favor of ebb velocity for Phase 0, but when adding the wind only a fraction of this difference remains. Phase 1 and 2 are further influenced

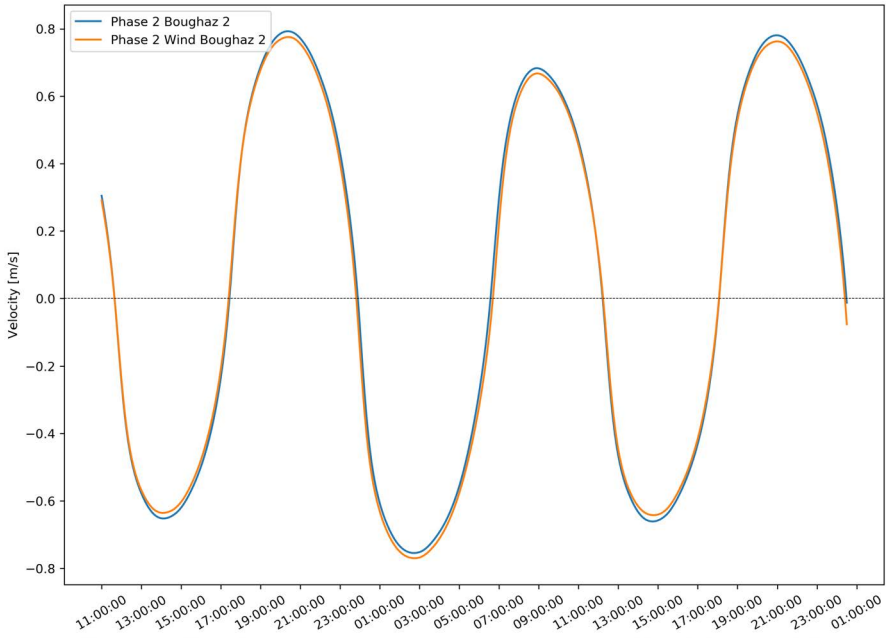

Figure 4.27: Tidal inlet velocity plot for Boughaz 2 during Phase 0 describing the case with only flow (blue line) and the situation with flow and wind (orange line)

by the wind with a change of sign in dominant transport current with a favor for the flood transport. Boughaz 2 initially (Phase 0) is characterised by higher flood transport without wind, but the added wind changes this to a higher ebb transport. In Phase 1 and 2 the trend is continued with an increased difference between the ebb and flood in favor of ebb transport.

No Wind Phase	Boughaz 1 Net transport 10^{-3} $[m^3/s]$	Boughaz 2 Net transport 10^{-3} $[m^3/s]$	System Net transport 10^{-3} $[m^3/s]$	System Dominant transport
0	-6.19	1.28	-4.91	Ebb
1	-1.29	-0.72	-2.02	Ebb
2	-2.96	-1.70	-4.66	Ebb
Wind Phase	Boughaz 1 Net transport 10^{-3} $[m^3/s]$	Boughaz 2 Net transport 10^{-3} $[m^3/s]$	System Net transport 10^{-3} $[m^3/s]$	System Dominant transport
0	-0.89	-2.77	-3.66	Ebb
1	0.82	-5.56	-4.75	Ebb
2	0.94	-7.43	-6.49	Ebb

Table 4.17: Tide averaged sediment bedload transport capacity for all phases for the situation with and without wind

From the previous section we know that, especially after adapting the West inlet (Boughaz 1), a small net flow from Boughaz 1 to Boughaz 2 is present. The model shows that the present wind climate contributes to this phenomenon. Table 4.18 shows the effect of the added wind climate on the observed tidal prism for each inlet and each phase. First of all the tide averaged tidal prism shows only minor changes with the added wind compared to the situation without wind, for all phases. But, when looking at Phase 0 (initial situation) a major difference can be found in the net flow. Looking at the Boughaz 1 inlet where initially a net flow of 0.6% of the tidal

prism is observed from Boughaz 2 to Boughaz 1, the added wind changes this flow to a net flow of 3.5% of the tidal prism from Boughaz 1 to Boughaz 2. Phase 1 and 2 show a similar trend for the increase in net transport from Boughaz 1 to Boughaz 2. The added wind increases the contribution of transport to 3% in the final design.

Because some uncertainties lay within the model the total net flow of the system does not equal zero. For the situation without wind a loss of water from the system is observed for all phases, which consists of about 0.04% of the total tidal prism. With wind a change in sign is observed and water is added to the system with a value of 0.02-0.06% of the total tide averaged tidal prism.

Inlet	Phase	Tide averaged prism [m^3]	Wind tide averaged prism [m^3]	Net flow [m^3]	Wind net flow [m^3]
Boughaz 1	0	10 425 000	10 432 000	-160 000	826 000
	1	23 378 000	23 305 000	301 000	1 456 000
	2	25 199 000	25 123 000	51 000	1 784 000
Boughaz 2	0	12 874 000	12 856 000	151 000	-849 000
	1	13 174 000	12 461 000	-311 000	-1 435 000
	2	37 363 000	37 342 000	-76 000	-1 772 000
System	0	23 299 000	23 288 000	-9 000	13 000
	1	36 552 000	36 494 000	-10 000	21 000
	2	62 562 000	62 465 000	-25 000	12 000

Table 4.18: The tidal prism for the first three phases for both inlets and the total system. Net flow is defined as the flood flow minus the ebb flow with a positive value indicating inflow and a negative value indicating a flow out of the lagoon

A visualisation of the hydraulic processes governing the lagoon under the prevailing wind conditions is shown in Figure 4.28. Noticeable is the little effect the prevailing winds have on the total tidal prism per inlet, but the significant effect on the net flow between the inlets.

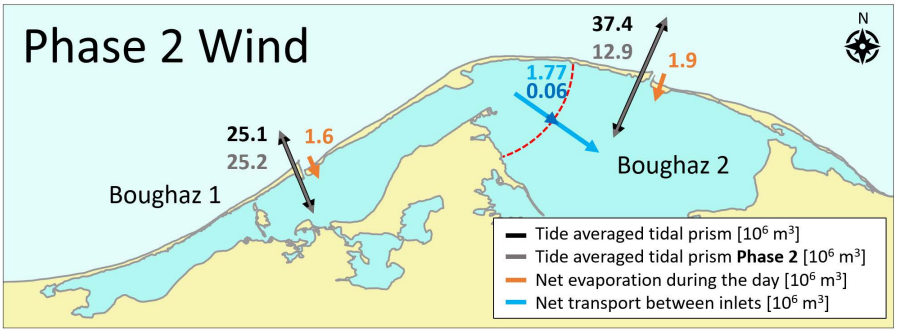

Figure 4.28: Overview of the hydraulic processes present in the Bardawil Lagoon inlet system in Phase 2 with the prevailing winds

Interpretation of the results

The added wind to the model shows immediate results on the observed maximum and minimum tidal elevations in and around the lagoon. For all phases a local increase in maximum elevation is observed, meaning more

water has to be transported through the lagoon. The minimum tidal elevation shows a reduced amplitude, especially in the South-Eastern borders of the lagoon where the highest wind set-up is expected. Although the velocity magnitude distribution map shows a local increase in velocity, especially along the barrier islands, no clear conclusions can be drawn from these plots. Initially still no connection can be observed between the inlets velocity wise, and the later phases lack a significant visual growth as well.

The data from the depth averaged cross-sectional velocity observations allows for drawing more profound conclusions. In previous studies the maximum ebb and flood velocities were used to determine the dominant transport character. Due to the changing wind pattern variations between the ebb velocities of different tidal cycles are observed, showing a slight increase in maximum velocity for one cycle, but a more significant decrease in maximum velocity for the other. Therefore it is chosen to assess the character of the inlets according to the sediment transport capacity for bed load transport. These results provide an interesting trend compared to the situation without wind. Boughaz 1 without wind was characterised as ebb dominant for all phases, but the prevailing North-Western winds causes flood dominance for Phase 1 and 2. This character suggests sediment import, although the differences between the ebb and flood currents are small. Boughaz 2 experiences flood dominance initially without wind, but the wind case transfers it to ebb dominance. Phase 1 and 2 for the Eastern inlet were already characterised by ebb dominance, but the effect of ebb transport is significantly increased. Hence, the total system can be characterised with an increased coarse sediment exporting character.

Looking at the inlet velocities and changes in tidal elevation, velocity and prism there is no reason to suggest that the wind conditions influence the stability of the inlets according to the methods of Bruun and Gerritsen and Escoffier. However, where for the no-wind situation the maximum observed net flow from Boughaz 1 to Boughaz 2 was observed to be 1.1%, after adopting Boughaz 1 in Phase 1 of the wind case an interaction of 5.4% is observed. The significance of this net flow might be significant enough for the inlets to influence the stability of the other.

In short, the wind has a positive influence on the net sediment transport characteristics of the lagoon and there is no significant influence on the inlet stability according to the Escoffier and Bruun method.

4.5 LAGOON FLUSHING

The flushing of the lagoon is assessed according to two methods: calculation of the renewal time following Pritchard (1960) and a determination of the flushing of the lagoon using a D-Water Quality model for fraction calculations. Both are elaborated in their respective sections. It should be noted that the renewal time is an estimation calculated with the purpose to get insight in results of the adaptations.

4.5.1 Renewal time

The rate of renewal of the lagoon can be determined by calculating the replacement time of lagoon water, which is a function of the total average lagoon volume (V) and the average tidal prism (Q) and is formulated as $t_{99\%}$. However, this relation assumes replacement of the entire water body,

which is never the case since new water will mix with old water, therefore the 50% renewal time $t_{50\%}$ is often calculated (Linnersund and Mårtensson, 2008). The 50% renewal time describes the time required to replace half of the lagoon water volume, assuming a well mixed lagoon. The complex geometry of Bardawil Lagoon is not included in the calculation, but can significantly influence the interaction. The derivation of the renewal time follows Pritchard (1960) and is as follows:

$$\frac{dV}{dt} = -r_v \cdot V \qquad where\, r_v = 2 \cdot k$$

The t_{50} is expressed as the renewal time in days and not in tidal cycles, therefore, for a semi-diurnal tidal pattern, the constant k is multiplied with 2. The value k represents the fractional change in volume, the ratio of the net intertidal volume to the total volume of the lagoon. Because of the semi-diurnal character this value has to be multiplied by two to express the renewal time in days.

Integration yields:

$$\int_{V_0}^{V_{new}} \frac{1}{V} \cdot dV = \int_{t_0}^{t_{50\%}} r_v \cdot dt$$

$$-\ln \frac{V_{new}}{V_0} = r_v \cdot (t_{50\%} - t_0)$$

$$\frac{V_{new}}{V_0} = 0.5 \qquad t_0 = 0$$

Solving for the renewal time, t_{50} gives:

$$t_{50\%} = \frac{0.693}{r_v}(days)$$

The 99% renewal time of the lagoon is found when $V_{new}/V_0 = 0.01$, determined as:

$$t_{99\%} = \frac{4.605}{r_v}(days)$$

Table 4.19 and Table 4.19 show the renewal time for the three design phases for the situation without and with wind added to the model. Due to the minimum effect of the wind on the tidal prism the differences in renewal time between the two cases is negligible. Each adaptation results in a significant increase of the renewal time for both the $t_{50\%}$ and $t_{99\%}$.

	Average prism (m^3)	T50 (days)	T99 (days)
Phase 0	23 299 000	9.3	61.7
Phase 1	36 552 000	5.9	39.4
Phase 2	62 562 000	3.5	23.0

Table 4.19: The renewal time for all phases determined for Bardawil Lagoon, no wind

	Average prism (m^3)	T50 (days)	T99 (days)
Phase 0	23 288 000	9.3	61.8
Phase 1	36 494 000	5.9	39.4
Phase 2	62 456 000	3.5	23.0

Table 4.20: The renewal time for all phases determined for Bardawil Lagoon, wind included in the model

4.5.2 Fraction calculations

Another method to get an indication of the flushing of Bardawil Lagoon is the use of a fraction computation, which uses unique tracers which are related to unique groups of boundaries, in this case the difference between the Mediterranean Sea and Bardawil Lagoon. These water fractions help understand the composition of water and are implemented using the D-Water Quality modelling software. The results of the calculations provide the percentage of lagoon water (start value of 1, color red) and the Mediterranean Sea (start value of 0, color blue) after one month of simulation time. For example, a value of 0.6 indicates 60% lagoon water and 40% seawater.

Figure 4.29 visualized the distribution of the fractions for all three phases. The top two figures depict the fraction distribution for Phase 0 without (left) and with (right) wind. It is clearly visible that without wind the interaction of the water bodies is concentrated around the inlets. When wind is added to the model significantly more interaction is visible around both inlets. The bottleneck becomes more flushed and the lagoon area East of Boughaz 2 appears to experience the effects of the prevailing Western winds. The most Western and central lagoon areas remain untouched during the simulation period. The visualisations of Phase 0 flushing coincide with the observed salinity values in Figure 2.9. Looking at the fraction concentration plotted over the time in Figure 4.30, insight is given in the rate in which the lagoon waters are renewed over time. Extrapolating this data to a 50% refreshing rate of Bardawil lagoon gives a t_{50} of 53 days without wind and 48 days with wind (Table 4.21).

After applying the new design of Boughaz 1 (Phase 1) it appears that an increase in flushing rate is observed (center figures). The area behind Boughaz 1 shows a lot more interaction with the Mediterranean Sea and the flushing is visible into the bottleneck. The wind contributes to these findings. No significant visual differences are observed for the Eastern area of the lagoon including Boughaz 2, the most Western area remains stagnant as well. However, looking at the average lagoon concentration over time (green lines) it appears that the fraction concentration for Phase 1 is similar to Phase 0, even with the significant increase around Boughaz 1. This could be due to a water level gradient between the two inlets inside the lagoon, with higher tidal elevation water from Boughaz 1 restricting the interaction of Boughaz 2 with the Mediterranean Sea. The t_{50} renewal time extrapolated from this data provides 52 days for Phase 1 without wind and 46 days with wind, which is only a minor gain compared to Phase 0.

In Phase 2 the whole lagoon experiences an increased interaction with the Mediterranean Sea (bottom two images in Figure 4.29). The area flushed at Boughaz 2 is significantly increased compared to Phase 0 and reaches into the areas far away from the inlets. The winds contribute to the interaction, almost connecting the two inlets inside the lagoon. After one month of simulation most areas of the lagoon experience at least some form of flushing,

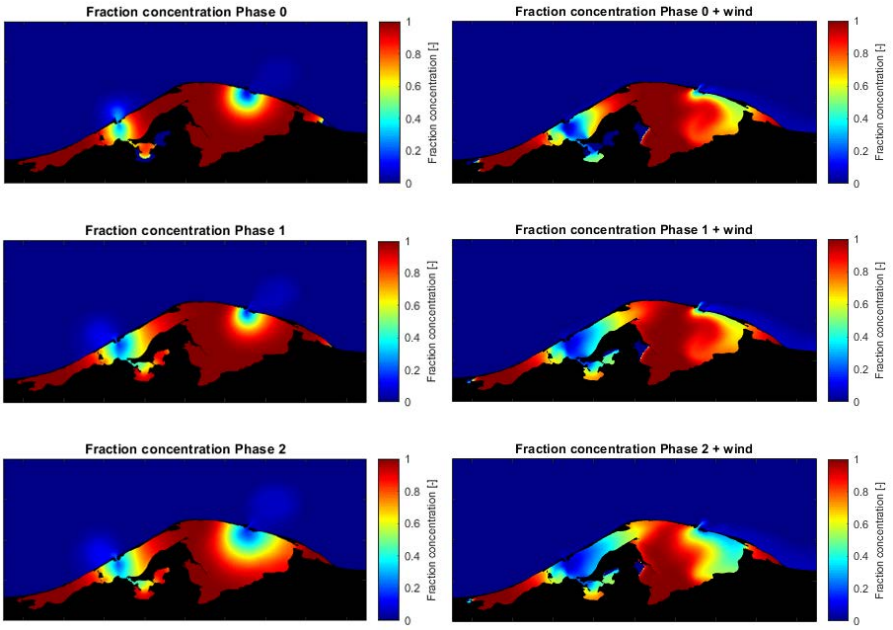

Figure 4.29: The results of a 30 day fraction calculation showing the situation without and with wind for Phase 0 (top), Phase 1 (middle), and Phase 2 (bottom). Red indicates 100% lagoon water and 0 represents 100% Mediterranean Seawater

however the most Western area and central lagoon area are still relatively untouched. The renewal time shows a reduction compared to Phase 0 and Phase 1, with a t_{50} of 48 days without wind and 42 days with wind.

No wind	Initial concentration residue after 30 days [-]	50% renewal time [days]
Phase 0	0,87	53
Phase 1	0,87	52
Phase 2	0,8	48
Wind		
Phase 0	0,78	48
Phase 1	0,77	46
Phase 2	0,69	42

Table 4.21: The average lagoon concentration after 30 days compared to the time in days required to refresh 50% of the lagoon waters

Interpretation of the results

The renewal time determined with the method of Pritchard provides an upper boundary of what might be possible in the lagoon should it be well mixed which, looking at the results, is not the case. The results of the renewal time calculations grow linearly with the increase of tidal prism. Phase 0 has a t_{50} of 9.3 days and after completion of Phase 2 the t_{50} renewal time is expected to be 3.5 days according to this method.

The fraction calculations with the D-Water Quality model provide a more realistic result of the flushing rate in the lagoon. Without wind the t_{50} with fraction calculations is respectively 53, 52 and 48 days for Phase 0, 1, and 2. The prevailing winds reduce these values with about 6 days. The reason the

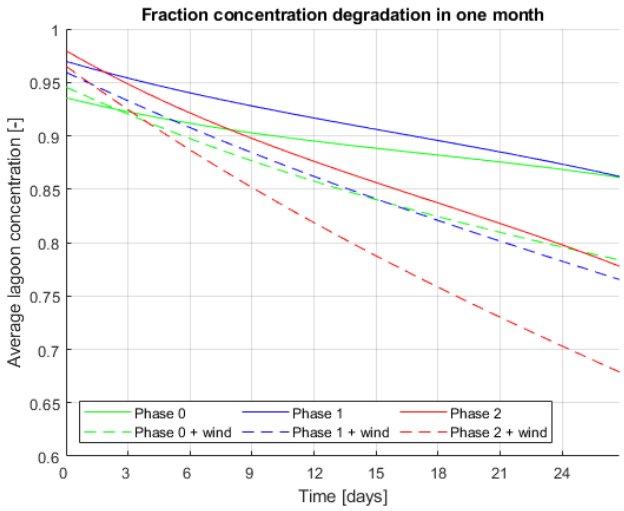

Figure 4.30: The average lagoon fraction concentration plotted over a 30 day time interval for all phases without and with wind

results of Phase 0 and Phase 1 are this close together is due to the increased water gradient in Phase 1 in the lagoon from Boughaz 1 towards Boughaz 2, which reduces the reach of the water from Boughaz 2. The adaptations made to Boughaz 2 in Phase 2 allow for an increase in interaction with the Mediterranean Sea and hence this effect is not as profound anymore, resulting in a decrease in t_{50}.

The values of the fraction calculations are considered a lot more reliable compared to the renewal time calculations at the beginning of this chapter. The fraction plots provide good insight in the reach of Mediterranean Sea water originating from the inlets into the lagoon and show that the lagoon is not well mixed. The Western and center lagoon areas are not well reached by the incoming tide, causing high saline zones.

5 DISCUSSION

The discussion is divided into two sections. First the effect of evaporation on the results is discussed. Thereafter the general discussion points of this thesis are elaborated.

5.1 EVAPORATION EFFECTS

The effect of evaporation is analytically included into the results to give an indication of the effects on the hydrodynamics and subsequently the sediment transport capacity due to water loss in the lagoon. For this approach the precipitation and evaporation data from Khalil and Shaltout (2006) is used, which are determined by Euroconsult (1995) (Table 5.1). The lagoon is divided into two segments, determined by the reach of each inlet. This is done according to the tidal divide previously mentioned by Lanters (2016) and Georgiou (2019). The tidal divide is visible in Figure 5.1, indicated with the red dashed line where the flows from the two inlets meet.

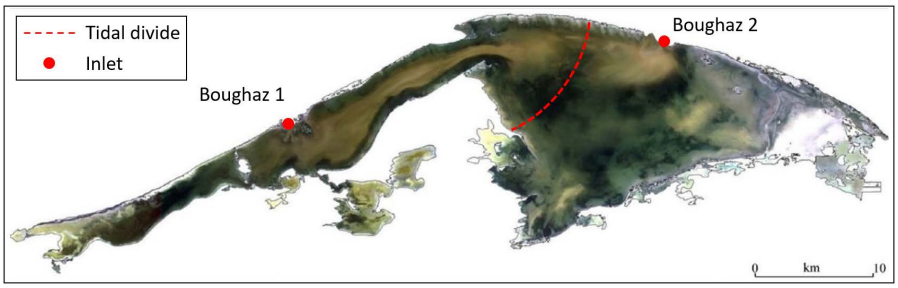

Figure 5.1: The tidal divide between the two inlets (Adapted from Embabi and Moawad (2014))

Three values of evaporation will be considered: High evaporation, low evaporation and average evaporation. High evaporation is defined as the highest observed evaporation during the year, which occurs during the summer months of June, July, and August. Low evaporation is the lowest evaporation during the year, present in December. The average evaporation is the average of all 12 months. The monthly water loss of the system is defined as the difference between the precipitation and evaporation divided by the number of days per month, which is then multiplied with the area of the lagoon to determine the daily net water loss of the system.

	j	f	m	a	m	j	j	a	s	o	n	d
Precipitation (mm)	13	10	9	7	5	0	0	0	0	0	18	20
Evaporation rate (mm)	56	84	96	132	167	189	192	177	153	146	63	50
Net water loss (mm/day)	1.4	2.6	2.8	4.2	5.2	6.3	6.2	5.7	5.1	4.7	1.5	1.0
Net water loss ($\cdot 10^6 m^3$)	0.77	1.43	1.54	2.31	2.86	3.47	3.41	3.14	2.81	2.59	0.83	0.55

Table 5.1: The precipitation, evaporation, and net water loss values of Bardawil Lagoon (Euroconsult, 1995)

With the tidal divide the influence areas of the inlets are determined to be roughly 250 km^2 for Boughaz 1 and 300 km^2 for Boughaz 2. Assuming most of the evaporation occurs between sunrise and sunset, the evaporation window is set to be between 06:00 and 18:00 hours. Like the previous results, the evaporation data will be processed on modelling runs of one month, including 2 spring tides and two neap tides. This is done for the case without and with wind and for Phase 0, Phase 1, and Phase 2.

5.1.1 Results

The addition of evaporation to the system has some effect on the maximum flow velocities in the inlets, especially for Phase 0 (without any adaptations to the system). When looking at high evaporation rates without changes to the inlets, the maximum increase (or reduction in case of ebb flow) in velocity to the system equals 0.038 m/s for Boughaz 1 and 0.032 m/s for Boughaz 2. The magnitude of the increased (or reduced) velocity significantly reduces after both inlets have been altered in Phase 2, to respectively 0.015 m/s for Boughaz 1 and 0.013 m/s for Boughaz 2. An increase in the maximum flow velocity positively benefits the stability of the inlets according to the Escoffier curve, because higher flow velocities are beneficial for erosion. However, the effects of evaporation on the sediment transport capacity of the inlets should also be considered, which is elaborated below.

Evaporation effects on the sediment transport capacity

Without considering the effects of evaporation, Boughaz 1 is classified as sediment exporting and Boughaz 2 is classified as sediment importing for Phase 0. The total system is considered sediment exporting as well, this in contrary with the current sediment importing character of the inlets. For both Phase 1 and Phase 2 both inlets and consequently the total system are sediment exporting for the tide only conditions.

When taking into account the evaporation effects as discussed earlier in this section a significant change in sediment transport character is visible, as can be seen in Table 5.2. All stages of evaporation (low, average, and high) have a contribution on the sediment transport character, of which the average and high evaporation have the most distinct effect. As can be seen in the table for low evaporation conditions, which occur during winter, the total system remains sediment exporting for all phases. However, the magnitude of the ebb dominant transport reduces, especially for Boughaz 2 which is only considered sediment exporting after Phase 2. Looking at the yearly average net water loss effects a more distinct trend is visible compared to the tide only and the low evaporation situation. The total system remains sediment importing in Phase 0 and Phase 1, only to achieve the desired sediment export after Phase 2. Moreover, Boughaz 2 remains sediment importing for all phases.

During the summer months the evaporation values have the largest magnitude and no precipitation is present, which causes a serious deficit of water. The high evaporation values cause a significant different trend compared to the system without evaporation. Both Boughaz 2 and the total system are considered sediment importing for all phases, with the highest values observed for Phase 0. Boughaz 1 is sediment exporting for Phase 0

and Phase 2, but the values are small compared to the import of Boughaz 2.

Situation	Phase	Net Boughaz 1 10^{-3} $[m^3/s]$	Net Boughaz 2 10^{-3} $[m^3/s]$	Net System 10^{-3} $[m^3/s]$
Tide only	0	-6.19	1.28	-4.91
	1	-1.30	-0.72	-2.02
	2	-2.96	-1.70	-4.66
Low Evaporation	0	-5.30	1.97	-3.33
	1	-0.97	0	-0.97
	2	-2.58	-1.22	-3.80
Average Evaporation	0	-2.60	4.06	1.46
	1	0.01	2.18	2.19
	2	-1.43	0.22	-1.21
High Evaporation	0	-0.37	5.79	5.42
	1	0.83	3.99	4.82
	2	-0.48	1.42	0.94

Table 5.2: The net sediment transport capacity under the evaporation conditions

Evaporation and wind effects on the sediment transport capacity

Table 5.3 depicts the evaporation effects on the behaviour of the system in which the prevailing wind conditions are included in the calculations. While a similar trend is visible compared to the situation without wind, there are some differences, as can be seen in the last column of the table. For Phase 0 the prevailing winds contribute to an flood dominated system, where significant import is observed for Boughaz 1. Boughaz 2 moves more towards an ebb dominant system in Phase 0, but the observed difference is less than the change visible at Boughaz 1, resulting in net import of sediments. Phase 1 shows the largest difference between the situation without and with wind, with a surge in ebb going transport. The same trend is visible for Phase 2, although the magnitude of the difference is less compared to Phase 1.

The most important difference between the evaporation cases without and with wind is the effect on the system after the adaptations made in Phase 1 and Phase 2. Without wind the system is still classified as having a sediment importing character, which is an undesired result. Boughaz 2 shows a distinct sediment exporting character under the prevailing winds in Phase 2, while Boughaz 1 becomes more sediment importing. Especially under high evaporation conditions the flood going transport stands out. However, when taking the prevailing winds into consideration, which occur in the same period as the highest evaporation values, the total system is expected to behave as a sediment exporting system.

5.1.2 Interpretation of the results

From these results it is obvious that the evaporation rates in Bardawil Lagoon play an important role in the character of the sediment transport in the inlets. The deficit of water inside the lagoon must be compensated with extra inflow of water from the Mediterranean Sea, which results in an increase in flood velocities and a reduction of ebb velocities during the day. These velocity changes are not considered significant enough to cause major changes in the inlet stability, but they do have significant effect on the transport capacity of the inlets, especially when looking at the high evaporation rates without the prevailing winds. The high evaporation changes the system from a solid sediment exporting system towards a sediment import-

Situation	Phase	Net Boughaz 1 10^{-3} $[m^3/s]$	Net Boughaz 2 10^{-3} $[m^3/s]$	Net System 10^{-3} $[m^3/s]$	Net System difference no wind 10^{-3} $[m^3/s]$
Tide only + Wind	0	-0.89	-2.77	-3.66	1.25
	1	0.82	-5.56	-4.75	-2.73
	2	0.94	-7.43	-6.49	-1.83
Low Evaporation + Wind	0	-0.02	-2.09	-2.11	1.22
	1	1.13	-4.86	-3.72	-2.75
	2	1.31	-6.96	-5.65	-1.85
Average Evaporation + Wind	0	2.63	-0.05	2.58	1.13
	1	2.10	-2.72	-0.62	-2.81
	2	2.44	-5.54	-3.10	-1.89
High Evaporation + Wind	0	4.84	1.65	6.49	1.07
	1	2.90	-0.94	1.96	-2.86
	2	3.37	-4.36	-0.99	-1.92

Table 5.3: The sediment transport capacity under the evaporation and prevailing wind conditions

ing system, even after the adaptations in Phase 2. However, the prevailing winds in combination with high evaporation bring the system back towards sediment exporting. Boughaz 1 is still importing sediments under these conditions, but for the low and average evaporation situation the export of Boughaz 2 is far exceeding the import of Boughaz 1.

5.2 GENERAL DISCUSSION

5.2.1 Bathymetry

The bathymetric data used in these studies originates from various resources, off which small parts of offshore data are dating back to the 19th century. This makes it difficult to establish a very accurate profile on the whole modelling area. Recent data is currently available for the Boughaz 2 inlet, but recent sources for other lagoon areas are scarce. While there are recent studies conducted on the bathymetry of Bardawil Lagoon, there was no success in establishing contact with these researchers. However, because this study is focused on the effect of different lagoon adaptations to the inlets, of which the bathymetry is relatively well known, this should not cause a significant problem. Since the goal of this study is to gain insight in the behaviour of the system to the adaptations in relation to the initial situation.

5.2.2 Wind

The daily wind pattern used in the model is obtained by averaging wind velocity data on specified time steps. This method gives solid insight into the effect of the prevailing winds present in the summer months. This is a useful method to visualize the effect of a daily wind pattern on the hydrodynamic behaviour of the lagoon. However, a seasonal variability is observed which is not implemented in the study. Applying a seasonal variability to the model could give further insight into the response of the system throughout the year, especially when morphology is included in the model. Furthermore, the effect of a storm event on the morphology and subsequently the stability of the system could give very insightful results.

5.2.3 Results from previous studies

The inlet cross-sectional area and approach channel design for Boughaz 1 is derived from the study of Georgiou (2019). The design adaptations showed promising results for Boughaz 1 in that study. For this study the design is implemented for both Boughaz 1 and Boughaz 2. While the results are promising, the morphological behaviour of this design at Boughaz 2 is unknown, because a morphological sensitivity analysis for Boughaz 2 could not be performed. It is therefore possible that a better design for Boughaz 2 could be achieved. For this study the new Boughaz 2 design functioned according to the expectations. The long term morphological behaviour of the approach channel proposed by Georgiou (2019) is yet to be determined. Initially a channel has to be dredged for the dredging vessels to enter the inlets, which makes it useful to develop it in in the most efficient design.

5.2.4 Morphology

At the time the model runs were done the version of Delft3D FM did not support multiple sediment fraction calculations, it could only perform calculations on a single sediment fraction size. Therefore, no conclusions could be conducted from simulations with morphology enabled. Running the model with just one fraction was not considered reliable because:

- Running the model with a small fraction (100 mu, observed inside the lagoon) caused major erosion inside the inlets, with values observed up to 10 meters in 2 months.
- Model runs with a large fraction (300 mu, observed outside the lagoon) showed promising results for the inlets, but no erosion was observed inside the lagoon where, due to the smaller fraction present erosion is expected, and the area of interest is located.

Thus, it was not possible to develop a model which accurately represents the inlet morphology combined with a representative erosion/sedimentation pattern inside the lagoon.

The model used for this study is a 2D-H model, thus varying in x and y dimension with a depth averaged flow velocity. This approach is considered suitable for a representative hydrodynamic analysis of the system, while keeping the required modelling time within acceptable time limits. However, the 2D approach neglects 3D effects, like density driven current, happening within the system. 3D effects are important to take into account when density differences are observed within a system, which might very well be the case for Bardawil Lagoon, as is described further down this chapter.

5.2.5 Processes affecting results

Results

The results of the model runs suggest that sediment export can already be expected in Phase 0 with the contribution of the prevailing winds on the system. Currently, yearly maintenance dredging is necessary to keep the inlets open, therefore it is thought that more processes are influencing the hydrodynamic (and thus morphodynamic) response of the system. The missing link in the calculations is thought to be evaporation, which is further

elaborated earlier in this chapter. The effect of the prevailing winds is shown in the previous chapter. These winds are included in the model, a model which is depth averaged. Wind forces act mainly on the surface of the water column, thus the effect of the wind on sediment transport could be an overestimation.

Salinity

The salinity values of the lagoon are exceeding the salinity values observed in the Mediterranean Sea. Moreover, the salinity inside the lagoon is not uniformly distributed. Density differences caused by the salinity gradient observed in the lagoon can contribute to a density driven circulation.

Stratification due to differences in salinity might occur on the shallow lagoon areas, although it must be noted that the average depth of 1.2 meter in combination with the prevailing winds could very well prevent stratification of happening. However, near the inlets, density driven currents are very likely to be present due to the increasing depth, especially after the adaptation of the inlets. The lighter, less dense, Mediterranean Seawater will float on top, while the denser lagoon waters are expected to flow near the bottom. This causes a so called 'lock exchange effect', with the lighter water flowing on top of the denser water. While this does not necessarily result in a net flow of water in any direction, it can have an effect on morphological behaviour of the inlet. The concentration of suspended sediments is higher near the bottom and bed load transport will always take place at this location, therefore a net export of sediments due to density driven currents is expected.

The increased interaction between the Mediterranean Sea and Bardawil Lagoon after Phase 1 and 2 is expected to decrease the salinity concentrations inside the lagoon, especially near the inlets. A reduction in salinity decreases the amount of flocculation, effectively reducing the fall velocity of finer sediments causing them to remain in suspension longer. Suspended sediments are more easily taken by the ebb going tide and consequently removed from the system, further enhancing sediment export. However, it should be noted that with a decreasing salinity the effect of the density driven currents on sediment transport will reduce over time.

5.2.6 Sediment transport character

Multiple processes have now been discussed which affect the sediment transport character of the inlets: evaporation, wind and baroclinic effects. All three are difficult to include in a depth averaged model, for their effect is non uniformly distributed over the water column. Evaporation results in a net inflow of Mediterranean Seawater into the lagoon, which is, due to the baroclinic effects situated at the top of the water column. The same holds for the wind driven circulation of water due to the prevailing winds conditions, for the wind acts as a surface force and effects mainly the top layer of water. Due to the lock exchange effect the heavier denser water inside the lagoon will move outwards near the bottom of the water column, where the highest concentration of sediments is located. Considering these processes the effect of evaporation and wind could possibly be less than the results now show, which is in favor of ebb directed sediment transport.

However, a seasonal variability is present at Bardawil Lagoon, which is not taken into account yet. The high evaporation rates in combination with the prevailing winds have a significant effect on the transport character of the system, especially when taking the surge in flood directed sediment transport at Boughaz 1. The wind direction and magnitude are more uniformly distributed in winter and the evaporation values are low. Looking at the current influence of the prevailing wind conditions during the summer months a winter climate could provide very different results. Morphological changes usually take place over long timescales (years), so possibly yearly averaged transport balance can be established for each inlets with flood dominance during the summer months and ebb dominance during the winter months.

5.2.7 Stability

The inlet stability in this research is assessed according to the method proposed by Escoffier (1940). The Escoffier method is based on the balance between the inward and outward sediment transport through the inlet and is visualised by a graph plotting the two processes: the equilibrium velocity curve and the close curve (Figure 2.12). The close curve is the result of the inlet geometry and present hydrodynamics and, in this study, is fitted according to the results obtained from the numerical model calculations. The equilibrium velocity curve used in this study is a constant of 1.0 m/s as described by Bruun (1978), however, according to van de Kreeke (2004) the value is a weak function of the littoral drift and cross-sectional area and could therefore have a different shape. In theory this could lead to different velocities defining the equilibrium stability points. Moreover, the Escoffier method assumes a constant basin level that fluctuates uniformly with the tide, which is not the case in this study. As described in Chapter 4 the bottom friction is significant and influences the tidal propagation into the lagoon. It is thought that with increasing the tidal intrusion into the basin the Escoffier curve may grow accordingly and the system may behave like it does to a change in basin area, effectively storing extra water inside the lagoon.

The Escoffier plots after Phase 1 and Phase 2 provide promising results which are supported by a sensitivity analysis. Especially the results of Boughaz 1 show a well defined location near the stable equilibrium velocity point. The location of Boughaz 2 is also determined near this location, but the slope of the curve is less distinct compared to Boughaz 1. This might compromise the stability of the inlet after a storm event. Immediate dredging operations after such event can bring the inlet back on track to the stable equilibrium point.

A method is developed by van de Van de Kreeke and Brouwer (2017) to assess the stability of a system composed of multiple inlets. Changing the size of one inlet could cause major disturbances on the other, which is visible for Boughaz 1, which shows an increase in maximum velocity after Boughaz 2 is adapted in Phase 2 Section B.1). However, the method is not yet validated on a natural multiple inlet system with a complex geometry. Therefore the application of the method on this study is not considered useful.

Moreover, the shape of the Escoffier curve is not fixed, it can change according to the characteristics of the system. An increase in average tidal prism shifts the curve to the right, a decrease in tidal prism will shift the curve to the left. If we take a closer look at the formula describing the curve below, one can see it involves three parameters: The tidal prism (P), the inlet cross-sectional area (A) and the tidal period (T).

$$u_e = \frac{\pi P}{AT}$$

Assuming the tidal period and inlet cross-sectional area are constant, a rise in tidal prism will always lead to an increase in velocity under these assumptions. This is visualized in Figure 5.2. The blue line indicates the original curve and the orange line the curve with an increase in tidal prism with the previous stated assumptions. The adaptations in this study are conducted on the inlets, no changes in inner basin geometry are present, and the inlets are located on point D, the stable equilibrium point. Should the lagoon experience natural deepening, the tidal prism is expected further increase due to a reduction in bottom friction, hence the curve will rise and the stable equilibrium point on the Escoffier plot will shift to the right, as can be seen in the figure. This would bring the inlet suddenly between point C and D, which of course will not be a sudden jump, because the inlet cross-sectional area is not fixed and will change according to the position on the Escoffier curve. The cross-sectional area size provided in this thesis brings the inlets to the stable equilibrium point (D) for the current lagoon characteristics, however a change in these characteristics will influence the stable cross-sectional inlet area. Hence with a natural deepening lagoon the tidal prism will gradually increase and with it the inlet cross-sectional area.

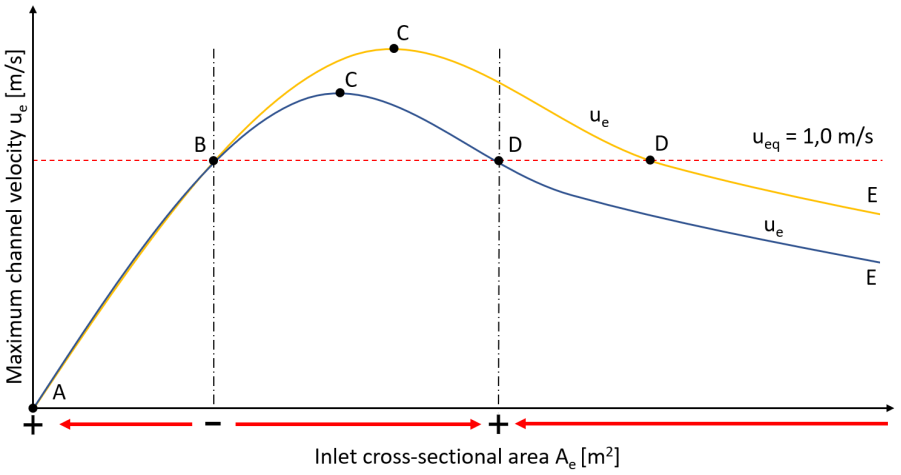

Figure 5.2: The change in Escoffier curve followed by an increase in tidal prism due to a deeper lagoon

6 CONCLUSION AND RECOMMENDATIONS

The goal of this thesis is to analyse the effect of inlet adaptations on the lagoon-sea interaction, with the goal of transforming the present, sediment importing system towards a stable, sediment exporting inlet system by adapting one or both of the present inlets. The study can be separated into four research phases; Phase 0 investigates the present functioning of Bardawil Lagoon without any interventions. Phase 1 and Phase 2 respectively investigate the effect of applying a new inlet design to the Boughaz 1 (west inlet) and Boughaz 2 (east inlet), of which consists of: increasing the inlet cross-sectional area, dredging an approach channel, addition of a nourishment, and removal of the present breakwaters. The final part of the thesis looks into the effect of a prevailing wind pattern on system behaviour.

The study is concluded by answering the research questions stated in Chapter 1. The main research question is as follows:

> **How can the Bardawil Lagoon multiple inlet system be transformed from a morphologically unstable towards a morphologically stable inlet system by adapting one or both inlets?**

The main research question is obtained by answering all sub questions, which is done below.

6.1 RESEARCH QUESTIONS

> **How can the current hydrodynamic and morphological character and inlet stability of Bardawil Lagoon be classified?**

Currently, in Phase 0, the Bardawil Lagoon does not function as a morphologically stable tidal lagoon inlet system as sedimentation occurs in both inlets. The restricted water exchange between the Mediterranean Sea and the lagoon indicates that the existing inlets are the limiting factor for proper functioning. For the assessment of the sediment character of both inlets the transport capacity is considered the most representative parameter for coarse sediment, because it takes the entire tidal cycle into account, instead of just the maximum flow velocities. According to the transport capacity Boughaz 1 is sediment exporting and Boughaz 2 tends towards sediment import, however the differences are small and it should be noted that residual currents due to evaporation are not included in these values. Higher flow velocities are only observed near the inlets and no net flow is observed between the inlets inside the lagoon. Hence, the two inlets act as separate basins separated by the tidal divide and the method of Escoffier (1940) can be applied for determining the stability of both inlets. Assessing the interaction with the Mediterranean Sea and the maximum flow velocities observed in the inlets, places both inlets near the unstable equilibrium point on the closure curve, indicating a morphologically unstable lagoon system. Thus

it is concluded that the current Bardawil Lagoon inlet system is morphologically unstable for both inlets following the results of sediment transport patterns and the evaluation of the Escoffier model.

What effect do the inlet adaptations have on the sediment transport character of the inlets?

Phase 1 characterises the new design of Boughaz 1. From the sediment transport capacity follows again ebb dominance for Boughaz 1, with a reduced transport magnitude relative to Phase 0. Boughaz 2 changes from flood to ebb dominant, although the difference is small and the values are relatively close to 0. However, taking average evaporation into account, the net sediment transport through the inlets in the system is still flood dominant. Hence, adapting only Boughaz 1 does not accomplish the goal of reaching a naturally deepening lagoon system.

The new design of Boughaz 2 in **Phase 2** shows promising results. From the tidal elevation data it is determined that the interaction between the Mediterranean Sea and Bardawil Lagoon, for both inlets, is no longer limited by the inlet characteristics, but by the bottom topography of the lagoon. The average tidal prism is increased by a factor 2.5, indicating an increase in interaction between the sea and lagoon. This increased interaction positively influences the flow velocities observed in both the inlets and the lagoon, which in their turn significantly increase the transport capacity for both inlets, with an observed growth of 10% for Boughaz 1 and 110% of Boughaz 2 compared to Phase 0. The entire system becomes more ebb dominant and the difference between ebb and flood flow is more distinct compared to the previous phase. This statement holds when looking at the average evaporation case, therefore with the adaptations of Phase 1 and Phase 2 it is concluded that the system is defined as sediment exporting.

What effect do the inlet adaptations have on the stability of the inlets?

Applying a new design on Boughaz 1 in **Phase 1** shows promising results regarding the stability of the inlet. The inlet moves on the Escoffier curve to a location near the stable equilibrium point, which is supported by the sensitivity analysis. This defines the inlet, in combination with the sediment exporting character, as a natural dynamically stable inlet. However, the desired stability change is not observed for Boughaz 2, and therefore the adaptations after Phase 1 are considered insufficient to reach the research goal.

After the completion of **Phase 2** it can be concluded that Boughaz 2 moves from the unstable, self closing, situation to the sustainable stable equilibrium point, which is clearly visible in the sensitivity analysis. The significant change in sediment transport capacity suggests the inlet will stimulate ebb directed transport. Furthermore, a minor stability increase of Boughaz 1 is observed with inlet velocities increasing from 0.95 to 1.01 m/s. A lack of a significant net flow between the inlets suggests they act as separate basins and can therefore still be assessed according to the model defined by Escoffier (1940). Following the stability ratio by Bruun and Gerritsen (1960) both inlets move from poor-to-fair stability in Phase 0 to a stability ratio which is considered fair in Phase 2. Different evaporation situations have only minor effect on the flow velocities and thus the inlet stability. To

conclude both inlets reach their stable equilibrium point after Phase 2 and thus are considered morphologically stable.

To what extent does the wind climate contribute to sediment transport and inlet stability of the system?

The effect of the morning Western winds and stronger afternoon North-Western winds is visible on the ebb and flood velocity magnitude. While the maximum inlet velocities show some small scale deviations, the cumulative effect over time provides the most significant differences. Boughaz 1 shows a large decrease in net ebb sediment transport capacity, but remains ebb dominated. However, Boughaz 2 changes from a flood dominant inlet towards an ebb dominant inlet. The same trend in visible for Phase 1 and Phase 2, with Boughaz 1 becoming more flood dominant and Boughaz 2 becoming more ebb dominant. While these results seem unlikely due to the current sediment importing situation stated in literature, the inlets both are considered sediment importing considering average-high evaporation. With a small increase in net flood transport for Boughaz 1 and a large increase in net ebb transport for Boughaz 2 the total inlet system moves towards a more ebb dominated inlet character with the prevailing wind conditions. No significant change in the spring tidal prism is observed in the wind-added model for all phases and, since the littoral drift value remains constant, it is determined that the wind does not influence the stability of the inlets according to the method of Bruun and Gerritsen (1960). However, an increase in net flow between the inlets is observed, although the value does not exceed 4% of the average tidal prism. Lagoon circulations due to prevailing wind patterns can influence the suitability of stability methods. Furthermore, it is concluded that the effect of the prevailing winds mainly influence the sediment transport character of the inlets, with the capability of changing the dominant transport direction.

What effect do the adaptations and wind climate have on the renewal time and flushing of the lagoon?

After the adaptations of Phase 1 and Phase 2 an increase in tidal prism is observed. The increased tidal prism reduces the $t_{50\%}$ renewal time by 63%, a reduction of 6 days from the original 9. However, it should be noted that this method assumes a well mixed lagoon, which is not the case for Bardawil. The wind has no influence in this calculation method. Modelling with the use of fractions gives better insight into the flushing behaviour of the lagoon under no wind and wind conditions. The results show, with a reduction in flushing time of 1%, only marginal gains on the flushing rate in Phase 1 after 30 days of simulation. However, after the adaptation of Boughaz 2 in Phase 2 a 12% increase in lagoon flushing is observed for the situation with wind and 8% for the situation without wind. The horizontal water distribution shows that the exchange with the Mediterranean Sea is concentrated around the inlets, where most of the fishing activities take place. The percentage mainly remains low due to the stagnant zones in the West and center of the lagoon, which experience little influence of the Mediterranean Sea. It therefore can be concluded that the combined adaptations of Phase 1 and Phase 2 shall result in an (limited) increase of the lagoon flushing rate. It will require further research to determine the additional measures which

are required to reach a well mixed lagoon, should this be desired by the Egyptian government.

How can the Bardawil Lagoon multiple inlet system be transformed from a morphologically unstable towards a morphologically stable inlet system by adapting one or both inlets?

After a careful assessment of the present Bardawil Lagoon hydrodynamic characteristics and their effect on the morphological stability of the inlet system, it is determined that the current situation at both inlets is not sustainable and system interventions are required to establish a morphologically stable lagoon inlet system. The application of the proposed designs in Phase 1 and Phase 2 removes the inlet limitations on the incoming tide, which is then mainly influenced by the friction imposed by the inner basin geometry. Moreover, taking into account both the prevailing winds and high evaporation effects, the total system is classified as sediment exporting after Phase 2, however baroclinic effects are not included in these calculations. High evaporation rates have significant importing effect on the sediment transport character of the inlets, however after Phase 2 these effects are reduced by a factor 3-5, depending on the wind. Due to the baroclinic instability resulting from the density difference between the Mediterranean Sea and Bardawil Lagoon a net export of sediments is expected, because the outgoing flow is located near the bottom where sediment transport takes place. The new cross-sectional area design brings both inlets near the stable equilibrium point on the Escoffier curve after Phase 2, which is supported by the sensitivity analysis. On this stable point the inlets are more robust and are able to remain open without interventions. The flushing rate of the lagoon shows an 8 to 12% increase after Phase 2, this increased flushing is mainly located near the inlets, where most of the fishing activities take place. Hence, it is concluded that the proposed adaptations achieve the goal of developing Bardawil Lagoon into a morphologically stable inlet system.

6.2 RECOMMENDATIONS

6.2.1 Data

Not surprisingly, taking into account the research of Lanters and Georgiou as well, the lack of data constraints the ability of constructing a well validated model. Recent field observations on wave, wind, tide, sediment, salinity and temperature data could significantly enhance the value of a numerical model. The current models allow for a qualitative evaluation of adaptations, but with proper insight these could become quantitative predictions.

6.2.2 Modelling

The current model provides only insight in the hydrodynamic behaviour of the lagoon for all phases. The morphodynamic changes are included analytically, which show promising results. But a validated (within the available data) 3D D-Flow in combination with D-Morphology model should be the start to gain insight in the current salt and water balance of Bardawil Lagoon. Furthermore, it could provide insight in the effect of inlet adaptations on the lagoon system, especially on the long term. The implementation of several sediment fractions would allow for a realistic approximation of morphodynamic behaviour inside and around the lagoon. It allows for determining the stability of the inlets over time under various conditions. In this study the sensitivity study is performed with 5 separate cross-sectional areas. In a morphological model this could be done with one large and one small cross-sectional area design chosen on the right places of the Escoffier curve, which according to the theory should converge them to one single point; the stable equilibrium point, as described by Tran et al. (2011). Long time morphological modelling provides insight in the dynamic stability of an inlet. Furthermore, including morphology, the effect of the adaptations on natural deepening can be investigated.

Moreover, constructing a 3D model instead of a 2D-H model should give more insight into the effect of baroclinic processes happening around the inlets and further into the lagoon. With an increased lagoon depth in later design stages the change of effects due to stratification increases. Such a 3D model allows for better insight in the long term response of system interventions.

6.2.3 Design adaptations

For the current study the inlet design proposed by Georgiou (2019) is, with small adaptations, applied to Boughaz 2. As described in the discussion this design performed well for this study, however this does not mean it is the most efficient design. Therefore it is recommended to conduct another study on the effect different design parameters have on the behaviour of Boughaz 2.

Besides adaptations to the inlets, adaptations to the lagoon interior can provide a lot of insight in the limiting effect of friction on the tidal propagation. Simple model runs with a uniform lagoon depth of -5 and -10 meter gave interesting results on the behaviour of the lagoon. It appeared that the basin moved from friction dominated in Phase 2 back to inlet dominated after applying an increased uniform depth. These assumptions along with

for example the dredging solutions provided by Lanters (2016) form a basis for next research.

6.2.4 Processes

This thesis is, within the known research, the first study on Bardawil Lagoon including a daily varying wind pattern, in contrast to investigating the separate effect of different wind directions and magnitudes. It provided an interesting insight in the behaviour of the lagoon under such conditions, but of course there are more events which can be investigated in the future. For example longer simulations can be done with the presence of both the summer and winter wind climate, as well as investigating the effect of storm events. The latter is especially interesting when looking at the morphological response of the inlets. As discussed, the shape of the Boughaz 2 Escoffier curve is not as steep as the one of Boughaz 1. A storm event could move the inlet back to an unstable equilibrium point. More research on this topic could give insight in the robustness of the system adaptations.

As has been described throughout the thesis evaporation is not included in the numerical model calculations. Nevertheless it is concluded that the net water loss due to evaporation has influence on the hydraulic behaviour of the inlets, as well as the salinity inside the lagoon. A model which incorporates the evaporation as a uniform sink within the lagoon should provide a more accurate representation of the natural behaviour of the system. When performing numerical model simulations including morphology these effects cannot be neglected. Hence the evaporation effect should be studies, which can be done by including for example a daily evaporation pattern (day-night difference), a yearly averaged pattern (for morphodynamic behaviour) or a summer/winter difference, which is interesting to investigate parallel to the seasonal wind variability.

6.2.5 Stability

The current study is performed on the Bardawil Lagoon double inlet system. However, there are plans on increasing the number from 2 inlets to 3 or even 4 inlets. This can completely change the interaction between the inlets and hence the behaviour of the total lagoon. While currently limited interaction is observed, increasing the number of inlets most likely amplifies these interactions. The conventional stability method of Escoffier is not applicable anymore in this situation. A method is developed by Van de Kreeke and Brouwer (2017), but not yet validated. Nevertheless, applying this method on Bardawil Lagoon could give insight into the stability behaviour of the inlets.

6.2.6 Flushing

Two methods are used in this thesis to gain insight in the flushing rate of the lagoon before and after the adaptations. However, a more thorough study on the flushing response of the system concerning adaptations could give more insight in the ecological response of the lagoon. A more ecological orientated study could provide insight in the direct effect of the adaptations on the salinity values and the amount of nutrients provided by the interaction with the Mediterranean Sea and hence the fish population.

LIST OF FIGURES

LIST OF TABLES

BIBLIOGRAPHY

Abd Ellah, R. G. and Hussein, M. M. (2009). Physical Limnology of Bardawil Lagoon, Egypt. *American-Eurasian J. Agric. & Environ. Sci*, 5(3):331–336.

Abohadima, S., El-Bagoury, D., and Rakha, K. A. (2013). Numerical simulation for flushing rate in Bardawil lagoon, Egypt. *Journal of Engineering and Applied Science*, 60(2):117–128.

Bek, M. and Cowles, G. (2018). A Three-Dimensional Circulation Model of Lake Bardawil, Egypt. 5:1–12.

Ben-Tuvia, A. (1979). Ten years of fisheries biology investigations of the Bardawil Lagoon. *Fish. Fish Breed.*, 14(2):29–37.

Bosboom, J. and Stive, M. J. (2015). *Coastal Dynamics 1*.

Brouwer, R. L., Van de Kreeke, J., and Schuttelaars, H. M. (2012). Entrance/exit losses and cross-sectional stability of double inlet systems. *Estuarine, Coastal and Shelf Science*, 107:69–80.

Bruun, P. (1978). Stability of tidal inlets, theory and engineering. *Developments in geotechnical engineering*, 23:510.

Bruun, P. and Gerritsen, F. (1959). Natural bypassing of sand at coastal inlets. *Joernal of the Waterways and Harbours Division*, 85:75–107.

Bruun, P. and Gerritsen, F. (1960). Stability of coastal inlets.

de Vriend, H. J., Dronkers, J., Stive, M. J. F., van Dongeren, A., and Wang, J. H. (2002). Coastal inlets and Tidal basins. *Delft University of Technology*.

Deltares (2019). D-Flow Flexible Mesh User Manual.

DHI (2019). *Shoreline Management Guidlines - DHI*.

El-Aiatt, A. A., Shalloof, K. A., and Saber, M. M. (2019). Bio-economic studies on the catch of Bardawil Lagoon, North Sinai, Egypt. *Egyptian Journal of Aquatic Research*, 45(1):59–65.

El-Bana, M., Khedr, A. H., Van Hecke, P., and Bogaert, J. (2002). Vegetation composition of a threatened hypersaline lake (Lake Bardawil), North Sinai. *Plant Ecology*, 163(1):63–75.

Emanuelsson, D. and Mirchi, A. (2007). Impact of coastal erosion and sedimentation along the northern coast of the sinai peninsula. 2(April):1049–1062.

Embabi, N. S. and Moawad, M. B. (2014). A semi-automated approach for mapping geomorphology of El Bardawil Lake, Northern Sinai, Egypt, using integrated Remote Sensing and GIS techniques. *Egyptian Journal of Remote Sensing and Space Science*, 17(1):41–60.

Escoffier, F. (1940). The stability of tidal inlets. *Shore and Beach*, 8(4):111–114.

Euroconsult (1995). Bardawil Development Project. Technical report.

Farahat, H. (2006). *Sedimentary processes act on Bardawil Lagoon, North Sinai, Egypt*. PhD thesis.

Ferrarin, C. and Umgiesser, G. (2005). Hydrodynamic modeling of a coastal lagoon: the Cobras lagoon in Sardinia, Italy. *Ecological Modelling*, 188:340–357.

FitzGerald, D., Kraus, N., and Hands, E. (2000). Natural Mechanisms of Sediment Bypassing at Tidal Inlets. *ERDC/CHL CHETN-IV-30, US Army Corps of Engineers*.

Folk, R. and Sanders, J. (1978). *Principles of sedimentology*.

Friedrichs, C., Aubrey, D., Giese, G., and Speer, P. (1993). Hydrodynamical modeling of a multiple-inlet estuary/barrier system: insight into tidal inlet formation and stability. In *Formation and Evolution of Multiple Tidal Inlets*, pages 95–112.

Frihy, O. E., Badr, A. A., Selim, M. A., and El sayed, W. R. (2002). Environmental impacts of El Arish power plant on the Mediterranean coast of Sinai, Egypt. *Environmental Geology*, 42(6):604–611.

Frihy, O. E. and Lotfy, M. F. (1997). Shoreline Changes and Beach-sand Sorting along the Northern Sinai Coast of Egypt. *Geo-Marine Letters*, 17:140–146.

Georgiou, M. (2019). Innovative Tidal Inlet Design.

Hamdan, M. and Hassan, F. (2020). Quaternary of Egypt. In *The Geology of Egypt*, pages 445–493.

Inman, D. (1970). Background information on Bardawil Lagoon.

Inman, D. and Jenkins, S. (1984). The Nile Littoral Cell and Man's Inpact on the Coastal Zone of the South Eastern Mediterranean. *Coastal Engineering*, pages 1600–1617.

Inman, D. L. and Jenkins, S. A. (1985). Nile Littoral Cell and Man'S Impact on the Coastal Zone of the Southeastern Mediterranean. *Proceedings of the Coastal Engineering Conference*, 2:1600–1617.

Kamphuis, J. (1991). Alongshore sediment transport rate. *Journal of Waterway, Port, Coastal and Ocean Engineering*, 117:624–640.

Khalil, M. T. and Shaltout, K. H. (2006). *Lake Bardawil and Zaranik Protected Area*. Number 15.

Klein, M. (1986). Morphological changes of the artificial inlets of the Bardawil lagoon. *Estuarine, Coastal and Shelf Science*, 22(4):487–493.

Lanters, M. (2016). A hydrological design of Lake Bardawil.

Linnersund, J. and Mårtensson, E. (2008). Hydrodynamic modelling and estimation of exchange rates for Bardawil Lagoon, Egypt. page 91.

Mil-Homens, J., Ranasinghe, R., Van Thiel de Vries, J., and Stive, M. (2013). Re-evaluation and improvement of three commonly used bulk longshore sediment transport formulas. *Coastal Engineering*, 75:29–39.

Miller, M., Pietrafesa, J. L., and Smith, N. (1990). Principles of hydraulic management of coastal lagoons for aquaculture and fisheries. *FAO Fisheries Technical Paper*, 314:88.

Nassar, K., Mahmod, W. E., Masria, A., Fath, H., and Nadaoka, K. (2018). Numerical simulation of shoreline responses in the vicinity of the western artificial inlet of the Bardawil Lagoon, Sinai Peninsula, Egypt. *Applied Ocean Research*, 74:87–101.

Oertel (1988). Processes of sediment exchange between tidal inlet, ebb deltas and barrier islands. *Lecture Notes on Coastal and Estuarine Studies*, 29:297–318.

Shore Protection Manual (1984). U.S. Army Corps of Engineers, Coastal Engineering Research Center, U.S. Governmeent Printing Office, Washington, D.C. Technical report.

Van de Kreeke, J. and Brouwer, R. L. (2017). *Tidal Inlets*. Cambridge University Press.

Van de Kreeke, J. and Robaczewska, K. (1993). Tide-induced residual transport of coarse sediment; Application to the EMS estuary. *Netherlands Journal of Sea Research*, 31(3):209–220.

van Rijn, L. (2013). A simple general expression for longshore transport of sand, gravel and shingle. Technical report.

Vinja, J. (1970). Coastal inlets of Bardawil Lagoon, Feasibility Study. *Waterloopkundig laboratorium Delft*.

A DATA

A.1 LITTORAL DRIFT

In Table A.1 below the literature values of the littoral drift from the studies of Inman (1970); Vinja (1970); Euroconsult (1995); Emanuelsson and Mirchi (2007) and Suez Canal Authority (1983) can be found.

Study	**Boughaz 1** (m^3/y)	**Boughaz 2** (m^3/y)	**Direction**
Inman (1970)	300 000	500 000	Gross
Vinja (1970)	340 000	600 000	East
	140 000	100 000	West
	200 000	500 000	Net East
	480 000	700 000	Gross
Suez Canal Authority (1983)	576000	360500	East
	149 500	54 500	West
	426 500	306 000	Net East
	725 500	415 000	Gross
Euroconsult (1995)	500 000	800 000	Gross
	300 000	500 000	Net East
Emanuelsson and Mirchi (2007)	40 000	258 000	Net East

Table A.1: Littoral drift studies along the North Sinai coastline, results obtained with aerial observations (Inman, 1970) and CERC formula (Shore Protection Manual, 1984), (Vinja, 1970; Euroconsult, 1995; Emanuelsson and Mirchi, 2007) (Suez Canal Authority, 1983)

As described in the main text a separate littoral drift study is performed for this thesis to gain insight in the longshore transport values according to the methods of Kamphuis (1991), CERC Shore Protection Manual (1984), Modified Kamphuis (Mil-Homens et al., 2013), and van Rijn (2013). The calculations are determined with a sheet provided by van Rijn and the results of this study can be found in Table A.3. The parameters used for these calculations can be found in Table A.2.

The wave climate which is used for the calculations is provided with the BMT Argoss model and is determined at two offshore locations in front of the respective inlet.

Parameter	Value
Sediment density [kg/m^3]	2650
Bulk density of sand bed [kg/m^3]	1600
Percentage of offshore swell waves (H>1m, T>10s) [-]	0.3
Calibration factor [-]	1
Breaker coefficient [-]	0.7
Slope surf zone [-]	0.02
Sediment size [m]	0.00025
Offshore water depth [m]	30
Shore normal angle to North Boughaz 1 [degrees]	345
Shore normal angle to North Boughaz 2 [degrees]	18

Table A.2: Values used for the calculation of the littoral drift

Study	Boughaz 1 (m^3/y)	Boughaz 2 (m^3/y)	Direction
Kamphuis (1991)	79 100	147800	Net east
	147 100	152 300	Gross
	113 100	150 100	Gross east
	34 000	2 300	Gross west
Kamphuis (2013)	57 600	88 400	Net east
	101 700	91 300	Gross
	79 700	89 900	Gross east
	22 100	1500	Gross west
CERC	239700	677800	Net east
	596800	700400	Gross
	418200	689100	Gross east
	178500	11300	Gross west
Van Rijn (2014)	99400	238400	Net east
	220300	245000	Gross
	159900	241700	Gross east
	60500	3300	Gross west

Table A.3: Littoral transport along the coastline stretches of Boughaz 1 and Boughaz 2 determined using the methods of Kamphuis (1991), Modified Kamphuis (Mil-Homens et al., 2013), CERC (Shore Protection Manual, 1984), and van Rijn (2013)

A.2 BATHYMETRY

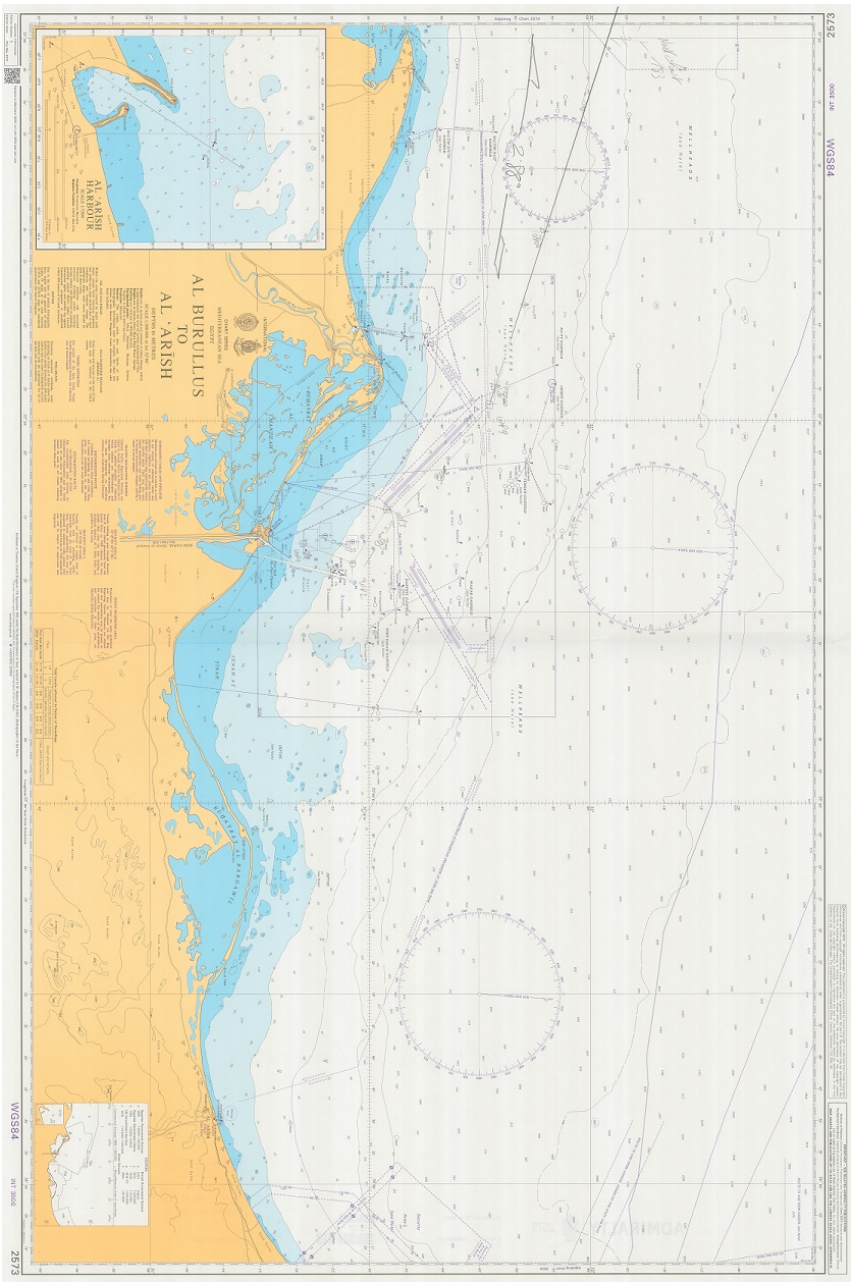

Figure A.1: Bathymetric map of the North Sinai published in 2011. Some map areas originate from data obtained in 1856

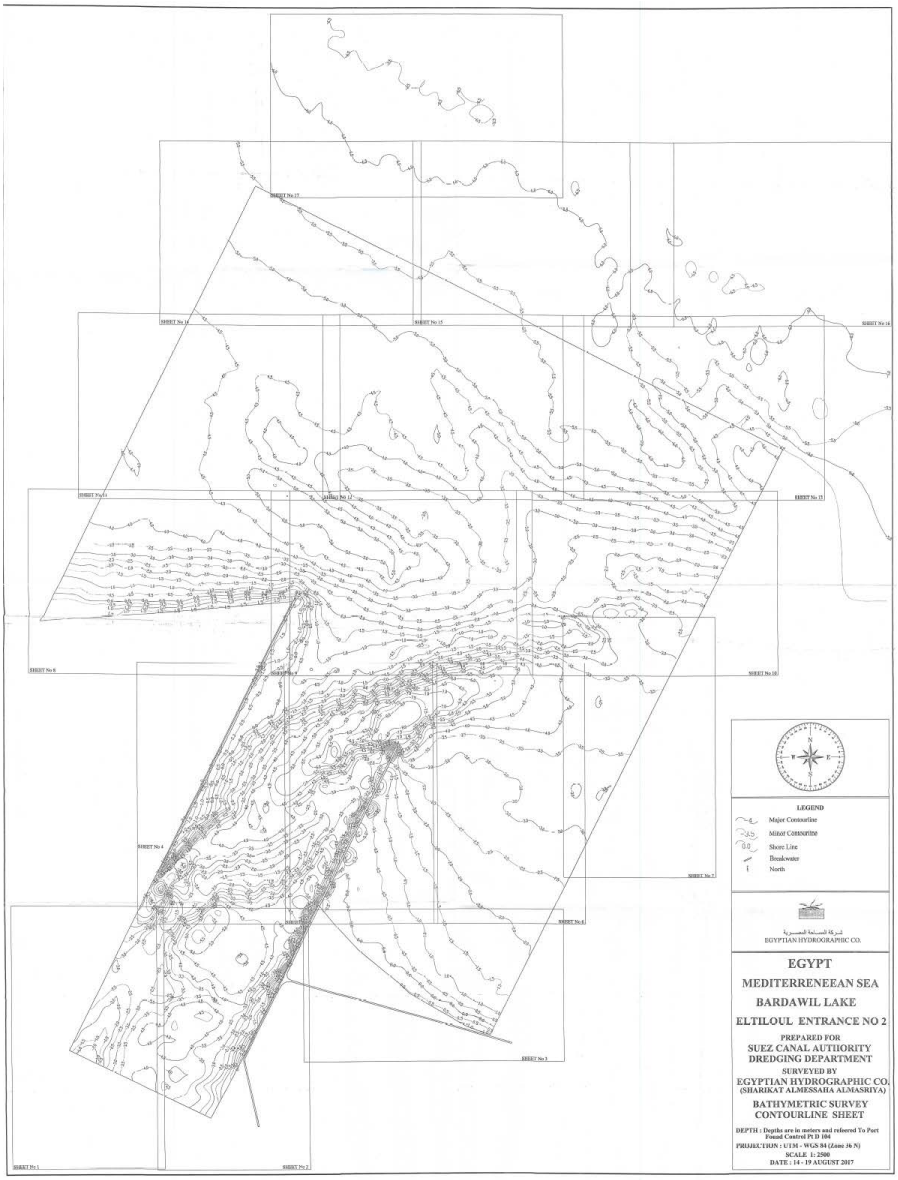

Figure A.2: Bathymetric survey conducted on Boughaz 2 in 2017

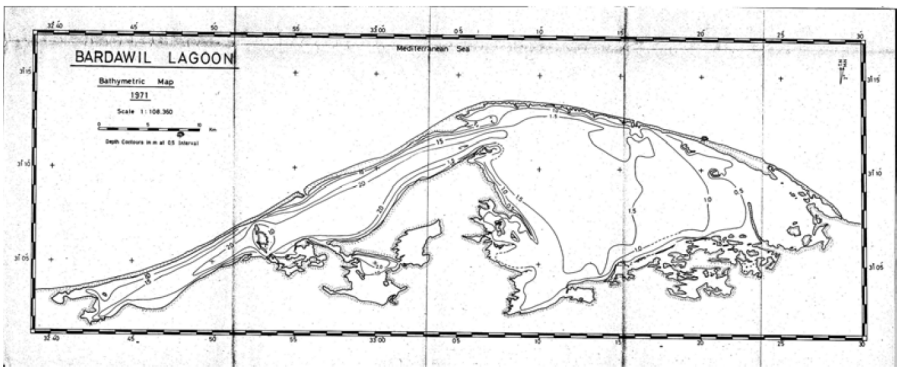

Figure A.3: Bathymetric map of the interior of Bardawil Lagoon from Linnersund and Mårtensson (2008)

B RESULTS

B.1 ESCOFFIER SENSITIVITY ANALYSIS

The proposed design changes for both Boughaz 1 and Boughaz 2 are designed in such a way to bring the inlets as close as possible to the stable equilibrium point on the Escoffier curve. To further support the choice of cross-section area a sensitivity analysis is conducted on the initial situation (Phase 0) and after the system interventions (Phase 1 and Phase 2), of which the results can be found in this section.

Because the system can be defined as a multiple inlet system the stability of one inlet is a function of the size of the other inlet. The sensitivity is therefore determined by choosing different cross-sectional area values for one inlet while the other inlet cross-sectional area remains constant. The Phase 0 model is used for both inlets in the initial situation, while the Phase 1 model is used for the analysis of Boughaz 1 and the Phase 2 model for the analysis of Boughaz 2.

B.1.1 Phase 0

The data from the sensitivity runs for Phase 0 can be found in Table B.1 for Boughaz 1 and in Table B.2 for Boughaz 2. A visualization of the Escoffier curve for Phase 0 can be found in Figure B.1. The trend shown for both situations indicates a position on upward slope of the Escoffier closure curve, indicating a point close to the unstable equilibrium point.

Boughaz 1	Cross-sectional area m^2	Max inlet velocity [m/s]
1	455	0.77
2	622	0.86
3 (Phase 0)	954	0.96
4	1253	1.05
5	1459	1.07

Table B.1: The maximum inlet velocity for different inlet cross-sectional areas for Boughaz 1 in Phase 0

Boughaz 2	Cross-sectional area m^2	Max inlet velocity [m/s]
1	1110	0.69
2	1206	0.74
3 (Phase 0)	1386	0.79
4	1647	0.85
5	1828	0.92

Table B.2: The maximum inlet velocity for different inlet cross-sectional areas for Boughaz 2 in Phase 0

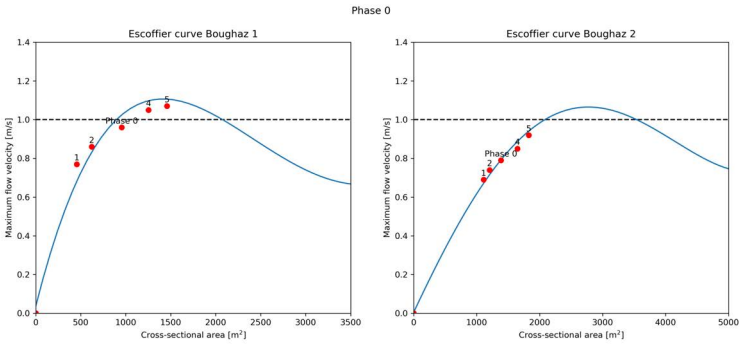

Figure B.1: Plot of the cross-sectional area and maximum depth averaged velocity of the sensitivity test runs for Phase 0. The closure curve is fitted according to the results of the sensitivity analysis

B.1.2 Phase 1

The results of the sensitivity analysis for Boughaz 1 can be found in Table B.3 below.

Case	Cross-sectional area m^2	Max inlet velocity [m/s]
1	1662	1.15
2	1961	1.07
3 (Phase 1)	2323	0.95
4	2627	0.88
5	3287	0.71

Table B.3: The maximum inlet velocity for different inlet cross-sectional areas for Boughaz 1 in Phase 1

Plotting the data from the table on to the Escoffier closure curve gives a good impression on the current status of the inlet stability wise (Figure B.2). Increasing the inlet leads to a decrease in velocity, indicating a point right of the stable equilibrium point, see Figure 2.12. The same principle holds for decreasing the inlet size, which in its turn leads to an increase in velocity, indicating a position left of the stable equilibrium point. Therefore it can be concluded that adapting Boughaz 1 to the cross-sectional area described in Chapter 3 leads to a position near the stable equilibrium point.

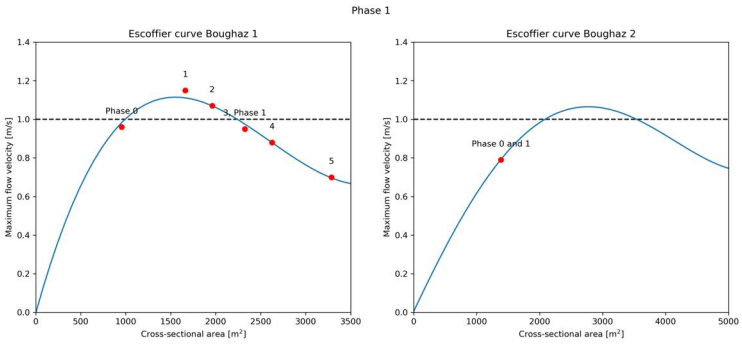

Figure B.2: Plot of the cross-sectional area and maximum depth averaged velocity of the sensitivity test runs for Phase 1. The closure curve is fitted according to the results of the sensitivity analysis

B.1.3 Phase 2

The results of the sensitivity analysis for Boughaz 2 can be found in Table B.4 below. For Boughaz 2 the same holds as was concluded for Boughaz 1. A decreased inlet size leads to larger flow velocities, while an increased inlet reduces the flow velocity. As can be seen in Figure B.3 the design for Boughaz 2 in Phase 2 leads to a stable situation.

Case	Cross-sectional area m^2	Max inlet velocity [m/s]
1	1872	1.10
2	2725	1.09
3 (Phase 2)	3221	1.00
4	4582	0.89

Table B.4: The maximum inlet velocity for different inlet cross-sectional areas for Boughaz 2 in Phase 2

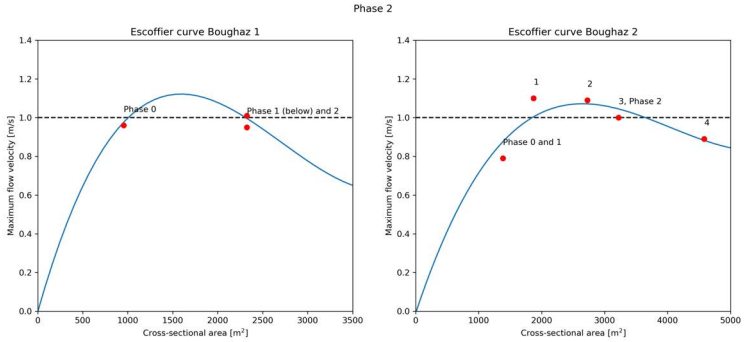

Figure B.3: Plot of the cross-sectional area and maximum depth averaged velocity of the sensitivity test runs for Phase 2. The closure curve is fitted according to the results of the sensitivity analysis